



**End Effects for Plane Deformations of an Elastic Anisotropic  
Semi-Infinite Strip**

---

A Dissertation  
Presented to  
the Faculty of the School of Engineering and Applied Science  
University of Virginia

---

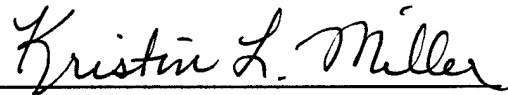
In Partial Fulfillment  
of the requirements for the Degree  
Doctor of Philosophy (Applied Mathematics)

by  
Kristin L. Miller  
May 1994

APPROVAL SHEET

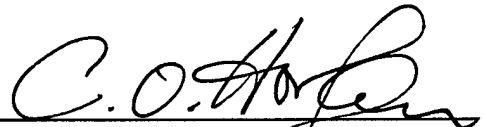
This dissertation is submitted in partial fulfillment of the  
requirements for the degree of

Doctor of Philosophy (Applied Mathematics)

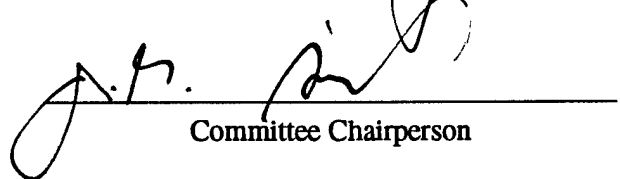


Kristin L. Miller

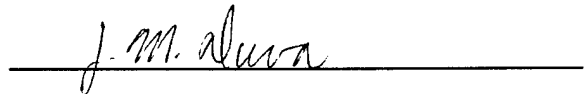
This dissertation has been read and approved by the examining Committee:

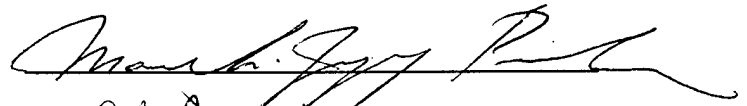


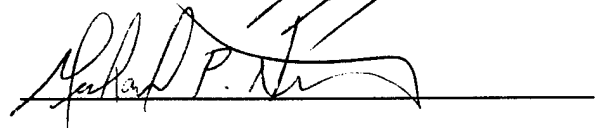
Dissertation Advisor



Committee Chairperson







Accepted for the School of Engineering and Applied Science:



Dean, School of Engineering and Applied Science

May 1994

## ABSTRACT

In the linear theory of elasticity, Saint-Venant's principle is used to justify the neglect of edge effects when determining stresses in a body. For isotropic materials, the validity of this is well established. However for anisotropic materials, experimental results have shown that edge effects may persist much farther into the material than for isotropic materials and as a result cannot be neglected. This research examines the effect of material anisotropy on the exponential decay rate for stresses in a semi-infinite elastic strip. A linear elastic semi-infinite strip in a state of plane stress/strain subject to a self-equilibrated end load is considered first for a specially orthotropic material and then for the general anisotropic material. The problem is governed by a fourth-order elliptic partial differential equation with constant coefficients. Conservation properties of the solution are derived to help to determine a stress decay rate estimate. Energy methods are then used to establish lower bounds on the actual stress decay rate. Both analytic and numerical estimates are obtained in terms of the elastic constants of the material and results are shown for several contemporary engineering materials. When compared with the exact stress decay rate computed numerically from the eigenvalues of a fourth-order ordinary differential equation, the results in some cases show a high degree of accuracy. Results of the type obtained here have several important practical applications. For example, the results provide physical insight into the mechanical testing of anisotropic and laminated composite structures and are useful in assessing the influence of fasteners, joints, etc. on the behavior of composite structures.

## Acknowledgements

I would like to express my appreciation to the members of my Ph.D committee: Dr. J.G. Simmonds (Chairman), Dr. C.O. Horgan (advisor) , Dr. J. M. Duva, Dr. M-J Pindera and Dr. M.P. Nemeth of NASA Langley Research Center, Hampton, VA. Their insight and helpful suggestions have been very important to the development of this research. In particular, the encouragement and advice offered by Dr. Nemeth during his visiting appointment in the Department of Applied Mathematics as a NASA Floyd L. Thompson Fellow is very much appreciated. I would especially like to acknowledge my advisor, Dr. C.O. Horgan, without whose guidance and direction I could not have accomplished this research. I greatly appreciate the time and effort he has devoted towards furthering my career as an applied mathematician. I am also grateful to Kay Holden and Beve Martin for the countless times they have helped me out during my graduate experience.

I want to thank the U.S. Air Force for their financial support of my doctoral study in awarding me a National Defense Science and Engineering Graduate Fellowship (NDSEGF). My work was also supported by grants from the Virginia Space Grant Consortium, the U.S. National Science Foundation and an Amelia Earhart Fellowship sponsored by the Zonta International Foundation. I am very grateful for the graduate research opportunities that have resulted from this support.

Finally, I would like to thank my fellow graduate students and friends who have helped me in the course of my research, in particular Ted Jackson who has provided much support and advice.

Dedicated to my father, Roger Miller, my stepmother, Phyllis Miller  
and to the memory of my mother, Mary-Lyn Miller, in appreciation for  
all the invaluable encouragement they have provided throughout the years.

# Contents

List of Figures	iii
List of Tables	v
<b>1 INTRODUCTION</b>	<b>1</b>
<b>2 ANISOTROPIC ELASTIC STRIP PROBLEM</b>	<b>5</b>
2.1 Problem Formulation . . . . .	5
2.2 Nondimensionalization . . . . .	10
2.3 Conservation Laws . . . . .	11
2.4 Positive-Definiteness of the Strain-Energy Density . . . . .	15
2.5 Energies . . . . .	17
2.5.1 Energy Methods . . . . .	18
2.5.2 Derivation of Energy Functionals . . . . .	20
2.5.3 Positive-Definiteness of the Energy Functionals . . . . .	25
<b>3 THE ORTHOTROPIC CASE</b>	<b>27</b>
3.1 Formulation . . . . .	27
3.2 Preliminary Inequalities . . . . .	30

3.3	Analytic Estimate . . . . .	31
3.3.1	General Estimate . . . . .	32
3.3.2	Asymptotic Estimate . . . . .	38
3.4	Conservation Law Estimate . . . . .	39
3.4.1	General Estimate . . . . .	40
3.4.2	Asymptotic Estimate . . . . .	46
3.5	Exact Decay Rates . . . . .	49
3.6	Discussion of Results . . . . .	51
<b>4</b>	<b>THE ANISOTROPIC CASE</b>	<b>62</b>
4.1	Formulation . . . . .	62
4.2	Basic Energy Estimate . . . . .	64
4.3	Nonlinear Optimization Estimate . . . . .	71
4.3.1	Nonlinear Optimization Analysis . . . . .	75
4.4	Higher-Order Energy Estimates . . . . .	83
4.4.1	Quadratic Estimate . . . . .	85
4.4.2	Quartic Estimate . . . . .	92
4.5	Exact Decay Rates . . . . .	100
4.6	Discussion of Results . . . . .	105
<b>5</b>	<b>SUMMARY AND CONCLUSIONS</b>	<b>119</b>



# List of Figures

2.1	Semi-infinite strip . . . . .	6
2.2	Cross section of strip . . . . .	12
2.3	Region $R_z$ . . . . .	18
4.1	Fiber angle $\theta$ . . . . .	102
4.2	Exact decay rates vs. fiber angle . . . . .	103
4.3	Exact decay rate and estimates for HS1 . . . . .	110
4.4	Exact decay rate and estimates for HS2 . . . . .	110
4.5	Exact decay rate and estimates for UM . . . . .	111
4.6	Basic energy estimate for HS1 with different energy functionals . . . .	111
4.7	Basic energy estimate for HS2 with different energy functionals . . . .	112
4.8	Basic energy estimate for UM with different energy functionals . . . .	112
4.9	Optimization estimate for HS1 with different energy functionals . . .	113
4.10	Optimization estimate for HS2 with different energy functionals . . .	113
4.11	Optimization estimate for UM with different energy functionals . . .	114
4.12	Materials for which the positive-definite condition (4.9) is satisfied .	114
4.13	Materials for which the positive-definite condition (4.9) fails . . . .	115
4.14	Upper bounds (4.138), (4.168) on estimated decay rate for HS1 . . .	115

4.15 Upper bounds (4.138), (4.168) on estimated decay rate for HS2 . . .	116
4.16 Upper bounds (4.138), (4.168) on estimated decay rate for UM . . .	116
4.17 Nondimensional parameters for HS1 . . . . .	118
4.18 Nondimensional parameters for KE . . . . .	118

# List of Tables

3.1	Orthotropic materials and elastic moduli . . . . .	58
3.2	Plane stress results for orthotropic materials . . . . .	59
3.3	Strongly orthotropic results . . . . .	60
3.4	Exact characteristic decay lengths . . . . .	61
4.1	Quartic estimate for orthotropic materials . . . . .	117

# Chapter 1

## INTRODUCTION

When considering plane deformations in the context of linear elasticity theory, Saint-Venant's principle is often used to justify approximations that neglect edge effects (see [1], [2] for recent reviews). As a result, this principle is also the basis for many approximate "strength of materials" formulae that are widely used in engineering practice. Experimental evidence has supported the use of Saint-Venant's principle in this manner. For instance, it is commonly known that for structures made of *homogeneous isotropic* materials, stress effects due to self-equilibrated edge loads decay with distance from the loaded ends over relatively short lengths, e.g. one strip width for a semi-infinite strip. For structures made of *homogeneous anisotropic* materials, however, it has been shown that these local stress effects may persist well into the interior of the body and thus cannot be neglected when making approximations (see [1] -[10]). It is the goal of this dissertation to investigate the behavior of local stress effects for anisotropic materials with a particular emphasis on determining the influence of the elastic constants of the material on the rate of stress decay.

The particular problem that we consider is that of a linearly elastic semi-infinite strip in a state of plane stress/strain subject to a self-equilibrated end load. For strips made of specially orthotropic materials, this stress decay problem may be formulated in terms of a single dimensionless material parameter. For strips made of general anisotropic materials, however, the problem is more complex and involves three dimensionless material parameters. In both cases, the elasticity problem is governed by a fourth-order elliptic partial differential equation with constant coefficients, whose exact analytical solutions are difficult to obtain. In studying the effects of material anisotropy on the exponential decay for stresses, we will develop methods of examining the relevant elasticity problems without having to find exact solutions. Energy methods and estimating techniques for partial differential equations will be used to obtain bounds on the solution and on the stresses (which are second derivatives of the solution) with an emphasis on obtaining bounds for their decay rates. In addition to the specific problem of plane elasticity for a semi-infinite strip, these methods can also be applied to other more general situations, i.e. problems with different geometries, problems with different governing equations, nonlinear problems, etc. (see e.g. [1], [2]). Through the use of such energy methods and estimating techniques, both analytic and numerical decay rate estimates are obtained in terms of the elastic constants of the material. For a set of specific materials, these estimates are compared with the exact decay rate computed numerically from the eigenvalues of a fourth-order ordinary differential equation. The results in some cases show a high degree of accuracy.

Much work has already been done with *isotropic* materials in a state of plane

stress/strain for which the governing equation is the biharmonic equation (see [3], [11] -[15]). Various energy methods and differential inequality techniques have been developed to obtain lower bounds for the decay rate that accurately estimate the exact decay rate of the solution. Fewer results are known for *anisotropic* materials in a state of plane stress/strain where the governing equation is a generalized fourth-order elliptic partial differential equation with constant coefficients. Much of the analysis that has already been done for anisotropic materials has been concerned with exact numerical solutions to the problem rather than analytic estimates. This dissertation will extend some of the known techniques used for the biharmonic equation and apply them to the generalized fourth-order problem. In the process, new techniques are also generated. Ultimately, an explicit "formula" for the decay rate of stresses is sought which, although it will be an estimate (in fact, a lower bound for the exact decay rate), will reveal how the elastic constants are involved.

This research has several applications in the field of structural analysis and design. For example, in the mechanical testing of anisotropic and composite materials, regions of uniform stress and strain fields are necessary for accurate measurements of material properties. Thus it is crucial to have an understanding of the local stress behavior and edge effects that may be induced through the testing procedure. Another area of application is in assessing the influence of fasteners, joints, rivets, etc. in composite materials. Here, an understanding of local stress effects and how far into the material they penetrate is of critical importance to the designer. Results of the type obtained in this research could also allow for "tailoring" a material with specific properties to ensure that local stresses attenuate at a desired rate.

The organization of this thesis is as follows. In Chapter 2, we formulate the *anisotropic strip problem* and its nondimensional form. Several conservation properties are derived for later use. The strain-energy for the problem is examined, the positive-definiteness of which leads to restrictions on the material constants. Energy methods that involve estimating techniques using differential inequalities are outlined and several energy norms are presented. In Chapter 3, we examine these energy methods for a special class of materials, namely orthotropic materials and the problem is reduced to the *orthotropic strip problem*. This serves as a simpler setting within which to illustrate the energy techniques of this dissertation. Several decay rate estimates are developed and then compared with exact solutions. Where possible, explicit formulae for the estimated decay rates are obtained and the results are compared with exact decay rates (computed from roots of a transcendental equation) for a variety of materials used in composites technology. Asymptotic results for strongly orthotropic materials are also developed. In Chapter 4, we return to the *anisotropic problem* and extend the techniques from Chapter 3 to cover more general materials. The complexity of the analysis is greatly increased. Several estimates are developed and numerical results are compared to exact solutions. The accuracy of these results and their implications for future estimating techniques are discussed. Finally, in Chapter 5 we summarize the important results obtained in this dissertation and indicate some directions for future research.

## Chapter 2

# ANISOTROPIC ELASTIC STRIP PROBLEM

In this chapter, the anisotropic elastic strip problem is formulated and preliminary material needed for the estimation techniques used in later chapters is presented. The chapter begins with a formulation of the physical problem, which is then nondimensionalized. Next, several conservation properties are examined as well as positive-definiteness of the strain-energy density. The chapter ends with an outline of the energy arguments that form the basis for subsequent estimation techniques.

### 2.1 Problem Formulation

Consider an homogeneous anisotropic linearly elastic body that occupies the following region described in the  $x_1, x_2, x_3$  Cartesian coordinate system by

$$x_1 \geq 0, \quad -H \leq x_2 \leq H, \quad -T \leq x_3 \leq T, \quad (2.1)$$



where  $2H$  is the height of the body and  $2T$  is the thickness that may be taken to be infinite or infinitesimal. For a material with the  $x_1 - x_2$  plane a plane of elastic symmetry, one can define a state of plane deformation such that the infinitely thick body is in a state of plane strain or such that the infinitesimally thin body is in a state of plane stress. All surfaces of the body will be traction free except for the surface  $x_1 = 0$ , where a prescribed self-equilibrated traction is applied. For this type of loading, it is assumed that the stresses decay to zero as  $x_1 \rightarrow \infty$ . The two plane strain and plane stress elastostatic problems are identical mathematically and differ only in the numerical value of the elastic constants used for each problem. Both result in the consideration of an anisotropic elastic semi-infinite strip occupying the region  $\mathfrak{R}$  in the  $x_1 - x_2$  plane defined by

$$\mathfrak{R}: \quad x_1 > 0, \quad -H < x_2 < H, \quad (2.2)$$

with traction-free lateral surfaces, a prescribed self-equilibrated edge load on the end  $x_1 = 0$  and stresses that decay to zero as  $x_1 \rightarrow \infty$  (see Figure 2.1).

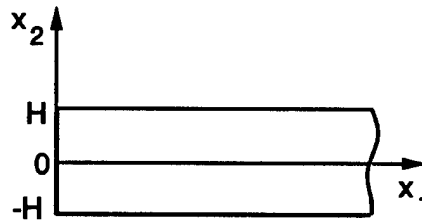


Figure 2.1: Semi-infinite strip

The in-plane components of the strain tensor  $e_{11}$ ,  $e_{12}$ ,  $e_{22}$  are related to the in-plane components of the stress tensor  $\tau_{11}$ ,  $\tau_{12}$ ,  $\tau_{22}$  by the following reduced constitutive

equations (see e.g. [4]),

$$\begin{aligned} e_{11} &= \beta_{11}\tau_{11} + \beta_{12}\tau_{22} + \beta_{16}\tau_{12}, \\ e_{22} &= \beta_{21}\tau_{11} + \beta_{22}\tau_{22} + \beta_{26}\tau_{12}, \\ 2e_{12} &= \beta_{61}\tau_{11} + \beta_{62}\tau_{22} + \beta_{66}\tau_{12}, \end{aligned} \quad (2.3)$$

or in matrix notation

$$\begin{bmatrix} e_{11} \\ e_{22} \\ 2e_{12} \end{bmatrix} = \begin{bmatrix} \beta_{11} & \beta_{12} & \beta_{16} \\ \beta_{21} & \beta_{22} & \beta_{26} \\ \beta_{61} & \beta_{62} & \beta_{66} \end{bmatrix} \begin{bmatrix} \tau_{11} \\ \tau_{22} \\ \tau_{12} \end{bmatrix}. \quad (2.4)$$

The constitutive equations are obtained from the general 3-D constitutive equations by invoking the assumptions of plane strain or plane stress to obtain a reduced 2-D form. The constants  $\beta_{pq} = \beta_{qp}$  ( $p, q = 1, 2, 6$ ) can be written in terms of the elastic compliances  $a_{pq}$ . In the case of plane stress, the  $\beta_{pq}$ 's are the elastic compliances themselves, while for plane strain they are related by

$$\beta_{pq} = a_{pq} - \frac{a_{p3}a_{q3}}{a_{33}}, \quad (a_{33} \neq 0). \quad (2.5)$$

For materials that are transversely isotropic about the  $x_1$  axis (or for specially orthotropic materials whose fibers run in the  $x_1$  direction), considerable simplification results from the fact that

$$a_{22} = a_{33}, \quad a_{12} = a_{13}, \quad a_{16} = a_{26} = a_{36} \equiv 0. \quad (2.6)$$

As a result,  $\beta_{16} = \beta_{26} \equiv 0$  and the elastic constants  $\beta_{pq}$  may be expressed in terms of the usual engineering constants  $\nu$ ,  $E$  and  $G$  which denote Poisson's ratio, Young's modulus and shear modulus respectively, so that one obtains

$$\begin{aligned}
\text{plane stress : } \beta_{11} &= \frac{1}{E_L}, & \beta_{12} &= -\frac{\nu_{LT}}{E_L} \\
\beta_{22} &= \frac{1}{E_T}, & \beta_{66} &= \frac{1}{G_{LT}}, & \beta_{16} &= \beta_{26} \equiv 0
\end{aligned} \tag{2.7}$$

$$\begin{aligned}
\text{plane strain : } \beta_{11} &= \frac{1}{E_L}(1 - \nu_{LT}^2 E_T/E_L), & \beta_{12} &= -\frac{\nu_{LT}}{E_L}(1 + \nu_{TT}) \\
\beta_{22} &= \frac{1}{E_T}(1 - \nu_{TT}^2), & \beta_{66} &= \frac{1}{G_{LT}}, & \beta_{16} &= \beta_{26} \equiv 0.
\end{aligned} \tag{2.8}$$

In these expressions,  $L$  denotes the longitudinal direction parallel to the  $x_1$  axis and  $T$  denotes the transverse direction. Further simplification arises in the case of isotropic materials such that

$$\begin{aligned}
\text{plane stress : } \beta_{11} &= \beta_{22} = \frac{1}{E}, & \beta_{12} &= -\frac{\nu}{E} \\
\beta_{66} &= \frac{1}{G}, & \beta_{16} &= \beta_{26} \equiv 0
\end{aligned} \tag{2.9}$$

$$\begin{aligned}
\text{plane strain : } \beta_{11} &= \beta_{22} = \frac{1}{E}(1 - \nu^2), & \beta_{12} &= -\frac{\nu}{E}(1 + \nu) \\
\beta_{66} &= \frac{1}{G}, & \beta_{16} &= \beta_{26} \equiv 0.
\end{aligned} \tag{2.10}$$

Returning to the anisotropic analysis, an Airy stress function  $\phi(x_1, x_2)$  is defined in terms of which the Cartesian components of the stress tensor  $\tau$  are given by

$$\tau_{11} = \phi_{,22}, \quad \tau_{22} = \phi_{,11}, \quad \tau_{12} = -\phi_{,12}, \tag{2.11}$$

where a comma denotes partial differentiation. With the Airy stress function defined in (2.11), the equations of equilibrium (with zero body force)

$$\tau_{\alpha\beta,\beta} = 0 \tag{2.12}$$

are identically satisfied. The compatibility equations then yield the following governing differential equation on  $\mathfrak{R}$  (see e.g. [4], [16]),

$$\begin{aligned} \beta_{22}\phi_{,1111} - 2\beta_{26}\phi_{,1112} + (2\beta_{12} + \beta_{66})\phi_{,1122} \\ - 2\beta_{16}\phi_{,1222} + \beta_{11}\phi_{,2222} = 0, \end{aligned} \quad (2.13)$$

which involves all six independent elastic constants. It is assumed that these elastic constants are such that the associated strain-energy density is positive-definite which ensures that the partial differential equation (2.13) is elliptic (see section 2.4 for further discussion). The traction-free boundary conditions on the surfaces of the strip may be written in terms of the Airy stress function and then integrated to yield, on using the self-equilibration conditions,

$$\phi = 0, \quad \phi_{,2} = 0 \quad \text{at } x_2 = \pm H, \quad (2.14)$$

$$\phi = f(x_2), \quad \phi_{,1} = g(x_2) \quad \text{at } x_1 = 0, \quad (2.15)$$

$$\phi_{,\alpha\beta} \rightarrow 0 \quad (\text{uniformly in } x_2) \quad \text{as } x_1 \rightarrow \infty, \quad (2.16)$$

where  $f(x_2)$  and  $g(x_2)$  are prescribed functions that satisfy certain continuity conditions at the corners of the strip. Since these continuity conditions will not be used here, their explicit forms are not given. Equations (2.13) - (2.16) constitute the fundamental boundary value problem associated with the semi-infinite anisotropic strip in a state of plane stress or plane strain, which is referred to henceforth as the *homogeneous anisotropic elastic strip problem*.

## 2.2 Nondimensionalization

In the analysis of this problem the governing partial differential equation is first nondimensionalized, reducing the number of independent elastic constants. Returning to equation (2.13), we define the dimensionless coordinates  $\xi, \eta$  as

$$\xi = \left( \frac{\beta_{11}}{\beta_{22}} \right)^{\frac{1}{4}} \frac{x_1}{H}, \quad \eta = \frac{x_2}{H}, \quad (2.17)$$

and obtain the nondimensional equation for the Airy function  $\phi(\xi, \eta)$ ,

$$\begin{aligned} \frac{\beta_{22}}{H^4} \left( \frac{\beta_{11}}{\beta_{22}} \right) \phi_{,\xi\xi\xi\xi} - \frac{2\beta_{26}}{H^4} \left( \frac{\beta_{11}}{\beta_{22}} \right)^{\frac{3}{4}} \phi_{,\xi\xi\xi\eta} + \left( \frac{2\beta_{12} + \beta_{66}}{H^4} \right) \left( \frac{\beta_{11}}{\beta_{22}} \right)^{\frac{1}{2}} \phi_{,\xi\xi\eta\eta} \\ - \frac{2\beta_{16}}{H^4} \left( \frac{\beta_{11}}{\beta_{22}} \right)^{\frac{1}{4}} \phi_{,\xi\eta\eta\eta} + \frac{\beta_{11}}{H^4} \phi_{,\eta\eta\eta\eta} = 0. \end{aligned} \quad (2.18)$$

Multiplying through both sides by  $\frac{H^4}{\beta_{11}}$  yields

$$\begin{aligned} \phi_{,\xi\xi\xi\xi} - \left[ \frac{2\beta_{26}}{\beta_{11}^{\frac{1}{4}}\beta_{22}^{\frac{3}{4}}} \right] \phi_{,\xi\xi\xi\eta} + \left[ \frac{2\beta_{12} + \beta_{66}}{(\beta_{11}\beta_{22})^{\frac{1}{2}}} \right] \phi_{,\xi\xi\eta\eta} \\ - \left[ \frac{2\beta_{16}}{\beta_{11}^{\frac{3}{4}}\beta_{22}^{\frac{1}{4}}} \right] \phi_{,\xi\eta\eta\eta} + \phi_{,\eta\eta\eta\eta} = 0, \end{aligned} \quad (2.19)$$

on the domain  $\xi > 0, -1 < \eta < 1$ . If one defines the following nondimensional quantities,

$$\epsilon_1 = \left[ \frac{2\beta_{12} + \beta_{66}}{(\beta_{11}\beta_{22})^{\frac{1}{2}}} \right]^{-1}, \quad \epsilon_2 = \left[ \frac{\beta_{26}}{\beta_{11}^{\frac{1}{4}}\beta_{22}^{\frac{3}{4}}} \right]^{-1}, \quad \epsilon_3 = \left[ \frac{\beta_{16}}{\beta_{11}^{\frac{3}{4}}\beta_{22}^{\frac{1}{4}}} \right]^{-1}, \quad (2.20)$$

then the nondimensional governing equation becomes

$$\phi_{,\xi\xi\xi\xi} - \frac{2}{\epsilon_2}\phi_{,\xi\xi\xi\eta} + \frac{1}{\epsilon_1}\phi_{,\xi\xi\eta\eta} - \frac{2}{\epsilon_3}\phi_{,\xi\eta\eta\eta} + \phi_{,\eta\eta\eta\eta} = 0, \quad (2.21)$$

on the new region  $R$  defined by

$$R: \quad \xi > 0, \quad -1 < \eta < 1. \quad (2.22)$$

This governing equation now involves the *three* nondimensional constants  $\epsilon_1$ ,  $\epsilon_2$  and  $\epsilon_3$ , rather than the *six* independent elastic constants  $\beta_{pq}$  originally present. Transforming the boundary conditions (2.14) - (2.15) to the nondimensional variables results in

$$\phi = 0, \quad \phi_{,\eta} = 0 \quad \text{at } \eta = \pm 1, \quad (2.23)$$

$$\phi = F(\eta), \quad \phi_{,\xi} = G(\eta) \quad \text{at } \xi = 0, \quad (2.24)$$

$$\phi_{,\alpha\beta} \rightarrow 0 \quad (\text{uniformly in } x_2) \quad \text{as } \xi \rightarrow \infty, \quad (2.25)$$

where  $\alpha, \beta \in \{\xi, \eta\}$  and  $F(\eta)$ ,  $G(\eta)$  are prescribed functions. We note that a similar nondimensionalization scheme for an orthotropic material weak in shear was carried out in [8]. Similar nondimensionalizations have also been used in the buckling of anisotropic structures (see e.g. [17] and the references therein).

## 2.3 Conservation Laws

Before proceeding further, several inequalities known as “conservation laws” are derived that will be used later to obtain the desired decay estimates. The basic method

to obtain the inequalities is the same in each case. The governing equation is first multiplied by an axial derivative of the Airy stress function and then integrated over the cross section of the strip. The result is simplified using integration by parts and the known homogeneous boundary conditions on the unloaded edges of the strip.

For the first conservation law, the governing equation (2.21) is multiplied by  $\phi_{,\xi}$  and then integrated over  $L_z$ , where  $L_z$  is the cross section of the nondimensional strip at  $\xi = z$ , (see Figure 2.2), so that we have

$$\int_{L_z} [\phi_{,\xi} (\phi_{,\xi\xi\xi\xi} - \frac{2}{\epsilon_2} \phi_{,\xi\xi\xi\eta} + \frac{1}{\epsilon_1} \phi_{,\xi\xi\eta\eta} - \frac{2}{\epsilon_3} \phi_{,\xi\eta\eta\eta} + \phi_{,\eta\eta\eta\eta})] d\eta = 0. \quad (2.26)$$

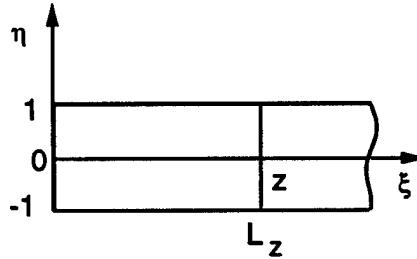


Figure 2.2: Cross section of strip

Performing integration by parts on some of the terms, making use of the boundary conditions  $\phi = 0$ ,  $\phi_{,\eta} = 0$  at  $\eta = \pm 1$ , and removing a  $\xi$ -derivative gives rise to

$$\frac{d}{d\xi} \int_{L_z} [\phi_{,\xi} \phi_{,\xi\xi\xi} - \frac{1}{2} \phi_{,\xi\xi}^2 + \frac{1}{2} \phi_{,\eta\eta}^2 - \frac{1}{2\epsilon_1} \phi_{,\xi\eta}^2 + \frac{2}{\epsilon_2} \phi_{,\xi\eta} \phi_{,\xi\xi}] d\eta = 0. \quad (2.27)$$

Upon integration, we obtain *Conservation Law 1*; i.e.,

$$\int_{L_z} [\phi_{,\xi} \phi_{,\xi\xi\xi} - \frac{1}{2} \phi_{,\xi\xi}^2 + \frac{1}{2} \phi_{,\eta\eta}^2 - \frac{1}{2\epsilon_1} \phi_{,\xi\eta}^2 + \frac{2}{\epsilon_2} \phi_{,\xi\eta} \phi_{,\xi\xi}] d\eta = C_1, \quad (2.28)$$

where  $C_1$  is a constant. The integral on the left hand side of (2.28) is independent of the axial coordinate  $\xi$ , and so is a "conserved" quantity. Using similar procedures, the second conservation law results from multiplying equation (2.21) by  $\phi_{,\xi\xi\xi}$  and integrating over the region  $L_z$ . Starting with

$$\int_{L_z} [\phi_{,\xi\xi\xi} (\phi_{,\xi\xi\xi\xi} - \frac{2}{\epsilon_2} \phi_{,\xi\xi\xi\eta} + \frac{1}{\epsilon_1} \phi_{,\xi\xi\eta\eta} - \frac{2}{\epsilon_3} \phi_{,\xi\eta\eta\eta} + \phi_{,\eta\eta\eta\eta})] d\eta = 0 \quad (2.29)$$

and using integration by parts along with the homogeneous boundary conditions, one obtains

$$\frac{d}{d\xi} \int_{L_z} [\phi_{,\xi\xi\eta} \phi_{,\eta\eta\eta} + \frac{1}{2} \phi_{,\xi\eta\eta}^2 - \frac{1}{2} \phi_{,\xi\xi\xi}^2 + \frac{1}{2\epsilon_1} \phi_{,\xi\xi\eta}^2 - \frac{2}{\epsilon_3} \phi_{,\xi\xi\eta} \phi_{,\xi\eta\eta}] d\eta = 0. \quad (2.30)$$

Upon integration, *Conservation Law 2* is obtained; i.e.,

$$\int_{L_z} [\phi_{,\xi\xi\eta} \phi_{,\eta\eta\eta} + \frac{1}{2} \phi_{,\xi\eta\eta}^2 - \frac{1}{2} \phi_{,\xi\xi\xi}^2 + \frac{1}{2\epsilon_1} \phi_{,\xi\xi\eta}^2 - \frac{2}{\epsilon_3} \phi_{,\xi\xi\eta} \phi_{,\xi\eta\eta}] d\eta = C_2, \quad (2.31)$$

where  $C_2$  is a constant.



The constants  $C_1$  and  $C_2$  are as yet unspecified. However by evaluating the integrals as  $z \rightarrow \infty$ , their signs may be determined and the conservation laws (2.28), (2.31) may be rewritten. To do this, we make a minor additional assumption on the behavior of a third derivative of  $\phi$  as  $\xi \rightarrow \infty$ , namely that

$$\phi_{,\xi\xi\xi} = O(1) \quad (\text{uniformly in } \eta) \quad \text{as } \xi \rightarrow \infty. \quad (2.32)$$

It then follows that

$$C_1 = 0, \quad C_2 = - \lim_{z \rightarrow \infty} \int_{L_z} \frac{1}{2} \phi_{,\xi\xi\xi}^2 d\eta \leq 0, \quad (2.33)$$

since  $\phi_{,\xi\xi}, \phi_{,\xi\eta}, \phi_{,\eta\eta} \rightarrow 0$  as  $\xi \rightarrow \infty$ . Thus, the first and second conservation laws imply

$$\int_{L_z} [2\phi_{,\xi}\phi_{,\xi\xi\xi} + \phi_{,\eta\eta}^2 + \frac{4}{\epsilon_2}\phi_{,\xi\eta}\phi_{,\xi\xi}] d\eta = \int_{L_z} [\phi_{,\xi\xi}^2 + \frac{1}{\epsilon_1}\phi_{,\xi\eta}^2] d\eta, \quad (2.34)$$

and

$$\int_{L_z} [2\phi_{,\xi\xi\eta}\phi_{,\eta\eta\eta} + \phi_{,\xi\eta\eta}^2 + \frac{1}{\epsilon_1}\phi_{,\xi\xi\eta}^2] d\eta \leq \int_{L_z} [\phi_{,\xi\xi\xi}^2 + \frac{4}{\epsilon_3}\phi_{,\xi\xi\eta}\phi_{,\xi\eta\eta}] d\eta, \quad (2.35)$$

respectively. These results will be used in later sections. It is worth noting here that the nondimensional parameter  $\epsilon_3$  (and so  $\beta_{16}$ ) does *not* appear explicitly in (2.34), while  $\epsilon_2$  (and so  $\beta_{26}$ ) does not appear explicitly in (2.35). The details of the derivations outlined above may be found in [18].

## 2.4 Positive-Definiteness of the Strain-Energy Density

It was observed in section 2.1 that the elastic constants  $\beta_{pq}$  in the governing equation (2.13) are such that the associated strain-energy density is positive-definite, ensuring ellipticity of the governing partial differential equation. This will now be discussed in more detail.

The total strain-energy for this boundary value problem is denoted by  $\int_{\mathfrak{R}} W dA$  where  $\mathfrak{R}$  is the original region occupied by the semi-infinite strip. The strain-energy density  $W$  can be expressed as

$$2W = \tau_{\alpha\beta} e_{\alpha\beta} \quad (2.36)$$

where upon using (2.4), one obtains

$$2W = \beta_{11}\tau_{11}^2 + \beta_{22}\tau_{22}^2 + \beta_{66}\tau_{12}^2 + 2\beta_{12}\tau_{11}\tau_{22} + 2\beta_{16}\tau_{11}\tau_{12} + 2\beta_{26}\tau_{22}\tau_{12}. \quad (2.37)$$

This quadratic form may be written in matrix notation as  $2W = \mathbf{t}^T \mathbf{B} \mathbf{t}$ , with

$$\mathbf{t} = \begin{bmatrix} \tau_{11} \\ \tau_{22} \\ \tau_{12} \end{bmatrix}, \quad \mathbf{B} = \begin{bmatrix} \beta_{11} & \beta_{12} & \beta_{16} \\ \beta_{21} & \beta_{22} & \beta_{26} \\ \beta_{61} & \beta_{62} & \beta_{66} \end{bmatrix} \quad (2.38)$$

where  $\mathbf{B}$  is the same symmetric matrix that appears in equation (2.4) and the superscript  $T$  denotes the transpose. The usual physical assumption that the strain-energy density is positive-definite, i.e.  $W(\tau) \geq 0$ ,  $\forall \tau \neq 0$  (with equality if and only if  $\tau \equiv 0$ ) is equivalent to the assumption that  $\mathbf{B}$  is a positive-definite matrix. Positive-definiteness of a symmetric matrix requires that the diagonal elements be positive

and that the determinants of the leading principal submatrices be positive as well.

Specifically, this requires

$$\beta_{11}, \beta_{22}, \beta_{66} > 0, \quad (2.39)$$

$$\beta_{11}\beta_{22} - \beta_{12}^2 > 0, \quad (2.40)$$

$$\beta_{11}\beta_{22}\beta_{66} + 2\beta_{16}\beta_{26}\beta_{12} - \beta_{11}\beta_{26}^2 - \beta_{22}\beta_{16}^2 - \beta_{66}\beta_{12}^2 > 0. \quad (2.41)$$

A further requirement is that the determinant of *any* submatrix, including principal minors, is positive. This yields, in addition,

$$\beta_{22}\beta_{66} - \beta_{26}^2 > 0, \quad (2.42)$$

$$\beta_{11}\beta_{66} - \beta_{16}^2 > 0. \quad (2.43)$$

For materials transversely isotropic about the  $x_1$  axis (or for specially orthotropic materials),  $\beta_{16} = \beta_{26} \equiv 0$ , and conditions (2.39) - (2.43) reduce to

$$\beta_{11}, \beta_{22}, \beta_{66} > 0, \quad (2.44)$$

$$\beta_{11}\beta_{22} - \beta_{12}^2 > 0, \quad (2.45)$$

It will now be shown that positive-definiteness of the strain-energy density  $W$  implies ellipticity of the governing equation (2.13). (Note that (2.13) is the original version of the governing equation rather than the nondimensionalized version (2.21). When working with the strain-energy it is more convenient to use the original  $x_1 - x_2$  domain since the strain-energy is not easily expressed in terms of the dimensionless parameters  $\epsilon_1, \epsilon_2, \epsilon_3$  in the  $\xi - \eta$  domain; see equation (2.59) below.) The governing partial differential equation

$$\begin{aligned} \beta_{22}\phi_{,1111} - 2\beta_{26}\phi_{,1112} + (2\beta_{12} + \beta_{66})\phi_{,1122} \\ - 2\beta_{16}\phi_{,1222} + \beta_{11}\phi_{,2222} = 0 \end{aligned} \quad (2.46)$$

is elliptic provided that the associated characteristic equation has *no real roots*, where the characteristic equation, denoted by  $P(\mu) = 0$ , is

$$P(\mu) = \beta_{11}\mu^4 + 2\beta_{16}\mu^3 + (2\beta_{12} + \beta_{66})\mu^2 + 2\beta_{26}\mu + \beta_{22} = 0. \quad (2.47)$$

As noted in Lekhnitskii [16] (see also [19]), choosing  $\mathbf{s}_\mu = [\mu^2, 1, \mu]^T$  and using the positive-definite assumptions on  $\mathbf{B}$  yields

$$\mathbf{s}_\mu^T \mathbf{B} \mathbf{s}_\mu = P(\mu) > 0 \quad \forall \mu \text{ real}. \quad (2.48)$$

Thus  $P(\mu)$  can have *no real roots* and (2.46), i.e. (2.13), is elliptic. The estimates of concern in this dissertation are relevant to elliptic partial differential equations.

The positive definite conditions (2.39) - (2.43) will be used in later sections to simplify expressions. Again it is noted that these conditions are in terms of  $\beta_{pq}$  rather than  $\epsilon_1$ ,  $\epsilon_2$  and  $\epsilon_3$ . Ideally, one would like to obtain these conditions in terms of the dimensionless variables, but this is not easily done as the strain-energy density  $W$  contains the constants  $\beta_{12}$  and  $\beta_{66}$  in separate terms rather than combined as they appear in  $\epsilon_1$  and the governing equation.

## 2.5 Energies

In this section, the ideas behind the energy methods used in later chapters will be developed. First, the methods themselves are outlined and then several specific energy functionals are derived.

### 2.5.1 Energy Methods

The stress decay estimates presented in the following chapters make use of energy arguments that produce bounds on energy functionals and thereby lead to decay rate estimates for the stresses in the material. To motivate the choice of energy functionals used in this dissertation, consider first an isotropic strip in a state of plane stress or plane strain. On using (2.9), (2.10) and (2.20), we find that

$$\epsilon_1 = \frac{1}{2}, \quad \frac{1}{\epsilon_2} = \frac{1}{\epsilon_3} \equiv 0, \quad (2.49)$$

and so (2.21) reduces to the biharmonic equation,

$$\phi_{,\xi\xi\xi\xi} + 2\phi_{,\xi\xi\eta\eta} + \phi_{,\eta\eta\eta\eta} = 0. \quad (2.50)$$

A natural energy functional associated with the biharmonic equation is the quadratic functional

$$E_1(z) = \int_{R_z} \phi_{,\alpha\beta} \phi_{,\alpha\beta} dA, \quad (2.51)$$

where the region  $R_z$  is the shaded region illustrated in Figure 2.3. In (2.51), the indices  $\alpha$  and  $\beta$  denote either  $\xi$  or  $\eta$  and the repeated index denotes summation over  $\xi$  and  $\eta$ .

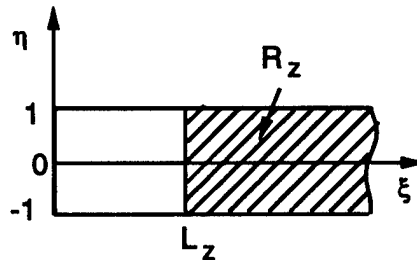


Figure 2.3: Region  $R_z$

This energy functional is related to the total strain-energy of the material stored

to the right of  $\xi = z$  (see [11]) and is referred to as a “first-order energy”, (see [15]).

Another energy functional associated with the biharmonic equation and referred to as a “second-order energy” has also been introduced (see [15]) as

$$E_2(z) = \int_{R_z} \phi_{,\xi\alpha\beta} \phi_{,\xi\alpha\beta} dA. \quad (2.52)$$

This energy can be viewed as the first-order energy defined on  $\phi_{,\xi}$ . The basic idea behind the energy methods used in later chapters of this dissertation is to consider a function  $F(z)$  that is a combination of these energy functionals. The goal is then to find the largest positive value of the constant  $k$  such that

$$F'(z) + 2kF(z) \leq 0, \quad (2.53)$$

where the prime denotes differentiation with respect to  $z$ . This may be accomplished through the use of the governing equation, conservation laws and various other inequalities. Equation (2.53) implies the first-order differential inequality

$$F'(z) \leq -2kF(z), \quad (2.54)$$

which leads to the exponential decay estimate

$$F(z) \leq F(0)e^{-2kz}, \quad z \geq 0. \quad (2.55)$$

It can further be shown, depending on the function  $F(z)$ , that the energies themselves have the same exponential behavior, i.e.

$$E_\alpha(z) \leq K_\alpha e^{-2kz}, \quad z \geq 0, \quad (2.56)$$

where  $K_\alpha$  ( $\alpha = 1, 2$ ) are constants. Since the energies are quadratic in the derivatives of  $\phi$  and the stresses  $\tau$  are defined as second derivatives of  $\phi$ , one can obtain bounds

on the stresses  $\tau$  such that the exponential decay from the end  $z = 0$  is of the form

$$\tau \sim Ke^{-kz}. \quad (2.57)$$

The value of this estimated decay rate  $k$  gives a *lower bound* for the decay rate of the stresses in the material occupying the domain in Figure 2.2.

## 2.5.2 Derivation of Energy Functionals

In the previous section, the first-order and second-order energies, (2.51) and (2.52), were described for an isotropic material. Their analogs for the anisotropic strip as well as additional energy functionals will now be derived.

There are two types of energy functionals that are used in this dissertation. The first type involves the *real physical* strain-energy of the material. The second type involves functionals that are not directly related to the physical strain-energy but are similar in structure. These "mathematical energies" are essentially norms for the problem. For the anisotropic strip, the strain-energy density  $W$  was expressed in terms of the stresses  $\tau$  in equation (2.37) of section 2.4. The total strain energy  $E = \int_{\mathfrak{R}} W dA$  is written in terms of the Airy stress function (2.11) as

$$\begin{aligned} 2E &= \int_{\mathfrak{R}} 2W dA \\ &= \int_{\mathfrak{R}} [\beta_{11}\phi_{,22}^2 + \beta_{22}\phi_{,11}^2 + \beta_{66}\phi_{,12}^2 + 2\beta_{12}\phi_{,11}\phi_{,22} \\ &\quad - 2\beta_{16}\phi_{,22}\phi_{,12} - 2\beta_{26}\phi_{,11}\phi_{,12}] dA. \end{aligned} \quad (2.58)$$

This energy  $E$  is the *total* physical energy of the semi-infinite strip in Figure 2.1, while  $E(z)$  is the stored physical energy in the strip region to the right of  $x_2 = z$ . Using the same nondimensionalization scheme presented in section 2.2, and letting

$E_p(z)$  now represent the nondimensional scaled *physical* energy, one obtains

$$E_p(z) = \int_{R_z} [\phi_{,\xi\xi}^2 + \phi_{,\eta\eta}^2 + \frac{2\beta_{12}}{\sqrt{\beta_{11}\beta_{22}}} \phi_{,\xi\xi} \phi_{,\eta\eta} + \frac{\beta_{66}}{\sqrt{\beta_{11}\beta_{22}}} \phi_{,\xi\eta}^2 - \frac{2}{\epsilon_2} \phi_{,\xi\eta} \phi_{,\xi\xi} - \frac{2}{\epsilon_3} \phi_{,\xi\eta} \phi_{,\eta\eta}] d\xi d\eta, \quad (2.59)$$

where  $R_z$  is the shaded region shown in Figure 2.3. The term  $\phi_{,\xi\xi} \phi_{,\eta\eta}$  in the integral (2.59) may be integrated by parts and simplified using the boundary conditions to yield

$$\int_{R_z} \phi_{,\xi\xi} \phi_{,\eta\eta} dA = \int_{R_z} \phi_{,\xi\eta}^2 dA - \int_{-1}^1 \phi_{,\xi}(z, \eta) \phi_{,\eta\eta}(z, \eta) d\eta \quad (2.60)$$

where the last term in (2.60) is a line integral contribution. Thus, one obtains

$$E_p(z) = \int_{R_z} [\phi_{,\xi\xi}^2 + \phi_{,\eta\eta}^2 + \frac{1}{\epsilon_1} \phi_{,\xi\eta}^2 - \frac{2}{\epsilon_2} \phi_{,\xi\eta} \phi_{,\xi\xi} - \frac{2}{\epsilon_3} \phi_{,\xi\eta} \phi_{,\eta\eta}] d\xi d\eta - \frac{2\beta_{12}}{\sqrt{\beta_{11}\beta_{22}}} \int_{-1}^1 \phi_{,\xi} \phi_{,\eta\eta} d\eta. \quad (2.61)$$

Either of the forms (2.59) or (2.61) may be used to express  $E_p(z)$ . In (2.61), we see the explicit dependence on the parameter  $\epsilon_1$ , while in (2.59) this parameter is not explicitly present. As was mentioned previously, this physical energy cannot be easily expressed solely in terms of the parameters  $\epsilon_1, \epsilon_2$  and  $\epsilon_3$ . A similar observation was made in the context of buckling of anisotropic plates [20]. This motivates the use of mathematical energy functionals that *can* be expressed solely in terms of the nondimensional parameters.

Next, several mathematical energies that are analogs to (2.51), (2.52) will be developed. The basic method in developing these functionals is to multiply the governing differential equation by the Airy stress function itself or an axial derivative and then integrate over the region  $R_z$  in Figure 2.3. This method is very similar to the



method used to derive the conservation laws in section 2.3, except that the integration now is over a two-dimensional region rather than a one-dimensional region (line integral). Upon use of the divergence theorem and simplification due to the homogeneous boundary conditions, the energy functional can also be conveniently expressed as a line integral. The following analysis is carried out in the nondimensional domain.

To obtain the first-order energy functional for the anisotropic strip, the nondimensionalized governing equation (2.21) is multiplied by  $\phi$  and integrated over  $R_z$ ,

$$\int_{R_z} \phi \left[ \phi_{,\xi\xi\xi\xi} - \frac{2}{\epsilon_2} \phi_{,\xi\xi\xi\eta} + \frac{1}{\epsilon_1} \phi_{,\xi\xi\eta\eta} - \frac{2}{\epsilon_3} \phi_{,\xi\eta\eta\eta} + \phi_{,\eta\eta\eta\eta} \right] dA = 0. \quad (2.62)$$

Integration by parts and use of the divergence theorem once yields

$$\begin{aligned} & \int_{R_z} \left[ -\phi_{,\xi} \phi_{,\xi\xi\xi} - \phi_{,\eta} \phi_{,\eta\eta\eta} + \frac{2}{\epsilon_2} \phi_{,\xi} \phi_{,\xi\xi\eta} + \frac{2}{\epsilon_3} \phi_{,\eta} \phi_{,\xi\eta\eta} - \frac{1}{\epsilon_1} \phi_{,\eta} \phi_{,\xi\xi\eta} \right] d\xi d\eta \\ &= - \int_{\partial R_z} \left[ \left( \phi \phi_{,\xi\xi\xi} - \frac{2}{\epsilon_2} \phi \phi_{,\xi\xi\eta} \right) n_\xi + \left( \phi \phi_{,\eta\eta\eta} - \frac{2}{\epsilon_3} \phi \phi_{,\xi\eta\eta} + \frac{1}{\epsilon_3} \phi \phi_{,\xi\xi\eta} \right) n_\eta \right] ds \end{aligned} \quad (2.63)$$

where  $\partial R_z$  denotes the boundary of  $R_z$ , and  $n_\xi$ ,  $n_\eta$  are components of the outward unit normal to the boundary in the  $\xi$ ,  $\eta$  directions. Repeating this process results in

$$\begin{aligned} & \int_{R_z} \left[ \phi_{,\xi\xi}^2 - \frac{2}{\epsilon_2} \phi_{,\xi\xi} \phi_{,\xi\eta} + \frac{1}{\epsilon_1} \phi_{,\xi\eta}^2 - \frac{2}{\epsilon_3} \phi_{,\eta\eta} \phi_{,\xi\eta} + \phi_{,\eta\eta}^2 \right] d\xi d\eta \\ &= - \int_{\partial R_z} \left[ \left( \phi \phi_{,\xi\xi\xi} - \frac{2}{\epsilon_2} \phi \phi_{,\xi\xi\eta} - \phi_{,\xi} \phi_{,\xi\xi} + \frac{2}{\epsilon_2} \phi_{,\xi} \phi_{,\xi\eta} - \frac{1}{\epsilon_1} \phi_{,\eta} \phi_{,\xi\xi\eta} \right) n_\xi \right. \\ & \quad \left. + \left( \phi \phi_{,\eta\eta\eta} - \frac{2}{\epsilon_3} \phi \phi_{,\xi\eta\eta} + \frac{1}{\epsilon_3} \phi \phi_{,\xi\xi\eta} - \phi_{,\eta} \phi_{,\eta\eta} + \frac{2}{\epsilon_3} \phi_{,\eta} \phi_{,\xi\eta} \right) n_\eta \right] ds. \end{aligned} \quad (2.64)$$

The quadratic functional on the left-hand side is the anisotropic analog of (2.51). It

will be called a "first-order" anisotropic energy and denoted by  $E_1(z)$ , i.e.

$$E_1(z) = \int_{R_z} [\phi_{,\xi\xi}^2 - \frac{2}{\epsilon_2} \phi_{,\xi\xi} \phi_{,\xi\eta} + \frac{1}{\epsilon_1} \phi_{,\xi\eta}^2 - \frac{2}{\epsilon_3} \phi_{,\eta\eta} \phi_{,\xi\eta} + \phi_{,\eta\eta}^2] d\xi d\eta. \quad (2.65)$$

When  $\epsilon_1 = \frac{1}{2}$ ,  $\epsilon_2^{-1} = 0$ ,  $\epsilon_3^{-1} = 0$ , (2.65) reduces to (2.51). The boundary integral on the right-hand side of (2.64) may be evaluated and simplified using the boundary conditions on the lateral sides of the strip and at the far end, so that the energy functional can be expressed in terms of a line integral as

$$E_1(z) = - \int_{L_z} [-\phi \phi_{,\xi\xi\xi} + \phi_{,\xi} \phi_{,\xi\xi} + \frac{1}{\epsilon_1} \phi_{,\eta} \phi_{,\xi\eta} + \frac{2}{\epsilon_2} \phi \phi_{,\xi\xi\eta} - \frac{2}{\epsilon_2} \phi_{,\xi} \phi_{,\xi\eta}] d\eta, \quad (2.66)$$

where  $L_z$  denotes the line segment  $-1 < \eta < 1$ ,  $\xi = z$  (see Figure 2.2). Noting that

$$\int_{L_z} \phi \phi_{,\xi\xi\eta} d\eta = - \int_{L_z} \phi_{,\eta} \phi_{,\xi\xi} d\eta \quad (2.67)$$

and

$$\int_{L_z} \phi_{,\xi} \phi_{,\xi\eta} d\eta = \int_{L_z} [\frac{\phi_{,\xi}^2}{2}]_{,\eta} d\eta = 0, \quad (2.68)$$

we get

$$E_1(z) = - \int_{L_z} [-\phi \phi_{,\xi\xi\xi} + \phi_{,\xi} \phi_{,\xi\xi} + \frac{1}{\epsilon_1} \phi_{,\eta} \phi_{,\xi\eta} - \frac{2}{\epsilon_2} \phi_{,\eta} \phi_{,\xi\xi}] d\eta. \quad (2.69)$$

It is worth noting that the parameter  $\epsilon_3$  does not appear explicitly in (2.69). The energy  $E_1(z)$  given by (2.65) or (2.69) is one of two mathematical energies that will be used in later chapters.

To obtain a second anisotropic energy functional, the governing equation is mul-

multiplied by  $\phi_{,\xi\xi}$  and integrated over the region  $R_z$ ,

$$\int_{R_z} \phi_{,\xi\xi} [\phi_{,\xi\xi\xi\xi} - \frac{2}{\epsilon_2} \phi_{,\xi\xi\xi\xi} + \frac{1}{\epsilon_1} \phi_{,\xi\xi\xi\xi} - \frac{2}{\epsilon_3} \phi_{,\xi\xi\xi\xi} + \phi_{,\eta\xi\xi\xi}] dA = 0. \quad (2.70)$$

Following the same procedure as before, using integration by parts and the divergence theorem repeatedly, one obtains

$$\begin{aligned} & \int_{R_z} [\phi_{,\xi\xi\xi\xi}^2 - \frac{2}{\epsilon_2} \phi_{,\xi\xi\xi\xi} \phi_{,\xi\xi\xi} + \frac{1}{\epsilon_1} \phi_{,\xi\xi\xi\xi}^2 - \frac{2}{\epsilon_3} \phi_{,\xi\xi\xi\xi} \phi_{,\xi\xi\xi} + \phi_{,\xi\xi\xi\xi}^2] d\xi d\eta \\ &= \int_{\partial R_z} [(\phi_{,\xi\xi\xi\xi} \phi_{,\xi\xi\xi} - \phi_{,\xi\xi\xi\xi} \phi_{,\eta\xi\xi\xi}) n_\xi \\ &+ (\phi_{,\xi\xi\xi\xi} \phi_{,\eta\xi\xi\xi} + \phi_{,\xi\xi\xi\xi} \phi_{,\xi\xi\xi} - \frac{2}{\epsilon_2} \phi_{,\xi\xi\xi\xi} \phi_{,\xi\xi\xi} - \frac{2}{\epsilon_3} \phi_{,\xi\xi\xi\xi} \phi_{,\xi\xi\xi} + \frac{1}{\epsilon_1} \phi_{,\xi\xi\xi\xi} \phi_{,\xi\xi\xi}) n_\eta] ds. \end{aligned} \quad (2.71)$$

The quadratic functional on the left-hand side of (2.71) is the anisotropic analog of (2.52). It will be called a "second-order" anisotropic energy and denoted by  $E_2(z)$ , i.e.

$$E_2(z) = \int_{R_z} [\phi_{,\xi\xi\xi\xi}^2 - \frac{2}{\epsilon_2} \phi_{,\xi\xi\xi\xi} \phi_{,\xi\xi\xi} + \frac{1}{\epsilon_1} \phi_{,\xi\xi\xi\xi}^2 - \frac{2}{\epsilon_3} \phi_{,\xi\xi\xi\xi} \phi_{,\xi\xi\xi} + \phi_{,\xi\xi\xi\xi}^2] d\xi d\eta. \quad (2.72)$$

The boundary integral on the right-hand side of (2.71) may be evaluated and simplified using the boundary conditions on the lateral sides of the strip and at the far end, so that the energy functional can be expressed in terms of a line integral as

$$E_2(z) = - \int_{L_z} [\phi_{,\xi\xi\xi\xi} \phi_{,\xi\xi\xi} - \phi_{,\xi\xi\xi\xi} \phi_{,\eta\xi\xi\xi}] d\eta. \quad (2.73)$$

We note that none of the nondimensional material parameters  $\epsilon_i$  ( $i = 1, 2, 3$ ) appear explicitly in (2.73). The energy  $E_2(z)$  given by (2.72) or (2.73) is the second mathematical energy that will be used in this dissertation.

It should be noted that there are many additional energy-like functionals that can be obtained following the procedure used above. Depending on how the integration is performed, terms that are different than those presented here may arise. However, the energy functionals (2.65), (2.72) have been found to be the most useful in the present study. It is also noted that some of these alternate energy forms may *not* be positive-definite and hence would not be suitable norms.

### 2.5.3 Positive-Definiteness of the Energy Functionals

It was stated previously that the real physical strain-energy of the material must be positive-definite and the conditions that this imposed on the elastic constants  $\beta_{pq}$  were derived. These conditions result from physical properties and must hold for all materials regardless of which energy functionals, real or mathematical, are used in the estimation techniques. If other energy functionals different from the physical strain energy are introduced into the problem, then this may impose additional constraints on the elastic parameters. Since the mathematical energies presented in the previous section are to be used as norms, by definition they must be positive. This requires that the integrands be positive-definite quadratic forms in their arguments. This in turn imposes restrictions on  $\epsilon_1$ ,  $\epsilon_2$  and  $\epsilon_3$ .

Returning to (2.65), one can rewrite the integrand of  $E_1(z)$  as a quadratic form,  $\phi_1^T \mathbf{B}_1 \phi_1$ , where

$$\phi_1 = \begin{bmatrix} \phi_{,\xi\xi} \\ \phi_{,\eta\eta} \\ \sqrt{2}\phi_{,\xi\eta} \end{bmatrix} \quad \text{and} \quad \mathbf{B}_1 = \begin{bmatrix} 1 & 0 & -\frac{1}{\sqrt{2}\epsilon_2} \\ 0 & 1 & -\frac{1}{\sqrt{2}\epsilon_3} \\ -\frac{1}{\sqrt{2}\epsilon_2} & -\frac{1}{\sqrt{2}\epsilon_3} & \frac{1}{2\epsilon_1} \end{bmatrix}. \quad (2.74)$$

Positive-definiteness of  $E_1(z)$  imposes the following restrictions

$$\frac{1}{\epsilon_1} > 0, \quad (2.75)$$

$$\frac{1}{\epsilon_1} - \frac{1}{\epsilon_2^2} - \frac{1}{\epsilon_3^2} > 0. \quad (2.76)$$

(We observe that (2.75) is implied by (2.76).) Returning to (2.72), the integrand of  $E_2(z)$  can be expressed as a quadratic form,  $\phi_2^T \mathbf{B}_2 \phi_2$ , where

$$\phi_2 = \begin{bmatrix} \phi_{,\xi\xi\xi} \\ \phi_{,\xi\eta\eta} \\ \sqrt{2}\phi_{,\xi\xi\eta} \end{bmatrix} \quad \text{and} \quad \mathbf{B}_2 = \begin{bmatrix} 1 & 0 & -\frac{1}{\sqrt{2}\epsilon_2} \\ 0 & 1 & -\frac{1}{\sqrt{2}\epsilon_3} \\ -\frac{1}{\sqrt{2}\epsilon_2} & -\frac{1}{\sqrt{2}\epsilon_3} & \frac{1}{2\epsilon_1} \end{bmatrix}. \quad (2.77)$$

Positive-definiteness of  $E_2(z)$  again results in the requirement (2.76) since  $\mathbf{B}_2 \equiv \mathbf{B}_1$ .

The restrictions (2.75) and (2.76), which result from using the mathematical energies  $E_1(z)$  and  $E_2(z)$ , will be assumed henceforth *and are in addition* to the constraints (2.39) - (2.43) imposed by positive-definiteness of the physical strain energy. All of these constraints will be useful in simplifying expressions appearing in later chapters.

## Chapter 3

# THE ORTHOTROPIC CASE

In the previous chapter, the elastic strip problem was formulated for anisotropic materials. However, the problem is simplified when one considers specially orthotropic and transversely isotropic materials. These form a special class of materials for which some of the elastic constants vanish. This special case will be examined first and will be referred to as the *orthotropic case* (although it includes both specially orthotropic and transversely isotropic materials). Several estimation techniques, both analytical and numerical, will be presented. These estimates will be compared with exact numerical solutions and the results discussed.

### 3.1 Formulation

The governing partial differential equation, conservation laws, and energy functionals of the previous chapter have been derived for an anisotropic strip. Consider now a subclass of materials for which the anisotropic material constants  $\beta_{16}$  and  $\beta_{26}$  vanish,

i.e.

$$\beta_{16} = \beta_{26} \equiv 0. \quad (3.1)$$

(As pointed out in Chapter 2, this simplification includes both specially orthotropic and transversely isotropic materials.) In view of the definition (2.20), Equation (3.1) implies that

$$\frac{1}{\epsilon_2} = \frac{1}{\epsilon_3} \equiv 0. \quad (3.2)$$

Returning to the governing equation (2.21) and using (3.2), one obtains the reduced equation

$$\phi_{,\xi\xi\xi\xi} + \frac{1}{\epsilon_1} \phi_{,\xi\xi\eta\eta} + \phi_{,\eta\eta\eta\eta} = 0, \quad (3.3)$$

which contains only one elastic parameter  $\epsilon_1$  instead of the three parameters  $\epsilon_1, \epsilon_2, \epsilon_3$  present in the anisotropic case. (As we remarked in Chapter 2, when  $\epsilon_1 = \frac{1}{2}$  in (3.3), the familiar biharmonic equation (2.50) governing isotropic materials results.)

The corresponding reduced forms of the conservation laws may be obtained from (2.34) and (2.35) upon using (3.2). This results in the following orthotropic conservation properties,

$$\int_{L_x} [2\phi_{,\xi}\phi_{,\xi\xi\xi} + \phi_{,\eta\eta}^2] d\eta = \int_{L_x} [\phi_{,\xi\xi}^2 + \frac{1}{\epsilon_1}\phi_{,\xi\eta}^2] d\eta \quad (3.4)$$

and

$$\int_{L_x} [2\phi_{,\xi\xi\eta}\phi_{,\eta\eta\eta} + \phi_{,\xi\eta\eta}^2 + \frac{1}{\epsilon_1}\phi_{,\xi\xi\eta}^2] d\eta \leq \int_{L_x} [\phi_{,\xi\xi\xi}^2] d\eta. \quad (3.5)$$

The strain-energy density  $W$  must be positive-definite and the restrictions this im-

poses on the elastic constants  $\beta_{pq}$  for the orthotropic case were presented in section 2.4, see equations (2.44) and (2.45).

The orthotropic analogs of the energy functionals presented in section 2.5 may also be obtained by using (3.2). The nondimensionalized physical strain-energy  $E_p(z)$  given by (2.61) becomes

$$E_p^{orth}(z) = \int_{R_s} [\phi_{,\xi\xi}^2 + \frac{1}{\epsilon_1} \phi_{,\xi\eta}^2 + \phi_{,\eta\eta}^2] d\xi d\eta - \frac{2\beta_{12}}{\sqrt{\beta_{11}\beta_{22}}} \int_{-1}^1 \phi_{,\xi} \phi_{,\eta\eta} d\eta, \quad (3.6)$$

where the superscript *orth* refers to orthotropic materials. Again, it is noted that this physical energy cannot be written solely in terms of the dimensionless elastic parameters, owing to the line integral contribution. The mathematical energies  $E_1(z)$  and  $E_2(z)$ , given by (2.65) and (2.72), become

$$E_1^{orth}(z) = \int_{R_s} [\phi_{,\xi\xi}^2 + \frac{1}{\epsilon_1} \phi_{,\xi\eta}^2 + \phi_{,\eta\eta}^2] dA, \quad (3.7)$$

$$E_2^{orth}(z) = \int_{R_s} [\phi_{,\xi\xi\xi}^2 + \frac{1}{\epsilon_1} \phi_{,\xi\xi\eta}^2 + \phi_{,\xi\eta\eta}^2] dA, \quad (3.8)$$

respectively. Using (2.69) and (2.73), we can also express these energies as line integrals where

$$E_1^{orth}(z) = - \int_{L_s} [-\phi \phi_{,\xi\xi\xi} + \phi_{,\xi} \phi_{,\xi\xi} + \frac{1}{\epsilon_1} \phi_{,\eta} \phi_{,\xi\eta}] d\eta, \quad (3.9)$$

$$E_2^{orth}(z) = - \int_{L_s} [\phi_{,\xi\xi} \phi_{,\xi\xi\xi} - \phi_{,\xi\eta} \phi_{,\eta\eta\eta}] d\eta. \quad (3.10)$$

The assumption (2.75), i.e.  $\epsilon_1 > 0$ , ensures that the energies (3.7), (3.8) are positive-



definite. Several energy estimates using these energy functionals will be presented for this *orthotropic* elastic strip problem. We note that these orthotropic versions of the governing equation, conservation laws and energy functionals *all involve only one elastic parameter*  $\epsilon_1$ .

## 3.2 Preliminary Inequalities

Before proceeding further, it is convenient to record several inequalities which play an important role in the arguments to follow. The first group consists of the well known Wirtinger-type inequalities, which have been widely used in previous work on Saint-Venant's Principle (see e.g. [1], [2], [3]). These inequalities hold for sufficiently smooth functions  $w(\eta)$  defined on the domain  $(-1, 1)$  and are the following:

(i) If  $w(\eta) \in C^1(-1, 1)$  and  $w(-1) = 0$ ,  $w(1) = 0$ , then

$$\int_{-1}^1 w_{,\eta}^2 d\eta \geq \frac{\pi^2}{h^2} \int_{-1}^1 w^2 d\eta. \quad (3.11)$$

(ii) If  $w(\eta) \in C^2(-1, 1)$  and  $w(-1) = w_{,\eta}(-1) = 0$ ,  $w(1) = w_{,\eta}(1) = 0$ , then

$$\int_{-1}^1 w_{,\eta\eta}^2 d\eta \geq \frac{4\pi^2}{h^2} \int_{-1}^1 w_{,\eta}^2 d\eta. \quad (3.12)$$

(iii) If  $w(\eta) \in C^2(-1, 1)$  and  $w(-1) = w_{,\eta}(-1) = 0$ ,  $w(1) = w_{,\eta}(1) = 0$ , then

$$\int_{-1}^1 w_{,\eta\eta}^2 d\eta \geq \frac{\mu_0^4}{h^4} \int_{-1}^1 w^2 d\eta, \quad (3.13)$$

where  $\mu_0^4 = 4.73$ , a value slightly larger than  $\frac{3\pi}{2}$ . For convenience this latter quantity will be substituted in (iii) so that one obtains

$$\int_{-1}^1 w_{,\eta\eta}^2 d\eta > \left(\frac{3}{2}\right)^4 \frac{\pi^4}{h^4} \int_{-1}^1 w^2 d\eta. \quad (3.14)$$

In all of these inequalities,  $h$  is the length of the interval of integration, i.e.  $h = 2$ . When applied to the semi-infinite strip problem,  $h$  represents the nondimensionalized height of the strip. These inequalities may be derived from variational formulations and the optimal constants that appear on the right-hand sides of (3.11) - (3.13) correspond to the smallest eigenvalues in such formulations. Proofs of these inequalities may be found in [21], [22] and [23].

Another inequality that will prove useful in the subsequent analysis is the *arithmetic-geometric mean inequality* which has the following two forms,

$$-2ab \leq \alpha a^2 + \frac{b^2}{\alpha}, \quad (\alpha > 0) \quad (3.15)$$

or

$$2ab \leq \alpha a^2 + \frac{b^2}{\alpha}, \quad (\alpha > 0). \quad (3.16)$$

Both of these forms may be obtained by observing that

$$\left(\sqrt{\alpha}a \pm \frac{b}{\sqrt{\alpha}}\right)^2 \geq 0. \quad (3.17)$$

### 3.3 Analytic Estimate

The first energy estimate that will be developed is an analytic estimate which yields an explicit formula for the estimated decay rate in terms of the elastic parameter  $\epsilon_1$ .

The estimate will be derived first for the general case of  $\epsilon_1 > 0$  and then specialized to an asymptotic result for small  $\epsilon_1$ .

### 3.3.1 General Estimate

For this analytic estimate only one of the energy functionals,  $E_1^{orth}(z)$ , defined in (3.7) is used. Following an energy method first developed in [11] for the isotropic case, let the function  $F(z)$  be defined by

$$F(z) = E_1(z) + 2k \int_z^\infty E_1(s) ds, \quad (3.18)$$

where  $k > 0$  is an unspecified constant. Here, the superscript *orth* has been dropped for convenience but it will be assumed for the remainder of this chapter that the functionals refer to orthotropic versions. We then have

$$\begin{aligned} F'(z) + 2kF(z) &= E_1'(z) - 2kE_1(z) + 2kE_1(z) + 4k^2 \int_z^\infty E_1(s) ds \\ &= E_1'(z) + 4k^2 \int_z^\infty E_1(s) ds. \end{aligned} \quad (3.19)$$

In order to express the terms  $E_1'(z)$  and  $\int_z^\infty E_1(s) ds$  as line integrals, we first note a result derived in [11] that follows from the definition of derivative,

$$\frac{d}{dz} \int_{R_z} f dA = - \int_{L_z} f d\eta, \quad (3.20)$$

for functions  $f$  continuous on  $R_z$ . Using  $f = [\phi_{,\xi\xi}^2 + \frac{1}{\epsilon_1} \phi_{,\xi\eta}^2 + \phi_{,\eta\eta}^2]$  in (3.20) yields an expression for  $E_1'(z)$  as a line integral,

$$E_1'(z) = - \int_{L_z} [\phi_{,\xi\xi}^2 + \frac{1}{\epsilon_1} \phi_{,\xi\eta}^2 + \phi_{,\eta\eta}^2] d\eta. \quad (3.21)$$

Similarly, using  $f = [-\phi\phi_{,\xi\xi\xi} + \phi_{,\xi}\phi_{,\xi\xi} + \frac{1}{\epsilon_1}\phi_{,\eta}\phi_{,\xi\eta}]$  in (3.20) implies in addition, using (3.9), that

$$E_1(z) = \frac{d}{dz} \int_{R_z} [-\phi\phi_{,\xi\xi\xi} + \phi_{,\xi}\phi_{,\xi\xi} + \frac{1}{\epsilon_1}\phi_{,\eta}\phi_{,\xi\eta}] dA. \quad (3.22)$$

On integration, and using the divergence theorem and boundary conditions, one obtains an expression for  $\int_z^\infty E_1(s)ds$  as a line integral,

$$\begin{aligned} \int_z^\infty E_1(s)ds &= - \int_{R_z} [-\phi\phi_{,\xi\xi\xi} + \phi_{,\xi}\phi_{,\xi\xi} + \frac{1}{\epsilon_1}\phi_{,\eta}\phi_{,\xi\eta}] dA. \\ &= - \int_{L_z} [\phi\phi_{,\xi\xi} - \phi_{,\xi}^2 - \frac{1}{2\epsilon_1}\phi_{,\eta}^2] d\eta. \end{aligned} \quad (3.23)$$

Returning to (3.19), we then have

$$\begin{aligned} F'(z) + 2kF(z) &= - \int_{L_z} [\phi_{,\xi\xi}^2 + \frac{1}{\epsilon_1}\phi_{,\xi\eta}^2 + \phi_{,\eta\eta}^2 + 4k^2\phi\phi_{,\xi\xi} - 4k^2\phi_{,\xi}^2 - \frac{4k^2}{2\epsilon_1}\phi_{,\eta}^2] d\eta. \end{aligned} \quad (3.24)$$

Recall from section 2.5 that the objective is to find the largest positive value for  $k$  such that

$$F'(z) + 2kF(z) \leq 0. \quad (3.25)$$

Denoting the right-hand side of (3.24) by  $J(z)$  and completing squares, one obtains

$$\begin{aligned} J(z) &= - \int_{L_z} [(\phi_{,\xi\xi} + 2k^2\phi)^2 + \frac{1}{\epsilon_1}\phi_{,\xi\eta}^2 + \phi_{,\eta\eta}^2 \\ &\quad - 4k^2\phi_{,\xi}^2 - \frac{2k^2}{\epsilon_1}\phi_{,\eta}^2 - 4k^4\phi^2] d\eta \end{aligned} \quad (3.26)$$

which upon dropping the first squared term yields the inequality

$$J(z) \leq - \int_{L_z} [\frac{1}{\epsilon_1}\phi_{,\xi\eta}^2 + \phi_{,\eta\eta}^2 - 4k^4\phi^2 - 4k^2\phi_{,\xi}^2 - \frac{2k^2}{\epsilon_1}\phi_{,\eta}^2] d\eta. \quad (3.27)$$

This inequality will now be simplified using the Wirtinger inequalities of section 3.2.

Recalling the boundary conditions (2.23), an admissible choice for  $w$  in (3.11) is

$w = \phi_{,\xi}$ , which yields

$$\int_{L_x} \phi_{,\xi\eta}^2 d\eta \geq \frac{\pi^2}{h^2} \int_{L_x} \phi_{,\xi}^2 d\eta, \quad (3.28)$$

which may then be used in (3.27) to obtain

$$\begin{aligned} J(z) &\leq - \int_{L_x} \left[ \left( \frac{1}{\epsilon_1} \frac{\pi^2}{h^2} - 4k^2 \right) \phi_{,\xi}^2 + \phi_{,\eta\eta}^2 - \frac{2k^2}{\epsilon_1} \phi_{,\eta}^2 - 4k^4 \phi^2 \right] d\eta \\ &\leq - \int_{L_x} \left[ \phi_{,\eta\eta}^2 - \frac{2k^2}{\epsilon_1} \phi_{,\eta}^2 - 4k^4 \phi^2 \right] d\eta, \end{aligned} \quad (3.29)$$

provided

$$\left( \frac{1}{\epsilon_1} \frac{\pi^2}{h^2} - 4k^2 \right) \geq 0. \quad (3.30)$$

Now, choose  $w = \phi$  in (3.12) to yield

$$\int_{L_x} \phi_{,\eta\eta}^2 d\eta \geq \frac{4\pi^2}{h^2} \int_{L_x} \phi_{,\eta}^2 d\eta, \quad (3.31)$$

which may then be used in (3.29) to obtain

$$J(z) \leq - \int_{L_x} \left[ \left( \frac{4\pi^2}{h^2} - \frac{2k^2}{\epsilon_1} \right) \phi_{,\eta}^2 - 4k^4 \phi^2 \right] d\eta. \quad (3.32)$$

Finally, choose  $w = \phi$  in (3.11) to obtain

$$\int_{L_x} \phi_{,\eta}^2 d\eta \geq \frac{\pi^2}{h^2} \int_{L_x} \phi^2 d\eta \quad (3.33)$$

which when used in (3.32) leads to the result

$$J(z) \leq - \int_{L_x} \left[ 4 \left( \frac{\pi^2}{h^2} - \frac{k^2}{2\epsilon_1} \right) - 4k^4 \frac{h^2}{\pi^2} \right] \phi_{,\eta}^2 d\eta. \quad (3.34)$$

The problem is now to find those values of  $k$  for which  $J(z) \leq 0$  and condition (3.30) holds. Since the values of  $k$  so obtained will be lower bounds on the exact decay

rate for stresses, we seek the largest possible  $k$  in order to yield the best estimate.

This reduces to the following problem characterizing the appropriate choice of  $k$ :

*Choose the largest  $k$  such that*

$$\left( \frac{\pi^2}{h^2} - \frac{k^2}{2\epsilon_1} \right) \frac{\pi^2}{h^2} - k^4 \geq 0 \quad (3.35)$$

*subject to the constraint*

$$k \leq \frac{\pi}{2h\sqrt{\epsilon_1}}. \quad (3.36)$$

In these expressions,  $h = 2$  is the non-dimensional strip width. Rewriting (3.35)

as

$$k^4 + k^2 \frac{\pi^2}{2h^2\epsilon_1} - \frac{\pi^4}{h^4} \leq 0, \quad (3.37)$$

it is observed that the largest value of  $k$  for which this is satisfied occurs when equality holds in (3.37). Using the quadratic formula yields the roots of this equation as

$$k^2 = -\frac{\pi^2}{4\epsilon_1 h^2} \left( 1 - \sqrt{1 + 16\epsilon_1^2} \right) \quad (3.38)$$

so that

$$k = \frac{\pi}{2h\sqrt{\epsilon_1}} \left( \sqrt{1 + 16\epsilon_1^2} - 1 \right)^{\frac{1}{2}} \quad (3.39)$$

where signs have been chosen so that  $k$  and  $k^2$  are positive real quantities. With  $k$  given by (3.39), the condition (3.36) is satisfied if  $\epsilon_1 \leq \frac{\sqrt{3}}{4}$ . When  $\epsilon_1$  exceeds this value, we choose

$$k = \frac{\pi}{2h\sqrt{\epsilon_1}}, \quad \text{for } \epsilon_1 > \frac{\sqrt{3}}{4}. \quad (3.40)$$

It is easily verified that the choice of  $k$  given by (3.40) satisfies (3.35).

From (3.25), we obtain the decay estimate

$$F(z) \leq F(0)e^{-2kz}, \quad z \geq 0. \quad (3.41)$$

It will now be shown that the energy functional  $E_1(z)$  has this same exponential decay behavior. Following the arguments of [11], it follows from the definition (3.18) of  $F(z)$  that

$$E_1(z) \leq F(0)e^{-2kz}. \quad (3.42)$$

It remains to find an upper bound for  $F(0)$ . Substituting the definition of  $F(z)$  directly into the left-hand side of (3.41) leads to the inequality

$$-\frac{d}{dz} \left[ e^{-2kz} \int_z^\infty E_1(x) dx \right] \leq F(0)e^{-4kz}. \quad (3.43)$$

Integrating this inequality from  $z = 0$  to  $z = \infty$  results in

$$\int_0^\infty E_1(x) dx \leq \frac{F(0)}{4k} = \frac{1}{4k} \left[ E_1(0) + 2k \int_0^\infty E_1(x) dx \right]. \quad (3.44)$$

Solving for the integral of  $E_1$  gives

$$2k \int_0^\infty E_1(x) dx \leq E_1(0). \quad (3.45)$$

Combining (3.45) with (3.18) yields the following bound on  $F(0)$ ,

$$F(0) \leq 2E_1(0), \quad (3.46)$$

which when substituted back into (3.42) yields the desired result

$$E_1(z) \leq 2E_1(0)e^{-2kz}, \quad z \geq 0. \quad (3.47)$$

Notice that when  $z = 0$ , the inequality (3.47) is not sharp. It has been shown in [24] that the multiplicative factor of 2 on the right-hand side of (3.47) can be eliminated (see also the discussion on p. 228 of [1]), thus remedying this shortcoming.

It is reasonable to expect from the definition of  $E_1(z)$  as quadratic in the second derivatives of  $\phi$  and hence quadratic in the stresses  $\tau$ , that the stresses themselves have the exponential decay behavior

$$|\tau(\xi, \eta)| \leq K e^{-k\xi} \quad \text{for fixed } \eta, \quad (3.48)$$

where  $\tau$  denotes a typical stress component. The derivation of such *pointwise estimates* is technically elaborate (see [1] for a discussion) and we shall not pursue this here. The *estimated decay rate* is given by (3.39), (3.40) as

$$\begin{aligned} k &= \frac{\pi}{2h\sqrt{\epsilon_1}} \left( \sqrt{1 + 16\epsilon_1^2} - 1 \right)^{\frac{1}{2}} & \text{for } \epsilon_1 \leq \frac{\sqrt{3}}{4}, \\ k &= \frac{\pi}{2h\sqrt{\epsilon_1}} & \text{for } \epsilon_1 > \frac{\sqrt{3}}{4}. \end{aligned} \quad (3.49)$$

This value of  $k$  gives a lower bound on the nondimensional decay rate for stresses in the material. Transforming this result back into the original variables  $x_1$  and  $x_2$ , using the change of variable presented in section 2.2, implies that the exponential decay factor in the stresses is given by

$$e^{-k\xi} = e^{-k\left(\frac{\beta_{11}}{\beta_{22}}\right)^{\frac{1}{4}} \frac{x_1}{H}} = e^{-k^* \frac{x_1}{H}} \quad (3.50)$$

where

$$\begin{aligned} k^* &= \frac{\pi}{4\sqrt{\epsilon_1}} \left( \sqrt{1 + 16\epsilon_1^2} - 1 \right)^{\frac{1}{2}} \left( \frac{\beta_{11}}{\beta_{22}} \right)^{\frac{1}{4}} & \text{for } \epsilon_1 \leq \frac{\sqrt{3}}{4}, \\ k^* &= \frac{\pi}{4\sqrt{\epsilon_1}} \left( \frac{\beta_{11}}{\beta_{22}} \right)^{\frac{1}{4}} & \text{for } \epsilon_1 > \frac{\sqrt{3}}{4} \end{aligned} \quad (3.51)$$

To obtain these expressions, we have set  $h = 2$ . We note that  $\frac{\sqrt{3}}{4} \approx 0.433$ . The fraction  $\frac{k^*}{H}$  is the estimated decay rate in the original domain where  $H$  denotes the



half-width of the original strip. The dependence of the decay rate on the strip width may be more conveniently expressed by writing the decay rate as  $\frac{2k^*}{2H}$  where  $2H$  is now the total width of the strip. The analytic estimate (3.51) gives a formula for the decay rate in terms of the elastic parameter  $\epsilon_1$  and the quantity  $\left(\frac{\beta_{11}}{\beta_{22}}\right)^{\frac{1}{4}}$  which will be referred to as the "beta ratio".

For isotropic materials where  $\epsilon_1 = \frac{1}{2}$ ,  $\left(\frac{\beta_{11}}{\beta_{22}}\right)^{\frac{1}{4}} = 1$ , we obtain from (3.51) that

$$\frac{k^*}{H} = \frac{\pi}{2\sqrt{2}H} \approx \frac{2.2}{2H}. \quad (3.52)$$

Note that this is precisely the same estimate that was obtained by Flavin [12] for the biharmonic equation, using a modification of the earlier arguments of Knowles [11]. This is also the result obtained by Oleinik and Yosifian [13], [14] using alternate methods. The decay rate estimate given by (3.52) improves upon the estimate in [11], which gives a decay rate of  $\left(\frac{\sqrt{2}-1}{2}\right)^{\frac{1}{2}} \frac{\pi}{2H} \approx \frac{1.4}{2H}$ .

### 3.3.2 Asymptotic Estimate

The previous estimate was derived for  $\epsilon_1 > 0$ . If  $\epsilon_1$  is small enough, a Taylor expansion may be introduced yielding an asymptotic version of the analytic estimate.

Recalling the Taylor expansion for  $\sqrt{1+x}$  as

$$\sqrt{1+x} = 1 + \frac{x}{2} - \frac{x^2}{8} + \frac{3}{48}x^3 + \dots \quad (|x| < 1) \quad (3.53)$$

and substituting this expansion into the first equation of (3.51), with  $x = 16\epsilon_1^2$ , yields

$$k^* = \frac{\pi}{4\sqrt{\epsilon_1}} (8\epsilon_1^2 - 32\epsilon_1^4 + \dots)^{\frac{1}{2}} \left(\frac{\beta_{11}}{\beta_{22}}\right)^{\frac{1}{4}}. \quad (3.54)$$

On retaining the leading order term, we find that

$$k^* \sim \frac{\pi\sqrt{\epsilon_1}}{\sqrt{2}} \left( \frac{\beta_{11}}{\beta_{22}} \right)^{\frac{1}{4}}, \quad \text{as } \epsilon_1 \rightarrow 0. \quad (3.55)$$

Note that the Taylor expansion for  $k^*$  is valid for  $\epsilon_1 < \frac{1}{4}$ . It is observed that for small  $\epsilon_1$  this asymptotic analytic estimate for  $k^*$  approaches the general analytic estimate (3.51) from *above* due to the alternating signs of the terms in (3.54). Thus, it is no longer guaranteed that (3.55) is strictly a *lower bound*. In fact, if the general analytic estimate is very close to the exact decay rate, then the asymptotic estimate may *overestimate* the exact decay rate. Hence, (3.55) must be viewed simply as an approximation rather than a lower bound.

The values of the two estimates (3.51), (3.55) for a set of materials (in plane stress) are shown in Table 3.2. The materials themselves are listed in Table 3.1 together with their elastic moduli. For all the materials listed, the result (3.51)<sub>1</sub> is applicable except in the isotropic case, where (3.51)<sub>2</sub> is used. We will discuss these results at the end of Chapter 3.

### 3.4 Conservation Law Estimate

The next estimate that will be developed is derived from similar arguments as the previous analytic estimate, using in addition the conservation property (3.4). It will be seen that this yields a significantly improved result. Again, this estimate is first derived for the most general case of  $\epsilon_1 > 0$  and then an asymptotic result is derived for small  $\epsilon_1$ .

### 3.4.1 General Estimate

For this estimate, both of the orthotropic energies  $E_1(z)$  and  $E_2(z)$  are used. Let  $F(z)$  be defined by

$$F(z) = [E_2(z) + mE_1(z)] + 2k \int_z^\infty [E_2(s) + mE_1(s)] ds, \quad (3.56)$$

where  $m$  and  $k$  are both positive constants to be determined. The detailed procedures for this estimate follow closely the arguments given in [3] for the isotropic strip where  $\epsilon_1 = \frac{1}{2}$ . With  $F(z)$  defined in (3.56), we have

$$F'(z) + 2kF(z) = E_2'(z) + mE_1'(z) + 4k^2 \int_z^\infty [E_2(s) + mE_1(s)] ds. \quad (3.57)$$

We now wish to express the quantities  $E_2'(z)$  and  $\int_z^\infty E_2(s)ds$  as line integrals, as was already done for  $E_1'(z)$  and  $\int_z^\infty E_1(s)ds$  in the previous section.

Following similar procedures, let  $f = [\phi_{,\xi\xi\xi}^2 + \frac{1}{\epsilon_1}\phi_{,\xi\xi\eta}^2 + \phi_{,\xi\eta\eta}^2]$  in (3.20) to obtain a line integral expression for  $E_2'(z)$ ,

$$E_2'(z) = - \int_z^\infty [\phi_{,\xi\xi\xi}^2 + \frac{1}{\epsilon_1}\phi_{,\xi\xi\eta}^2 + \phi_{,\xi\eta\eta}^2] d\eta. \quad (3.58)$$

Letting  $f = [\phi_{,\xi\xi}\phi_{,\xi\xi\xi} - \phi_{,\xi\eta}\phi_{,\eta\eta\eta}]$  in (3.20) yields

$$E_2(z) = \frac{d}{dz} \int_{R_z} [\phi_{,\xi\xi}\phi_{,\xi\xi\xi} - \phi_{,\xi\eta}\phi_{,\eta\eta\eta}] dA, \quad (3.59)$$

which, when combined with the divergence theorem and boundary conditions, yields

an expression for  $\int_z^\infty E_2(s)ds$  as a line integral,

$$\begin{aligned}\int_z^\infty E_2(s)ds &= -\int_{L_z} [\phi_{,\xi\xi}\phi_{,\xi\xi\xi} - \phi_{,\xi\eta}\phi_{,\eta\eta\eta}] dA \\ &= \int_{L_z} \left[ \frac{\phi_{,\xi\xi}^2}{2} + \frac{\phi_{,\eta\eta}^2}{2} \right] d\eta.\end{aligned}\quad (3.60)$$

Substituting (3.21), (3.23), (3.58) and (3.60) into (3.57) results in

$$\begin{aligned}F'(z) + 2kF(z) &= -\int_{L_z} [\phi_{,\xi\xi\xi}^2 + \frac{1}{\epsilon_1}\phi_{,\xi\xi\eta}^2 + \phi_{,\xi\eta\eta}^2 + (m-2k^2)\phi_{,\xi\xi}^2 \\ &\quad + (m-2k^2)\phi_{,\eta\eta}^2 + \frac{m}{\epsilon_1}\phi_{,\xi\eta}^2 - 4k^2m\phi_{,\xi}^2 \\ &\quad - \frac{4k^2m}{2\epsilon_1}\phi_{,\eta}^2 + 4k^2m\phi\phi_{,\xi\xi}] d\eta \\ &= -J(z).\end{aligned}\quad (3.61)$$

We now seek positive values for  $k$  and  $m$  such that the integral  $J(z)$  is nonnegative.

The first step in simplifying  $J(z)$  is to make use of the conservation property (3.4)

which may be rewritten, upon using the arithmetic-geometric mean inequality (3.15),

as

$$\begin{aligned}\int_{L_z} [\phi_{,\eta\eta}^2 - \phi_{,\xi\xi}^2 - \frac{1}{\epsilon_1}\phi_{,\xi\eta}^2] d\eta &\leq -\int_{L_z} 2\phi_{,\xi}\phi_{,\xi\xi\xi} d\eta \\ &\leq \int_{L_z} [\alpha\phi_{,\xi}^2 + \frac{1}{\alpha}\phi_{,\xi\xi\xi}^2] d\eta\end{aligned}\quad (3.62)$$

for  $\alpha > 0$ . Thus we have from (3.62) that

$$\int_{L_z} \phi_{,\xi\xi\xi}^2 d\eta \geq \int_{L_z} [\alpha\phi_{,\eta\eta}^2 - \alpha\phi_{,\xi\xi}^2 - \frac{\alpha}{\epsilon_1}\phi_{,\xi\eta}^2 - \alpha^2\phi_{,\xi}^2] d\eta.\quad (3.63)$$

Using (3.63) in (3.61), we obtain

$$\begin{aligned}J(z) &\geq \int_{L_z} [(m-2k^2+\alpha)\phi_{,\eta\eta}^2 + (m-2k^2-\alpha)\phi_{,\xi\xi}^2 + (\frac{m}{\epsilon_1}-\frac{\alpha}{\epsilon_1})\phi_{,\xi\eta}^2 \\ &\quad - (4k^2m+\alpha^2)\phi_{,\xi}^2 - \frac{2k^2m}{\epsilon_1}\phi_{,\eta}^2 + 4k^2m\phi\phi_{,\xi\xi} \\ &\quad + \frac{1}{\epsilon_1}\phi_{,\xi\xi\eta}^2 + \phi_{,\xi\eta\eta}^2] d\eta.\end{aligned}\quad (3.64)$$

On using again the arithmetic-geometric mean inequality (3.15), we obtain

$$\int_{L_x} 2\phi\phi_{,\xi\xi} d\eta \geq -\gamma \int_{L_x} \phi^2 d\eta - \frac{1}{\gamma} \int_{L_x} \phi_{,\xi\xi}^2 d\eta, \quad \gamma > 0. \quad (3.65)$$

On employing the Wirtinger inequality (3.14) with the choice  $w = \phi$ , we obtain from (3.65)

$$\int_{L_x} 2\phi\phi_{,\xi\xi} d\eta > -\frac{\gamma h^4}{(\frac{3\pi}{2})^4} \int_{L_x} \phi_{,\eta\eta}^2 d\eta - \frac{1}{\gamma} \int_{L_x} \phi_{,\xi\xi}^2 d\eta, \quad (3.66)$$

which may be used in (3.64) to yield

$$\begin{aligned} J(z) > \int_{L_x} \left[ \phi_{,\xi\eta\eta}^2 + \frac{1}{\epsilon_1} \phi_{,\xi\xi\eta}^2 + (m - 2k^2 - \alpha - \frac{2k^2 m}{\gamma}) \phi_{,\xi\xi}^2 \right. \\ &\quad \left. + (m - 2k^2 + \alpha - \frac{2k^2 m \gamma h^4}{(\frac{3\pi}{4})^4}) \phi_{,\eta\eta}^2 + \frac{(m - \alpha)}{\epsilon_1} \phi_{,\xi\eta}^2 \right. \\ &\quad \left. - (4k^2 m + \alpha^2) \phi_{,\xi}^2 - \frac{2k^2 m}{\epsilon_1} \phi_{,\eta}^2 \right] d\eta. \end{aligned} \quad (3.67)$$

Next several Wirtinger inequalities will be used, the validity of which make use of the boundary conditions (2.23). The choices  $w = \phi$  and  $w = \phi_{,\xi}$  in the inequality (3.12) yield

$$\int_{L_x} \phi_{,\eta}^2 d\eta \leq \frac{h^2}{4\pi^2} \int_{L_x} \phi_{,\eta\eta}^2 d\eta \quad (3.68)$$

and

$$\int_{L_x} \phi_{,\xi\eta}^2 d\eta \leq \frac{h^2}{4\pi^2} \int_{L_x} \phi_{,\xi\eta\eta}^2 d\eta, \quad (3.69)$$

respectively. Similarly, the choices of  $w = \phi_{,\xi\xi}$  in (3.11) and  $w = \phi_{,\xi}$  in (3.14) yield

$$\int_{L_x} \phi_{,\xi\xi\eta}^2 d\eta \geq \frac{\pi^2}{h^2} \int_{L_x} \phi_{,\xi\xi}^2 d\eta \quad (3.70)$$

and

$$\int_{L_z} \phi_{,\xi}^2 d\eta < \frac{h^4}{(\frac{3\pi}{2})^4} \int_{L_z} \phi_{,\xi\eta\eta}^2 d\eta, \quad (3.71)$$

respectively. Using (3.68) - (3.71) in (3.67), provided that  $(m - \alpha) \leq 0$ , we obtain

$$\begin{aligned} J(z) > \int_{L_z} \left[ \left\{ 1 + \frac{m - \alpha}{\epsilon_1} \frac{h^2}{4\pi^2} - (4k^2m + \alpha^2) \frac{h^4}{(\frac{3\pi}{2})^4} \right\} \phi_{,\xi\eta\eta}^2 \right. \\ &\quad + \left\{ \frac{\pi^2}{h^2\epsilon_1} + m - 2k^2 - \alpha - \frac{2k^2m}{\gamma} \right\} \phi_{,\xi\xi}^2 \\ &\quad \left. + \left\{ m - 2k^2 + \alpha - \frac{2k^2m\gamma h^4}{(\frac{3\pi}{2})^4} - \frac{k^2m}{2\epsilon_1} \frac{h^2}{\pi^2} \right\} \phi_{,\eta\eta}^2 \right] d\eta. \quad (3.72) \end{aligned}$$

It then follows that the integral  $J(z)$  will be nonnegative if we can choose positive constants  $m$ ,  $\alpha$ ,  $\gamma$  and  $k$ , such that the coefficients of  $\phi_{,\xi\eta\eta}^2$ ,  $\phi_{,\xi\xi}^2$ , and  $\phi_{,\eta\eta}^2$  in (3.72) are nonnegative. Following the notation introduced in [3], we let

$$m = \frac{\pi^2}{h^2}M, \quad k^2 = \frac{\pi^2}{h^2}K^2, \quad \alpha = \frac{\pi^2}{h^2}\beta, \quad \gamma = \frac{\pi^2}{h^2}\delta, \quad (3.73)$$

where  $h = 2$ . The problem is then to find positive constants  $M$ ,  $\beta$ ,  $\delta$  and  $K$ , such that

$$\beta \geq M, \quad (3.74)$$

$$1 + \frac{(M - \beta)}{4\epsilon_1} - \frac{\beta^2}{(\frac{3}{2})^4} - \frac{4K^2M}{(\frac{3}{2})^4} \geq 0, \quad (3.75)$$

$$\frac{1}{\epsilon_1} + M - 2K^2 - \beta - \frac{2K^2M}{\delta} \geq 0, \quad (3.76)$$

$$M - 2K^2 + \beta - \frac{K^2M}{2\epsilon_1} - \frac{2K^2M\delta}{(\frac{3}{2})^4} \geq 0. \quad (3.77)$$

We desire the choice of constants, satisfying (3.74) - (3.77), to maximize the value of  $K$  and hence maximize  $k$ . In [3] it was shown that choosing

$$\beta = M \quad (3.78)$$

resulted in the maximum value of  $k$  for the case where  $\epsilon_1 = \frac{1}{2}$ , i.e. for isotropic materials. Similar arguments can be used to show that (3.78) also provides the *maximum* value of  $k$  in the present case. On choosing (3.78), the remaining conditions (3.75) - (3.77) become

$$K^2 \leq \frac{[(\frac{3}{2})^4 - M^2]}{4M}, \quad (3.79)$$

$$K^2 \leq \frac{1}{2\epsilon_1} \left( \frac{\delta}{\delta + M} \right), \quad (3.80)$$

$$K^2 \leq \frac{2M}{\left[ 2 + \frac{M}{2\epsilon_1} + \frac{2M\delta}{(\frac{3}{2})^4} \right]}. \quad (3.81)$$

It is readily verified that the right-hand sides of (3.79), (3.80) and (3.81) are strictly monotone functions of the variables  $M$  and  $\delta$ . Thus the maximum choice for  $K$  satisfying (3.79) - (3.81) results from equating these three expressions. Equating (3.79) and (3.80) results in the following expression for  $\delta$ ,

$$\delta = -\frac{2\epsilon_1 M [(\frac{3}{2})^4 - M^2]}{\{2\epsilon_1 [(\frac{3}{2})^4 - M^2] - 4M\}}. \quad (3.82)$$

Equating (3.79) and (3.81), and using (3.82), results in a sixth order polynomial equation for  $M$ ,

$$\begin{aligned} \left(\frac{3}{2}\right)^4 \left[ M^3 + 20\epsilon_1 M^2 - \left(\frac{3}{2}\right)^4 M - 4\left(\frac{3}{2}\right)^4 \epsilon_1 \right] & \left[ 2\epsilon_1 M^2 + 4M - 2\left(\frac{3}{2}\right)^4 \epsilon_1 \right] \\ & - 8M^2 \epsilon_1^2 \left[ \left(\frac{3}{2}\right)^4 - M^2 \right]^2 = 0. \end{aligned} \quad (3.83)$$

The roots of (3.83) may then be used to obtain  $K$  by taking equality in (3.79), where it can be observed that the smallest value of  $M$  yields the largest value for  $K$ . The sixth order polynomial (3.83) was solved using MACSYMA for the set of materials

given in Table 3.1. For each specific material,  $\epsilon_1$  was determined and substituted into (3.83), which was then solved numerically. For all of the materials, the six roots  $M_i$ ,  $i \in \{1, 2, 3, 4, 5, 6\}$  were such that the smallest positive root resulted in a negative choice for  $\delta$ , and hence was inadmissible. The second positive root in each case gave the desired maximum value for  $K$  satisfying (3.79) - (3.81) and hence from (3.73) the maximum value for  $k$ .

We see from (3.61) that this value for  $k$  yields an exponential decay for  $F(z)$  of the form

$$F(z) \leq F(0)e^{-2kz}, \quad z \geq 0. \quad (3.84)$$

From the definition of  $F(z)$  in (3.56), we find that

$$E_2(z) + mE_1(z) \leq F(0)e^{-2kz}, \quad z \geq 0. \quad (3.85)$$

Adapting the arguments given in (3.42) - (3.46) and modelled after [11], it can be shown that

$$F(0) \leq 2[E_2(0) + mE_1(0)]. \quad (3.86)$$

It then follows from (3.85) and (3.86) that

$$E_2(z) + mE_1(z) \leq 2[E_2(0) + mE_1(0)]e^{-2kz}, \quad z \geq 0, \quad (3.87)$$

and hence, since  $E_1(z)$  and  $E_2(z)$  are nonnegative,

$$E_1(z) \leq 2 \left[ E_1(0) + \frac{1}{m}E_2(0) \right] e^{-2kz}, \quad z \geq 0, \quad (3.88)$$

$$E_2(z) \leq 2[E_2(0) + mE_1(0)]e^{-2kz}, \quad z \geq 0, \quad (3.89)$$



showing that the energies  $E_1(z)$  and  $E_2(z)$  have the same exponential decay as  $F(z)$ . Again, it can be shown using arguments in [24] that the multiplicative factors of 2 on the right-hand sides of (3.88) and (3.89) can be eliminated.

The derivation of pointwise estimates for the stresses  $\tau$  of the form (3.48) is again technically elaborate (see e.g. [1], [2], [3]). Assuming a result of the form (3.48), and transforming this result back into the original domain leads to an estimated stress decay rate of  $\frac{2k^*}{2H}$  where  $k^*$  is given by

$$k^* = k \left( \frac{\beta_{11}}{\beta_{22}} \right)^{\frac{1}{4}}. \quad (3.90)$$

Although this conservation law estimate does not give an *explicit formula* for the decay rate in terms of the elastic constants, the numerical results show a considerable improvement over the analytic estimate (3.51). These results are shown in Table 3.2. The results for the isotropic case, which coincide with [3], are also shown in Table 3.2.

### 3.4.2 Asymptotic Estimate

The technique based on the conservation property (3.4) can also be used to obtain an asymptotic estimate for small  $\epsilon_1$ . Using perturbation methods, we look for roots  $M$  of (3.83) of the form

$$M = m_0 + m_1\epsilon_1 + m_2\epsilon_1^2 + \dots \quad (3.91)$$

where  $M$  has been expanded in powers of the small parameter  $\epsilon_1$  and  $m_0$ ,  $m_1$  and  $m_2$  are constants to be determined. Keeping only the first three terms, we substitute

(3.91) into (3.83) and collect like powers of  $\epsilon_1$ . This results in an equation of the form

$$A_0 + A_1\epsilon_1 + A_2\epsilon_1^2 + \dots + A_N\epsilon_1^N + O(\epsilon_1^{N+1}) = 0. \quad (3.92)$$

Using the Fundamental Theorem of Perturbation Theory (see [25]), we set each of the coefficients  $A_i$  in (3.92) equal to zero, which in turn gives values for  $m_0$ ,  $m_1$  and  $m_2$ . This process results in four roots of the form (3.91),

$$M_1 = \left(\frac{3}{2}\right)^2 - 8\epsilon_1 + \frac{256}{9}\epsilon_1^2 + \dots \quad (3.93)$$

$$M_2 = -\left(\frac{3}{2}\right)^2 - 8\epsilon_1 - \frac{256}{9}\epsilon_1^2 + \dots \quad (3.94)$$

$$M_3 = \frac{1}{2}\left(\frac{3}{2}\right)^4 \epsilon_1 + \dots \quad (3.95)$$

$$M_4 = -4\epsilon_1 + \dots, \quad (3.96)$$

while the remaining two roots of (3.83) take on a different expansion that is proportional to  $\epsilon_1^{-1}$ . It is observed that  $M_1$  and  $M_3$  give two positive roots while  $M_2$  and  $M_4$  give two negative roots. Furthermore, it is seen that  $M_1$  given by (3.93) yields the *second* positive root, which was the root of (3.83) obtained using MACSYMA that yielded the maximum value for  $K$ . Taking the first two terms in (3.93) as an approximation for  $M$ , i.e.

$$M \sim \frac{9}{4} - 8\epsilon_1, \quad \text{as } \epsilon_1 \rightarrow 0, \quad (3.97)$$

and substituting into (3.79) with equality holding, we find that

$$\begin{aligned} K &\sim \frac{[(\frac{3}{2})^4 - (\frac{9}{4} - 8\epsilon_1)^2]^{\frac{1}{2}}}{2(\frac{9}{4} - 8\epsilon_1)^{\frac{1}{2}}} \\ &= \frac{(36\epsilon_1 - 64\epsilon_1^2)^{\frac{1}{2}}}{(9 - 32\epsilon_1)^{\frac{1}{2}}} \\ &= 2\sqrt{\epsilon_1} \left(1 - \frac{16}{9}\epsilon_1\right)^{\frac{1}{2}} \left(1 - \frac{32}{9}\epsilon_1\right)^{-\frac{1}{2}}, \quad \text{as } \epsilon_1 \rightarrow 0. \end{aligned} \quad (3.98)$$

Noting the Taylor expansions

$$(1 + x)^{\frac{1}{2}} = 1 + \frac{x}{2} - \frac{x^2}{8} + \dots \quad (|x| < 1) \quad (3.99)$$

$$(1 + x)^{-\frac{1}{2}} = 1 - \frac{x}{2} + \frac{3x^2}{8} + \dots \quad (|x| < 1) \quad (3.100)$$

we obtain from (3.98),

$$\begin{aligned} K &\sim 2\sqrt{\epsilon_1}(1 - \frac{8}{9}\epsilon_1 + \dots)(1 + \frac{16}{9}\epsilon_1 + \dots) \\ &\sim 2\sqrt{\epsilon_1}(1 + \frac{8}{9}\epsilon_1 + \dots) \\ &\sim 2\sqrt{\epsilon_1}, \quad \text{as } \epsilon_1 \rightarrow 0, \end{aligned} \quad (3.101)$$

where the leading order term has been retained in the last step.

Returning to (3.73) and (3.90) we have the following asymptotic conservation law estimate for  $k^*$ ,

$$k^* \sim \pi\sqrt{\epsilon_1} \left( \frac{\beta_{11}}{\beta_{22}} \right)^{\frac{1}{4}} \quad \text{as } \epsilon_1 \rightarrow 0 \quad (3.102)$$

which improves upon the asymptotic analytic estimate (3.55) by a factor of  $\sqrt{2}$ . Note that this estimate is valid for  $\epsilon_1 < \frac{9}{32} \approx .28$ . It has also been shown in [6], [7] that (3.102) follows from an asymptotic analysis of the *exact decay rate*, so that *the conservation law argument yields an estimate for the decay rate which is asymptotically exact*. This asymptotic conservation law estimate is shown for a set of orthotropic materials in Table 3.2. We again observe that (3.102) is not guaranteed to be a *lower bound* for the exact decay rate but rather an approximation, valid for small  $\epsilon_1$ . Further discussion of the result (3.102) will be given later in this section.

### 3.5 Exact Decay Rates

The exact solution to (3.3) subject to the boundary conditions (2.23) - (2.25) may be obtained using a separation of variables technique. First, we seek solutions of the form

$$\phi = e^{-\gamma \xi} F(\eta), \quad \gamma = \text{constant}. \quad (3.103)$$

This form is chosen since we seek stresses that decay exponentially in the axial direction. Substituting this form for  $\phi$  directly into the governing equation and boundary conditions gives

$$\begin{aligned} F'''' + \frac{\gamma^2}{\epsilon_1} F'' + \gamma^4 F &= 0, \quad \text{on } (-1, 1) \\ F(-1) &= F(1) = 0, \\ F'(-1) &= F'(1) = 0. \end{aligned} \quad (3.104)$$

This is a fourth-order eigenvalue problem for an ordinary differential equation. Solutions to (3.104) are sought in the form

$$F = Ae^{m\eta}, \quad m = \text{constant}, \quad (3.105)$$

which when substituted back into the boundary conditions (3.104) yields one of three separate characteristic equations (or eigenconditions) for  $\gamma$ , depending on the range of  $\epsilon_1$  (see [6], [19]). The eigenvalues  $\gamma$  are complex in general. Numerical solutions to these eigenconditions have been computed in [6] and [19]. The decay rate is obtained from the eigenvalue with the smallest positive real part. Once obtained, this result must be transformed back to the original variables  $x_1$  and  $x_2$  to arrive at the exact

decay rate for the material. Exact decay rates for a set of orthotropic materials (in plane stress) are shown in Table 3.2 using the methods of [19] which will be discussed more fully in the next chapter. In this table, note that for all the materials other than isotropic, the exact decay rate is just the *purely real* first eigenvalue. In fact it can be shown from [19] that the transition point where the eigenvalue changes from a purely real value to a complex value occurs when  $\epsilon_1 = \frac{3}{10}$ . For  $\epsilon_1 \leq \frac{3}{10}$ , (a condition satisfied by all of the orthotropic materials in the table), the first eigenvalue is purely real.

In the case of isotropic materials where  $\epsilon_1 = \frac{1}{2}$ , the eigenvalue problem (3.104) reduces to

$$\begin{aligned} F'''' + 2\gamma^2 F'' + \gamma^4 F &= 0, \quad \text{on } (-1, 1) \\ F(-1) &= F(1) = 0, \\ F'(-1) &= F'(1) = 0. \end{aligned} \tag{3.106}$$

This is a well-known eigenvalue problem whose solutions  $F$  are known as the Fadde-Papkovich eigenfunctions (see e.g. p. 231 of [1] for a discussion). Seeking solutions of the form (3.105) and using the boundary conditions (3.106) leads to an eigencondition for  $\gamma$ ,

$$\sin(2\gamma) = \pm 2\gamma. \tag{3.107}$$

The smallest real part of an eigenvalue  $\gamma$  arises from the taking the minus sign in (3.107), (corresponding to symmetric deformations), and is given by

$$\operatorname{Re} \gamma \approx 2.106, \tag{3.108}$$

so that the stresses decay as

$$e^{-2.106\xi}. \quad (3.109)$$

Transforming this result back into the original variables, we see that the stresses decay as

$$e^{-\frac{4.212}{2H}x_1}, \quad (3.110)$$

and so we recover the well-known result (see e.g. [1], [26]) that the exact decay rate for stresses in the isotropic material is  $\frac{4.212}{2H}$ .

### 3.6 Discussion of Results

We now discuss the stress decay estimates for orthotropic strips obtained in this chapter and compare them with the corresponding exact decay rates that were computed numerically. The materials used for comparison are contemporary engineering materials, and are listed in Table 3.1 along with their elastic moduli and Poisson's ratios. All of the materials are specially orthotropic with the fibers parallel to the  $x_1$  direction. Decay estimates were evaluated for each of the materials in Table 3.1 and the results are shown in Table 3.2 along with the exact decay rates. All of the results were computed for plane stress (and thus, from (2.7), the values of  $\nu_{TT}$  were not needed). The isotropic case is included in the last row of the table for comparison.

The analytic estimate (3.51), asymptotic analytic estimate (3.55) and asymptotic conservation law estimate (3.102) all yield an explicit formula for the decay rate in terms of the parameter  $\epsilon_1$  and the beta ratio  $(\frac{\beta_{11}}{\beta_{22}})^{\frac{1}{4}}$ . (Recall that the general conservation law estimate did *not* yield an explicit formula and thus was purely a numerical

estimate.) It is now useful to express these decay estimates in terms of the engineering constants of the material. Using the definition (2.20) of  $\epsilon_1$  and recalling (2.7), we obtain that for plane stress,

$$\epsilon_1 = \sqrt{\frac{E_L}{E_T}} \left( \frac{G_{LT}}{E_L - 2\nu_{LT}G_{LT}} \right), \quad \left( \frac{\beta_{11}}{\beta_{22}} \right)^{\frac{1}{4}} = \left( \frac{E_T}{E_L} \right)^{\frac{1}{4}}. \quad (3.111)$$

Here  $E$ ,  $\nu$  and  $G$  are the Young's Modulus, Poisson ratio and shear modulus respectively. Using (3.111), the *analytic estimate* (3.51) becomes

$$k^* = \frac{\pi}{4} \sqrt{\frac{E_T}{G_{LT}} - \frac{2E_T\nu_{LT}}{E_L}} \left( \sqrt{1 + 16G_{LT}^2 \frac{E_L}{E_T} \left( \frac{1}{E_L - 2\nu_{LT}G_{LT}} \right)^2} - 1 \right)^{\frac{1}{2}},$$

$$\text{if } \sqrt{\frac{E_L}{E_T}} \left( \frac{G_{LT}}{E_L - 2\nu_{LT}G_{LT}} \right) \leq \frac{\sqrt{3}}{4},$$

$$k^* = \frac{\pi}{4} \sqrt{\frac{E_T}{G_{LT}} - \frac{2E_T\nu_{LT}}{E_L}}, \quad \text{if } \sqrt{\frac{E_L}{E_T}} \left( \frac{G_{LT}}{E_L - 2\nu_{LT}G_{LT}} \right) > \frac{\sqrt{3}}{4}. \quad (3.112)$$

Similarly, the *asymptotic analytic estimate* (3.55) becomes

$$k^* \sim \frac{\pi}{\sqrt{2}} \sqrt{\frac{G_{LT}}{E_L - 2\nu_{LT}G_{LT}}}, \quad \text{as } \sqrt{\frac{E_L}{E_T}} \left( \frac{G_{LT}}{E_L - 2\nu_{LT}G_{LT}} \right) \rightarrow 0, \quad (3.113)$$

while the *asymptotic conservation law estimate* (3.102) becomes

$$k^* \sim \pi \sqrt{\frac{G_{LT}}{E_L - 2\nu_{LT}G_{LT}}}, \quad \text{as } \sqrt{\frac{E_L}{E_T}} \left( \frac{G_{LT}}{E_L - 2\nu_{LT}G_{LT}} \right) \rightarrow 0. \quad (3.114)$$

To discuss these results, we refer to Table 3.2 where it is observed from examining the first column that the materials are ordered according to increasing values of  $\epsilon_1$ . It is also observed that all of the decay estimates presented in the table have the same *relative* ordering as the exact decay rates given in the far right column. The second column shows the analytic estimate (3.51) (or equivalently (3.112)) for each of the materials. For the isotropic case, the analytic decay estimate is roughly half of the exact decay rate. However, as one moves upward in the table (i.e. as  $\epsilon_1$  decreases) the analytic estimate improves in accuracy so that for boron epoxy which has the smallest value of  $\epsilon_1$ , the analytic decay estimate is about 70% of the exact decay rate. As was mentioned previously,  $(3.51)_1$  was used for all materials except for the isotropic case where  $(3.51)_2$  was used.

The asymptotic analytic estimate (3.55) (or equivalently (3.113)) is presented in the third column of Table 3.2. For the materials for which this estimate is applicable (i.e.  $\epsilon_1 < \frac{1}{4}$ ), we see a slight improvement over the general analytic estimate. Again, we see that as  $\epsilon_1$  decreases the agreement between the asymptotic analytic estimate and the exact decay rate improves as expected.

The fourth column in Table 3.2 shows the general conservation law estimate that arises from solving the sixth order polynomial given by (3.83). While this estimate does not provide an explicit formula for the decay rate, obtaining it is not computationally intensive. The results show much better agreement with the exact decay rates than obtained by either of the analytic estimates. The improvement for the isotropic case is only slight, *but as  $\epsilon_1$  decreases the improved agreement becomes much better*. For materials with small values of  $\epsilon_1$  *the conservation law estimate yields a*



*fairly accurate approximation to the exact decay rate.*

Finally, the fifth column shows the asymptotic conservation law estimate (3.102) (or equivalently (3.114)). For the range of  $\epsilon_1$  where this decay estimate is valid i.e.  $\epsilon_1 < 0.28$ , we see a further improvement over the general conservation law estimate. Again, as  $\epsilon_1$  decreases this asymptotic estimate more closely approximates the exact decay rate so that for small  $\epsilon_1$  there is very little error. This is to be expected since, as mentioned previously, (3.102) *also results from an asymptotic analysis of the eigencondition characterizing the exact decay rate.*

The results in Table 3.2 indicate that the orthotropic decay estimates obtained in this chapter yield the best agreement with corresponding exact results for the materials with small values of  $\epsilon_1$ . This may be related to the fact that for small values of  $\epsilon_1$  the smallest eigenvalue of equation (3.104) is purely real, and the methods used in this chapter make use of real analysis arguments to estimate this quantity. It is also observed that the conservation law approach yields the best estimate, asymptotically approaching the exact decay rate. This suggests that the conservation laws derived in Chapter 2 play an important role in estimating the exact decay rate since they provide results that are in good agreement with corresponding exact results and are not computationally intensive. For both the analytic and conservation law estimates, their asymptotic versions yield improvements suggesting again that the energy methods of this chapter work best for materials with small values of  $\epsilon_1$ .

While it appears from Table 3.2 that the decay estimates are ordered in terms of increasing  $\epsilon_1$  (with the boron epoxy as an exception), this is somewhat misleading. From the formulae (3.51), (3.55) and (3.102), we see that the decay estimates are

dependent on both  $\epsilon_1$  and the beta ratio  $(\frac{\beta_{11}}{\beta_{22}})^{\frac{1}{4}}$  and are thus ordered by a combination of these quantities. An interesting simplification results when one considers specially orthotropic (or transversely isotropic) materials with a high degree of orthotropy in the axial direction. For such *strongly orthotropic* materials, we assume (see [6], [7]) that

$$\frac{E_T}{E_L} \ll 1, \quad \frac{G_{LT}}{E_L} \ll 1, \quad \frac{G_{LT}}{E_T} \leq 1. \quad (3.115)$$

Using (3.115) in (3.111) we obtain

$$\epsilon_1 \sim \frac{G_{LT}}{\sqrt{E_L E_T}}, \quad \left( \frac{\beta_{11}}{\beta_{22}} \right)^{\frac{1}{4}} = \left( \frac{E_T}{E_L} \right)^{\frac{1}{4}}. \quad (3.116)$$

It follows from (3.115) and (3.116) that  $\epsilon_1 \ll 1$  and that the decay estimates for small  $\epsilon_1$  are valid for strongly orthotropic materials. Upon using (3.116), the asymptotic analytic estimate (3.55) and asymptotic conservation law estimate (3.102) reduce to

$$k^* \sim \frac{\pi}{\sqrt{2}} \left( \frac{G_{LT}}{E_L} \right)^{\frac{1}{2}}, \quad \text{as } \frac{G_{LT}}{E_L} \rightarrow 0, \quad (3.117)$$

and

$$k^* \sim \pi \left( \frac{G_{LT}}{E_L} \right)^{\frac{1}{2}}, \quad \text{as } \frac{G_{LT}}{E_L} \rightarrow 0, \quad (3.118)$$

respectively. Both of these decay estimates are of the form

$$k^* = O \left[ \left( \frac{G_{LT}}{E_L} \right)^{\frac{1}{2}} \right], \quad \text{as } \frac{G_{LT}}{E_L} \rightarrow 0, \quad (3.119)$$

a result which was first established in [5] using the energy decay arguments of [4].

The result (3.118) was also obtained in [6], [7] from an asymptotic analysis of the exact decay rate.

The material constant ratios given in (3.115), the asymptotic conservation law estimate for strongly orthotropic materials (3.118), and the exact decay rates (repeated from Table 3.2 for convenience) are tabulated in Table 3.3. In this table, the materials are now ordered by increasing values of  $\frac{G_{LT}}{E_L}$ , thus switching the order of boron epoxy and ultra-high modulus graphite epoxy from Table 3.2. The estimate (3.118) and the exact decay rates are seen to increase with  $\frac{G_{LT}}{E_L}$ . All but the last two materials in the table may be considered *strongly orthotropic*. The result (3.118) provides an extremely accurate estimate for the exact decay rate for the strongly orthotropic materials. (See e.g. [2], [7], [9], [10] for a discussion of the utility of (3.118) in the mechanics of laminated composite structures.)

The results of this chapter have been obtained for the case of plane stress. Numerical results for the case of plane strain have also been calculated. The results are not presented here as they differ very little from the plane stress case. Recall that the only difference between these two formulations is in the values of the elastic constants  $\beta_{pq}$ . For the case of strongly orthotropic materials, we still obtain (3.118) in plane strain.

The decay rate results presented here may also be expressed in terms of decay lengths. If we denote the *characteristic decay length*  $d$  as the length over which the solution  $\phi$  and hence the stresses  $\tau$  decay to 1% of their original value, i.e.

$$|\tau(d, x_2)| = K e^{-k^* \frac{d}{H}} = \frac{1}{100} K, \quad \text{for fixed } x_2, \quad (3.120)$$

then we obtain that

$$d = \frac{\ln 100}{2k^*} (2H) \quad (3.121)$$

where  $2H$  is one strip width of the material. Thus the decay length is inversely proportional to the decay rate  $k^*$ , and underestimates of  $k^*$  provide conservative overestimates of  $d$ . Table 3.4 shows the exact characteristic decay lengths for each of the materials previously mentioned. (The exact decay rates are repeated from Table 3.2 for convenience.) From the last row of Table 3.4 we recover the well known result that the *isotropic material* has a characteristic decay length of roughly one strip width, meaning that approximately one strip width away from the edge the end effects are negligible. This is the general rule often invoked when using Saint-Venant's principle for isotropic materials (see e.g. [1]). However, for orthotropic materials the decay length may be much larger. As seen in Table 3.4, the decay lengths vary from roughly one strip width to six strip widths in the case of ultra-high modulus graphite epoxy. For this situation, end effects may persist much farther into the strip than for the corresponding isotropic case. Thus for orthotropic materials Saint-Venant's principle cannot be routinely applied as for isotropic materials. This fact poses a serious deficiency in the use of Saint-Venant's principle to obtain approximate solutions to anisotropic boundary-value problems. This emphasizes the importance, particularly in the case of strongly orthotropic materials, of obtaining accurate decay rate estimates such as (3.118). Here, very high aspect ratios (ratio of length to width) are necessary before end effects can be neglected.

Material	$E_L$ (psi)	$E_T$ (psi)	$\nu_{LT}$	$\nu_{TT}$	$G_{LT}$ (psi)
Boron Epoxy	$30.0 \times 10^6$	$3.0 \times 10^6$	.21	.35	$0.7 \times 10^6$
Ultra-high Modulus Graphite Epoxy	$45.0 \times 10^6$	$0.9 \times 10^6$	.26	NA	$0.6 \times 10^6$
Kevlar Epoxy	$11.0 \times 10^6$	$0.8 \times 10^6$	.34	NA	$0.3 \times 10^6$
High Strength Graphite Epoxy 1	$20.0 \times 10^6$	$1.0 \times 10^6$	.25	.25	$0.6 \times 10^6$
High Strength Graphite Epoxy 2	$18.5 \times 10^6$	$1.6 \times 10^6$	.35	.20	$0.832 \times 10^6$
S-glass Epoxy	$7.5 \times 10^6$	$1.7 \times 10^6$	.25	NA	$0.8 \times 10^6$
Boron Aluminum	$33.0 \times 10^6$	$21.0 \times 10^6$	.23	.30	$7.0 \times 10^6$

Table 3.1: Orthotropic materials and elastic moduli

Material ( $\epsilon_1$ )	Analytic Estimate (3.51)	Analytic Estimate for small $\epsilon_1$ (3.55)	Cons. Law Estimate	Cons. Law Estimate for small $\epsilon_1$ (3.102)	Exact Decay Rate $k^*$
<b>BE</b> (0.0745)	0.337	0.341	0.445	0.482	0.487
<b>UM</b> (0.0949)	0.253	0.257	0.328	0.364	0.369
<b>KE</b> (0.1030)	0.363	0.370	0.467	0.524	0.534
<b>HS1</b> (0.1362)	0.375	0.388	0.468	0.548	0.567
<b>HS2</b> (0.1578)	0.458	0.478	0.564	0.677	0.708
<b>SE</b> (0.2366)	0.684	0.745	0.794	1.054	1.195
<b>BA</b> (0.2946)	0.955	NA	1.069	NA	1.942
<b>Isotropic</b> (0.500)	1.111	NA	1.220	NA	2.106

Table 3.2: Plane stress results for orthotropic materials :  $\tau \sim e^{-\frac{k^* x_1}{H}}$  as  $x_1 \rightarrow \infty$ .

#### Key for Materials

BE = boron epoxy  
 UM = ultra-high modulus graphite epoxy  
 KE = kevlar epoxy  
 HS1 = high strength graphite epoxy 1  
 HS2 = high strength graphite epoxy 2  
 SE = s-glass epoxy  
 BA = boron aluminum

Material ( $\epsilon_1$ )	$G_{LT}/E_L$	$E_T/E_L$	$G_{LT}/E_T$	Cons. Law Estimate (3.118)	Exact Decay Rate $k^*$
<b>UM</b> (0.0949)	0.013	0.02	0.66	0.358	0.369
<b>BE</b> (0.0745)	0.023	0.10	0.23	0.476	0.487
<b>KE</b> (0.1030)	0.027	0.072	0.37	0.516	0.534
<b>HS1</b> (0.1362)	0.03	0.05	0.6	0.544	0.567
<b>HS2</b> (0.1578)	0.045	0.086	0.52	0.666	0.708
<b>SE</b> (0.2366)	0.106	0.226	0.47	NA	1.195
<b>BA</b> (0.2946)	0.212	0.636	0.33	NA	1.942

Table 3.3: Strongly orthotropic results:  $\tau \sim e^{-\frac{k^* x_1}{H}}$  as  $x_1 \rightarrow \infty$ .

Material ( $\epsilon_1$ )	Exact Decay Rate $k^*$	Exact Characteristic Decay Length $d$
<b>UM</b> (0.0949)	0.369	$6.24 \times 2H$
<b>BE</b> (0.0745)	0.487	$4.73 \times 2H$
<b>KE</b> (0.1030)	0.534	$4.31 \times 2H$
<b>HS1</b> (0.1362)	0.567	$4.06 \times 2H$
<b>HS2</b> (0.1578)	0.708	$3.25 \times 2H$
<b>SE</b> (0.2366)	1.195	$1.92 \times 2H$
<b>BA</b> (0.2946)	1.942	$1.18 \times 2H$
<b>Isotropic</b> (0.500)	2.106	$1.09 \times 2H$

Table 3.4: Exact characteristic decay lengths:  $d = \frac{\ln 100}{2k^*}(2H)$



## Chapter 4

# THE ANISOTROPIC CASE

The techniques described in the previous chapter will now be extended to the generalized fourth-order problem for the *anisotropic* strip. First, for the reader's convenience, we will recall several results that were derived in Chapter 2. Several estimates will then be presented and the results discussed.

### 4.1 Formulation

From (2.21), the nondimensional governing equation for the anisotropic strip is given by

$$\phi_{,\xi\xi\xi\xi} - \frac{2}{\epsilon_2}\phi_{,\xi\xi\xi\eta} + \frac{1}{\epsilon_1}\phi_{,\xi\xi\eta\eta} - \frac{2}{\epsilon_3}\phi_{,\xi\eta\eta\eta} + \phi_{,\eta\eta\eta\eta} = 0. \quad (4.1)$$

From (2.34) and (2.35), the final reduced form of the first and second Conservation Laws are

$$\int_{L_z} [2\phi_{,\xi}\phi_{,\xi\xi\xi} + \phi_{,\eta\eta}^2 + \frac{4}{\epsilon_2}\phi_{,\xi\eta}\phi_{,\xi\xi}] d\eta = \int_{L_z} [\phi_{,\xi\xi}^2 + \frac{1}{\epsilon_1}\phi_{,\xi\eta}^2] d\eta \quad (4.2)$$

and

$$\int_{L_z} [2\phi_{,\xi\xi\eta}\phi_{,\eta\eta\eta} + \phi_{,\xi\eta\eta}^2 + \frac{1}{\epsilon_1}\phi_{,\xi\xi\eta}^2] d\eta \leq \int_{L_z} [\phi_{,\xi\xi\xi}^2 + \frac{4}{\epsilon_3}\phi_{,\xi\xi\eta}\phi_{,\xi\eta\eta}] d\eta, \quad (4.3)$$

respectively. From (2.61), the nondimensional physical strain-energy is given by

$$\begin{aligned} E_p(z) = & \int_{R_z} [\phi_{,\xi\xi}^2 + \phi_{,\eta\eta}^2 + \frac{1}{\epsilon_1}\phi_{,\xi\eta}^2 - \frac{2}{\epsilon_2}\phi_{,\xi\eta}\phi_{,\xi\xi} - \frac{2}{\epsilon_3}\phi_{,\xi\eta}\phi_{,\eta\eta}] d\xi d\eta \\ & - \frac{2\beta_{12}}{\sqrt{\beta_{11}\beta_{22}}} \int_{-1}^1 \phi_{,\xi}\phi_{,\eta\eta} d\eta. \end{aligned} \quad (4.4)$$

From (2.65) and (2.72), the energy functionals  $E_1(z)$  and  $E_2(z)$  are given by

$$E_1(z) = \int_{R_z} [\phi_{,\xi\xi}^2 - \frac{2}{\epsilon_2}\phi_{,\xi\xi}\phi_{,\xi\eta} + \frac{1}{\epsilon_1}\phi_{,\xi\eta}^2 - \frac{2}{\epsilon_3}\phi_{,\eta\eta}\phi_{,\xi\eta} + \phi_{,\eta\eta}^2] d\xi d\eta, \quad (4.5)$$

$$E_2(z) = \int_{R_z} [\phi_{,\xi\xi\xi}^2 - \frac{2}{\epsilon_2}\phi_{,\xi\xi\xi}\phi_{,\xi\xi\eta} + \frac{1}{\epsilon_1}\phi_{,\xi\xi\eta}^2 - \frac{2}{\epsilon_3}\phi_{,\xi\xi\eta}\phi_{,\xi\eta\eta} + \phi_{,\xi\eta\eta}^2] d\xi d\eta. \quad (4.6)$$

From (2.69) and (2.73), the line integral representations for these energies are

$$E_1(z) = - \int_{L_z} [-\phi\phi_{,\xi\xi\xi} + \phi_{,\xi}\phi_{,\xi\xi} + \frac{1}{\epsilon_1}\phi_{,\eta}\phi_{,\xi\eta} - \frac{2}{\epsilon_2}\phi_{,\eta}\phi_{,\xi\xi}] d\eta, \quad (4.7)$$

$$E_2(z) = - \int_{L_z} [\phi_{,\xi\xi}\phi_{,\xi\xi\xi} - \phi_{,\xi\eta}\phi_{,\eta\eta\eta}] d\eta. \quad (4.8)$$

Furthermore, it is assumed that

$$\frac{1}{\epsilon_1} > \frac{1}{\epsilon_2^2} + \frac{1}{\epsilon_3^2}, \quad (4.9)$$

so that the integrands in the energies  $E_1(z)$  and  $E_2(z)$  are positive-definite quadratic forms in their arguments.

## 4.2 Basic Energy Estimate

For the basic energy estimate only one of the energies  $E_1(z)$  is used. As in (3.18) for the orthotropic case, let the function  $F(z)$  be defined by

$$F(z) = E_1(z) + 2k \int_z^\infty E_1(s) ds, \quad (4.10)$$

where  $k > 0$  is, as yet, an unspecified constant. From (4.10), we have that

$$F'(z) + 2kF(z) = E_1'(z) + 4k^2 \int_z^\infty E_1(s) ds. \quad (4.11)$$

Returning to (3.20) and letting  $f = [\phi_{,\xi\xi}^2 - \frac{2}{\epsilon_2}\phi_{,\xi\xi}\phi_{,\xi\eta} + \frac{1}{\epsilon_1}\phi_{,\xi\eta}^2 - \frac{2}{\epsilon_3}\phi_{,\eta\eta}\phi_{,\xi\eta} + \phi_{,\eta\eta}^2]$  yields an expression for  $E_1'(z)$  in terms of a line integral as

$$E_1'(z) = - \int_{L_z} [\phi_{,\xi\xi}^2 - \frac{2}{\epsilon_2}\phi_{,\xi\xi}\phi_{,\xi\eta} + \frac{1}{\epsilon_1}\phi_{,\xi\eta}^2 - \frac{2}{\epsilon_3}\phi_{,\eta\eta}\phi_{,\xi\eta} + \phi_{,\eta\eta}^2] d\eta. \quad (4.12)$$

Similarly, letting  $f = [-\phi\phi_{,\xi\xi\xi} + \phi_{,\xi}\phi_{,\xi\xi} + \frac{1}{\epsilon_1}\phi_{,\eta}\phi_{,\xi\eta} - \frac{2}{\epsilon_2}\phi_{,\eta}\phi_{,\xi\xi}]$  in (3.20) yields

$$E_1(z) = \frac{d}{dz} \int_{R_z} [-\phi\phi_{,\xi\xi\xi} + \phi_{,\xi}\phi_{,\xi\xi} + \frac{1}{\epsilon_1}\phi_{,\eta}\phi_{,\xi\eta} - \frac{2}{\epsilon_2}\phi_{,\eta}\phi_{,\xi\xi}] dA, \quad (4.13)$$

which when integrated using the divergence theorem and boundary conditions gives an expression for  $\int_z^\infty E_1(s)ds$  in terms of a line integral as

$$\begin{aligned}\int_z^\infty E_1(s)ds &= - \int_{R_z} [-\phi\phi_{,\xi\xi\xi} + \phi_{,\xi}\phi_{,\xi\xi} + \frac{1}{\epsilon_1}\phi_{,\eta}\phi_{,\xi\eta} - \frac{2}{\epsilon_2}\phi_{,\eta}\phi_{,\xi\xi}] dA \\ &= - \int_{L_z} [\phi\phi_{,\xi\xi} - \phi_{,\xi}^2 - \frac{1}{2\epsilon_1}\phi_{,\eta}^2 + \frac{2}{\epsilon_3}\phi_{,\eta}\phi_{,\xi}] d\eta.\end{aligned}\quad (4.14)$$

Returning to (4.11), we have that

$$\begin{aligned}F'(z) + 2kF(z) &= - \int_{L_z} [\phi_{,\xi\xi}^2 + \phi_{,\eta\eta}^2 - \frac{2}{\epsilon_2}\phi_{,\xi\xi}\phi_{,\xi\eta} \\ &\quad - \frac{2}{\epsilon_3}\phi_{,\xi\eta}\phi_{,\eta\eta} + \frac{1}{\epsilon_1}\phi_{,\xi\eta}^2 + 4k^2\phi\phi_{,\xi\xi} \\ &\quad - 4k^2\phi_{,\xi}^2 - \frac{2k^2}{\epsilon_1}\phi_{,\eta}^2 + \frac{8k^2}{\epsilon_2}\phi_{,\eta}\phi_{,\xi}] d\eta \\ &= J(z).\end{aligned}\quad (4.15)$$

As before, we want to find values of  $k$  such that  $J(z) \leq 0$ . The steps that follow are modelled essentially after Horgan [4], except that here we use the energy functional (4.5) (rather than the physical energy used in [4]) and a sharper Wirtinger inequality than that employed in [4].

If we define  $E_1(z) = \int_{R_z} 2W_1 dA$ , where

$$2W_1 = \phi_{,\xi\xi}^2 + \phi_{,\eta\eta}^2 - \frac{2}{\epsilon_2}\phi_{,\xi\xi}\phi_{,\xi\eta} - \frac{2}{\epsilon_3}\phi_{,\xi\eta}\phi_{,\eta\eta} + \frac{1}{\epsilon_1}\phi_{,\xi\eta}^2, \quad (4.16)$$

then from (4.15) we obtain

$$J(z) = - \int_{L_z} [2W_1 - 4k^2(\phi_{,\xi}^2 - \phi\phi_{,\xi\xi} + \frac{1}{2\epsilon_1}\phi_{,\eta}^2 - \frac{2}{\epsilon_2}\phi_{,\eta}\phi_{,\xi})] d\eta. \quad (4.17)$$

We can write  $2W_1$  as a quadratic form as  $\mathbf{s}^T \mathbf{B} \mathbf{s}$ , where

$$\mathbf{s} = \begin{bmatrix} \phi_{,\xi\xi} \\ \phi_{,\eta\eta} \\ \sqrt{2}\phi_{,\xi\eta} \end{bmatrix} \quad \text{and} \quad \mathbf{B} = \begin{bmatrix} 1 & 0 & -\frac{1}{\sqrt{2}\epsilon_2} \\ 0 & 1 & \frac{1}{\sqrt{2}\epsilon_3} \\ -\frac{1}{\sqrt{2}\epsilon_2} & -\frac{1}{\sqrt{2}\epsilon_3} & \frac{1}{2\epsilon_1} \end{bmatrix}. \quad (4.18)$$

By virtue of (4.9), we know that  $2W_1$  is positive-definite and we have the result that

$$2W_1 \geq \lambda_m (\phi_{,\xi\xi}^2 + \phi_{,\eta\eta}^2 + 2\phi_{,\xi\eta}^2), \quad (4.19)$$

where  $\lambda_m > 0$  is the minimum eigenvalue of  $\mathbf{B}$  (see [27]). This leads to the inequality

$$\begin{aligned} J(z) \leq & - \int_{L_x} [\lambda_m (\phi_{,\xi\xi}^2 + \phi_{,\eta\eta}^2 + 2\phi_{,\xi\eta}^2) \\ & - 4k^2 (\phi_{,\xi}^2 - \phi\phi_{,\xi\xi} + \frac{1}{2\epsilon_1}\phi_{,\eta}^2 - \frac{2}{\epsilon_2}\phi_{,\eta}\phi_{,\xi})] d\eta \end{aligned} \quad (4.20)$$

$$\begin{aligned} = & - \int_{L_x} [\lambda_m (\phi_{,\xi\xi}^2 + \frac{2}{\lambda_m}k^2\phi)^2 + \lambda_m\phi_{,\eta\eta}^2 + 2\lambda_m\phi_{,\xi\eta}^2 \\ & - 4k^2\phi_{,\xi}^2 - \frac{2k^2}{\epsilon_1}\phi_{,\eta}^2 + \frac{8k^2}{\epsilon_2}\phi_{,\eta}\phi_{,\xi} - \frac{4k^4}{\lambda_m}\phi^2] d\eta \end{aligned} \quad (4.21)$$

$$\begin{aligned} \leq & - \int_{L_x} [\lambda_m\phi_{,\eta\eta}^2 + 2\lambda_m\phi_{,\xi\eta}^2 - 4k^2\phi_{,\xi}^2 - \frac{2k^2}{\epsilon_1}\phi_{,\eta}^2 \\ & + \frac{8k^2}{\epsilon_2}\phi_{,\eta}\phi_{,\xi} - \frac{4k^4}{\lambda_m}\phi^2] d\eta. \end{aligned} \quad (4.22)$$

We now use the following two Wirtinger inequalities obtained by choosing  $w = \phi$  in

(3.12) and  $w = \phi_{,\xi}$  in (3.11),

$$\int_{L_x} \phi_{,\eta\eta}^2 d\eta \geq \frac{4\pi^2}{h^2} \int_{L_x} \phi_{,\eta}^2 d\eta, \quad (4.23)$$

$$\int_{L_x} \phi_{,\xi\eta}^2 d\eta \geq \frac{\pi^2}{h^2} \int_{L_x} \phi_{,\xi}^2 d\eta, \quad (4.24)$$

respectively. We shall set  $h = 2$  (i.e. equal to the strip width) later. Thus we obtain

from (4.22) that

$$\begin{aligned}
J(z) \leq & - \int_{L_z} [(\lambda_m \frac{2\pi^2}{h^2} - 4k^2)\phi_{,\xi}^2 + (\frac{4\pi^2}{h^2}\lambda_m - \frac{2k^2}{\epsilon_1})\phi_{,\eta}^2 \\
& + \frac{8k^2}{\epsilon_2}\phi_{,\eta}\phi_{,\xi} - \frac{4k^4}{\lambda_m}\phi^2] d\eta.
\end{aligned} \tag{4.25}$$

Observe that the first three terms in the integrand may be written as a quadratic form as  $Q = \mathbf{d}^T \mathbf{D} \mathbf{d}$ , where

$$\mathbf{d} = \begin{bmatrix} \phi_{,\xi} \\ \phi_{,\eta} \end{bmatrix} \quad \text{and} \quad \mathbf{D} = \begin{bmatrix} (2\lambda \frac{\pi^2}{h^2} - 4k^2) & \frac{4k^2}{\epsilon_2} \\ \frac{4k^2}{\epsilon_2} & (4\lambda \frac{\pi^2}{h^2} - \frac{2k^2}{\epsilon_1}) \end{bmatrix}. \tag{4.26}$$

Here,  $\mathbf{D}$  is a symmetric matrix and for convenience the subscript  $m$  has been dropped from the eigenvalue  $\lambda$ . If we choose the constant  $k$  such that the eigenvalues of  $\mathbf{D}$  are positive, i.e.  $\mathbf{D}$  is positive-definite, then we obtain

$$Q \geq \omega(\mathbf{d}^T \mathbf{d}) = \omega(\phi_{,\xi}^2 + \phi_{,\eta}^2) \tag{4.27}$$

where  $\omega > 0$  is the minimum eigenvalue of  $\mathbf{D}$ . Equation (4.25) then leads to the inequality

$$J(z) \leq - \int_{L_z} [\omega(\phi_{,\xi}^2 + \phi_{,\eta}^2) - \frac{4k^4}{\lambda}\phi^2] d\eta. \tag{4.28}$$

Dropping the first term and using the inequality

$$\int_{L_z} \phi_{,\eta}^2 d\eta \geq \frac{\pi^2}{h^2} \int_{L_z} \phi^2 d\eta, \tag{4.29}$$

which is obtained from (3.11) with the choice  $w = \phi$ , we then have

$$J(z) \leq - \int_{L_z} [(\frac{\omega\pi^2}{h^2} - \frac{4k^4}{\lambda})\phi^2] d\eta. \tag{4.30}$$

We now choose  $k$  to be the positive root of the equation

$$\frac{\omega\pi^2}{h^2} - \frac{4k^4}{\lambda} = 0 \quad (4.31)$$

which, since  $\lambda > 0$ , is consistent with the earlier assumption that  $w > 0$ . This is the largest positive value for  $k$  such the right-hand side of (4.30) is nonpositive.

The problem may now be simplified using the following notation. Let

$$k^2 = \frac{\lambda\pi^2}{8}s, \quad \alpha = \frac{1}{2\epsilon_1}. \quad (4.32)$$

The matrix  $\mathbf{D}$  in (4.26) can then be written as

$$\mathbf{D} = \frac{\lambda\pi^2}{2} \begin{bmatrix} 1-s & \frac{s}{\epsilon_2} \\ \frac{s}{\epsilon_2} & 2-\alpha s \end{bmatrix}, \quad (4.33)$$

where  $h = 2$  has been used. The new notation now implies that in order to solve for the positive root  $k$  of (4.31), we must solve for the positive root  $s$  of the equation

$$s^2 = 2\nu \quad (4.34)$$

where

$$\nu = \frac{2w}{\lambda\pi^2} > 0 \quad (4.35)$$

is the minimum eigenvalue of

$$\mathbf{E} = \begin{bmatrix} 1-s & \frac{s}{\epsilon_2} \\ \frac{s}{\epsilon_2} & 2-\alpha s \end{bmatrix}. \quad (4.36)$$

Solving for  $\nu$  in the equation

$$\det|\mathbf{E} - \nu\mathbf{I}| = 0, \quad (4.37)$$

and returning to (4.34), we seek the positive root of

$$s^2 = 3 - (\alpha + 1)s - \sqrt{\{(\alpha - 1)s - 1\}^2 + \frac{4}{\epsilon_2^2}s^2}. \quad (4.38)$$

This is equivalent to seeking the *smallest* positive root of the quartic equation

$$s^4 + 2(\alpha + 1)s^3 + (4\alpha - 6 - \frac{4}{\epsilon_2^2})s^2 - 4(\alpha + 2)s + 8 = 0, \quad (4.39)$$

where, from (4.32),  $\alpha = \frac{1}{2\epsilon_1}$ . Returning to (4.32) thus yields the following value for the nondimensional decay rate  $k$ ,

$$k = \frac{\pi}{2\sqrt{2}}\sqrt{\lambda s}, \quad (4.40)$$

where  $s$  is the smallest positive root of (4.39) and  $\lambda$  is the minimum eigenvalue of (4.18). From (4.18), it can be shown that  $\lambda$  is the smallest root of the characteristic polynomial

$$\lambda^3 - (\frac{1}{2\epsilon_1} + 2)\lambda^2 - (\frac{1}{2\epsilon_2^2} + \frac{1}{2\epsilon_3^2} - 1 - \frac{1}{\epsilon_1})\lambda - \frac{1}{2\epsilon_1} + \frac{1}{2\epsilon_2^2} + \frac{1}{2\epsilon_3^2} = 0. \quad (4.41)$$

With (4.40) as our value for  $k$ , (4.15) implies

$$F(z) \leq F(0)e^{-2kz}, \quad z \geq 0. \quad (4.42)$$

Following exactly the arguments given in Chapter 3 (in (3.42) - (3.47)), with  $E_1(z)$  now representing the anisotropic energy functional (4.5), we obtain

$$E_1(z) \leq 2E_1(0)e^{-2kz}, \quad z \geq 0. \quad (4.43)$$

Again, this can be shown to lead to pointwise estimates for the stresses  $\tau$  such that

$$|\tau(\xi, \eta)| \leq Ke^{-k\xi} \quad \text{for fixed } \eta. \quad (4.44)$$



In the original variables, we obtain a decay estimate for  $\tau$  with exponential decay rate  $\frac{2k^*}{2H}$  where

$$k^* = k \left( \frac{\beta_{11}}{\beta_{22}} \right)^{\frac{1}{4}}. \quad (4.45)$$

While this estimate does not produce an explicit formula for the decay estimate in terms of the parameters  $\epsilon_1, \epsilon_2, \epsilon_3$ , the calculation of  $k$  is a straightforward procedure, involving the solution of the quartic and cubic algebraic equations (4.39) and (4.41) respectively. Numerical results are discussed at the end of this chapter.

This energy method may also be carried out using the nondimensional physical energy  $E_p(z)$  given by (4.4) instead of the mathematical energy  $E_1(z)$ . (Note that the analysis in [4] makes use of the physical strain energy.) The line integral representation of  $E_p(z)$  is easily obtained by using (4.7) and observing that

$$E_p(z) = E_1(z) - \frac{2\beta_{12}}{\sqrt{\beta_{11}\beta_{22}}} \int_{L_s} \phi_{,\xi} \phi_{,\eta\eta} d\eta. \quad (4.46)$$

The steps that follow using  $E_p(z)$  are essentially the same as those presented in the preceding analysis for  $E_1(z)$ , the main difference being that the problem now involves the constants  $\beta_{pq}$  in addition to the parameters  $\epsilon_1, \epsilon_2$  and  $\epsilon_3$ . The end result is that

$$k^* = k \left( \frac{\beta_{11}}{\beta_{22}} \right)^{\frac{1}{4}} = \frac{\pi}{2\sqrt{2}} \sqrt{\lambda s} \left( \frac{\beta_{11}}{\beta_{22}} \right)^{\frac{1}{4}} \quad (4.47)$$

where  $s$  satisfies the quartic equation given by (4.39) but now  $\alpha = \frac{\beta_{66}}{2\sqrt{\beta_{11}\beta_{22}}}$ , and  $\lambda$  is the smallest root of the characteristic polynomial

$$\begin{aligned} \lambda^3 - \left( \frac{\beta_{66}}{2\sqrt{\beta_{11}\beta_{22}}} + 2 \right) \lambda^2 - \left( \frac{1}{2\epsilon_2^2} + \frac{1}{2\epsilon_3^2} - 1 - \frac{\beta_{66}}{\sqrt{\beta_{11}\beta_{22}}} + \frac{\beta_{12}^2}{\beta_{11}\beta_{22}} \right) \lambda \\ - \left[ \frac{1}{\sqrt{\beta_{11}\beta_{22}}} \left( \frac{\beta_{66}}{2} + \frac{\beta_{12}}{\epsilon_2\epsilon_3} - \frac{\beta_{12}^2\beta_{66}}{2\beta_{11}\beta_{22}} \right) - \frac{1}{2\epsilon_2^2} - \frac{1}{2\epsilon_3^2} \right] = 0. \end{aligned} \quad (4.48)$$

Numerical results for this  $E_p(z)$  formulation were calculated and compared with the results from the  $E_1(z)$  formulation (see Discussion of Results section). For all of the materials considered, the difference between the two results is rather insignificant. The mathematical energy  $E_1(z)$  involving the parameters  $\epsilon_1$ ,  $\epsilon_2$  and  $\epsilon_3$  only is algebraically simpler to use than the physical energy  $E_p(z)$ . An advantage, however, to using the energy  $E_p(z)$  is that the results will be applicable to *all physical materials*, while the results using  $E_1(z)$  depend upon the condition (4.9) being satisfied. This condition, which guarantees the positive-definiteness of the mathematical energy norm  $E_1(z)$ , fails to hold for some materials (see Discussion of Results section).

### 4.3 Nonlinear Optimization Estimate

This estimate makes use of three weighted arithmetic-geometric mean inequalities, introducing three new parameters  $\alpha$ ,  $\beta$  and  $\gamma$  into the problem. Using the same function  $F(z)$ , given by (4.10), as in the basic energy estimate, we recall from (4.15) that

$$\begin{aligned}
 J(z) = - \int_{L_x} [ & \phi_{,\xi\xi}^2 + \phi_{,\eta\eta}^2 - \frac{2}{\epsilon_2} \phi_{,\xi\xi} \phi_{,\xi\eta} \\
 & - \frac{2}{\epsilon_3} \phi_{,\xi\eta} \phi_{,\eta\eta} + \frac{1}{\epsilon_1} \phi_{,\xi\eta}^2 + 4k^2 \phi \phi_{,\xi\xi} \\
 & - 4k^2 \phi_{,\xi}^2 - \frac{2k^2}{\epsilon_1} \phi_{,\eta}^2 + \frac{8k^2}{\epsilon_2} \phi_{,\eta} \phi_{,\xi} ] d\eta. \quad (4.49)
 \end{aligned}$$

We seek positive values for  $k$  such that  $J(z) \leq 0$ . From the arithmetic-geometric mean inequalities (3.15) and (3.16), we have the following three results

$$\frac{2}{\epsilon_2} \phi_{,\xi\xi} \phi_{,\xi\eta} \leq \frac{2}{|\epsilon_2|} |\phi_{,\xi\xi}| |\phi_{,\xi\eta}| \leq \frac{1}{|\epsilon_2|} (\alpha \phi_{,\xi\xi}^2 + \frac{1}{\alpha} \phi_{,\xi\eta}^2), \quad (4.50)$$

$$\frac{2}{\epsilon_3} \phi_{,\xi\eta} \phi_{,\eta\eta} \leq \frac{2}{|\epsilon_3|} |\phi_{,\xi\eta}| |\phi_{,\eta\eta}| \leq \frac{1}{|\epsilon_3|} (\beta \phi_{,\eta\eta}^2 + \frac{1}{\beta} \phi_{,\xi\eta}^2), \quad (4.51)$$

$$-\frac{8k^2}{\epsilon_2} \phi_{,\eta} \phi_{,\xi} \leq \frac{8k^2}{|\epsilon_2|} |\phi_{,\eta}| |\phi_{,\xi}| \leq \frac{4k^2}{|\epsilon_2|} (\gamma \phi_{,\eta}^2 + \frac{1}{\gamma} \phi_{,\xi}^2), \quad (4.52)$$

where  $\alpha$ ,  $\beta$  and  $\gamma$  are positive weights to be determined. Using (4.50) - (4.52) in (4.49) we obtain

$$\begin{aligned} J(z) \leq & - \int_{L_z} \left[ \left(1 - \frac{\alpha}{|\epsilon_2|}\right) \phi_{,\xi\xi}^2 + \left(1 - \frac{\beta}{|\epsilon_3|}\right) \phi_{,\eta\eta}^2 \right. \\ & + \left( \frac{1}{\epsilon_1} - \frac{1}{\alpha|\epsilon_2|} - \frac{1}{\beta|\epsilon_3|} \right) \phi_{,\xi\eta}^2 + 4k^2 \phi_{,\xi} \phi_{,\xi\xi} \\ & \left. - 4k^2 \left( \frac{1}{\gamma|\epsilon_2|} + 1 \right) \phi_{,\xi}^2 - 4k^2 \left( \frac{\gamma}{|\epsilon_2|} + \frac{1}{2\epsilon_1} \right) \phi_{,\eta}^2 \right] d\eta. \end{aligned} \quad (4.53)$$

Completing squares in (4.53) leads to the inequality

$$\begin{aligned} J(z) \leq & - \int_{L_z} \left[ \left(1 - \frac{\alpha}{|\epsilon_2|}\right) \left\{ \phi_{,\xi\xi} + \frac{2k^2}{(1 - \frac{\alpha}{|\epsilon_2|})} \phi \right\}^2 - \frac{4k^4}{(1 - \frac{\alpha}{|\epsilon_2|})} \phi^2 \right. \\ & + \left(1 - \frac{\beta}{|\epsilon_3|}\right) \phi_{,\eta\eta}^2 + \left( \frac{1}{\epsilon_1} - \frac{1}{\alpha|\epsilon_2|} - \frac{1}{\beta|\epsilon_3|} \right) \phi_{,\xi\eta}^2 \\ & \left. - 4k^2 \left( \frac{1}{\gamma|\epsilon_2|} + 1 \right) \phi_{,\xi}^2 - 4k^2 \left( \frac{\gamma}{|\epsilon_2|} + \frac{1}{2\epsilon_1} \right) \phi_{,\eta}^2 \right] d\eta, \end{aligned} \quad (4.54)$$

which, on discarding the first term, yields

$$\begin{aligned} J(z) \leq & - \int_{L_z} \left[ \left(1 - \frac{\beta}{|\epsilon_3|}\right) \phi_{,\eta\eta}^2 + \left( \frac{1}{\epsilon_1} - \frac{1}{\alpha|\epsilon_2|} - \frac{1}{\beta|\epsilon_3|} \right) \phi_{,\xi\eta}^2 \right. \\ & - 4k^2 \left( \frac{1}{\gamma|\epsilon_2|} + 1 \right) \phi_{,\xi}^2 - 4k^2 \left( \frac{\gamma}{|\epsilon_2|} + \frac{1}{2\epsilon_1} \right) \phi_{,\eta}^2 \\ & \left. - \frac{4k^4}{(1 - \frac{\alpha}{|\epsilon_2|})} \phi^2 \right] d\eta \end{aligned} \quad (4.55)$$

provided

$$\left(1 - \frac{\alpha}{|\epsilon_2|}\right) > 0. \quad (4.56)$$

Using the inequality (4.24) in (4.55) yields

$$\begin{aligned} J(z) \leq & - \int_{L_x} \left[ \left(1 - \frac{\beta}{|\epsilon_3|}\right) \phi_{,\eta\eta}^2 - 4k^2 \left(\frac{\gamma}{|\epsilon_2|} + \frac{1}{2\epsilon_1}\right) \phi_{,\eta}^2 - \frac{4k^4}{(1 - \frac{\alpha}{|\epsilon_2|})} \phi^2 \right. \\ & \left. + \left\{ \left(\frac{1}{\epsilon_1} - \frac{1}{\alpha|\epsilon_2|} - \frac{1}{\beta|\epsilon_3|}\right) - \frac{4k^2 h^2}{\pi^2} \left(\frac{1}{\gamma|\epsilon_2|} + 1\right) \right\} \phi_{,\xi\eta}^2 \right] d\eta \quad (4.57) \end{aligned}$$

$$\leq - \int_{L_x} \left[ \left(1 - \frac{\beta}{|\epsilon_3|}\right) \phi_{,\eta\eta}^2 - 4k^2 \left(\frac{\gamma}{|\epsilon_2|} + \frac{1}{2\epsilon_1}\right) \phi_{,\eta}^2 - \frac{4k^4}{(1 - \frac{\alpha}{|\epsilon_2|})} \phi^2 \right] d\eta, \quad (4.58)$$

provided

$$\left(\frac{1}{\epsilon_1} - \frac{1}{\alpha|\epsilon_2|} - \frac{1}{\beta|\epsilon_3|}\right) - \frac{4k^2 h^2}{\pi^2} \left(\frac{1}{\gamma|\epsilon_2|} + 1\right) \geq 0. \quad (4.59)$$

Using the Wirtinger inequalities (4.23) and (4.29), we get from (4.58) that

$$J(z) \leq - \int_{L_x} \left[ \left\{ \left(1 - \frac{\beta}{|\epsilon_3|}\right) \frac{4\pi^2}{h^2} - 4k^2 \left(\frac{\gamma}{|\epsilon_2|} + \frac{1}{2\epsilon_1}\right) - \frac{4k^4 h^2}{(1 - \frac{\alpha}{|\epsilon_2|})\pi^2} \right\} \phi_{,\eta}^2 \right] d\eta \quad (4.60)$$

provided

$$\left(1 - \frac{\beta}{|\epsilon_3|}\right) \geq 0. \quad (4.61)$$

We now seek the maximum positive  $k$  such that  $J(z) \leq 0$  i.e., from (4.60), the maximum positive  $k$  such that

$$k^4 + \frac{\pi^2}{h^2} \left(1 - \frac{\alpha}{|\epsilon_2|}\right) \left(\frac{\gamma}{|\epsilon_2|} + \frac{1}{2\epsilon_1}\right) k^2 - \left(1 - \frac{\alpha}{|\epsilon_2|}\right) \left(1 - \frac{\beta}{|\epsilon_3|}\right) \frac{\pi^4}{h^4} \leq 0. \quad (4.62)$$

It is clear that the maximum value for  $k$  occurs when equality is chosen in (4.62), which upon using the quadratic formula yields

$$2k^2 = -\frac{\pi^2}{h^2} \left(1 - \frac{\alpha}{|\epsilon_2|}\right) \left(\frac{\gamma}{|\epsilon_2|} + \frac{1}{2\epsilon_1}\right) + \frac{\pi^2}{h^2} \sqrt{\left(1 - \frac{\alpha}{|\epsilon_2|}\right)^2 \left(\frac{\gamma}{|\epsilon_2|} + \frac{1}{2\epsilon_1}\right)^2 + 4 \left(1 - \frac{\alpha}{|\epsilon_2|}\right) \left(1 - \frac{\beta}{|\epsilon_3|}\right)}. \quad (4.63)$$

Equation (4.63) guarantees a positive value for  $k^2$  due to the conditions (4.56) and (4.61), which in turn guarantees a *real* value for  $k$ . We observe that the formula for  $k$  given by (4.63) involves the parameters  $\alpha$ ,  $\beta$  and  $\gamma$  which have not yet been determined. It remains to choose positive values for these parameters such that  $k$  is maximized and such that the conditions (4.56), (4.59) and (4.61) hold. Since  $k$  given by (4.63) is a nonlinear function of the parameters  $\alpha$ ,  $\beta$  and  $\gamma$ , and the constraints (4.56), (4.59) and (4.61) also involve nonlinear functions of these parameters, this formulation is called *the nonlinear optimization estimate*.

We observe that the constraints (4.56) and (4.61) may always be satisfied by a proper choice of  $\alpha$  and  $\beta$ . The constraint (4.59), however, involves  $k$  as well as  $\alpha$ ,  $\beta$ ,  $\gamma$ , and may or may not be satisfied by the choice of  $k^2$  in (4.63). If  $\alpha$ ,  $\beta$  and  $\gamma$  are chosen such that the constraints (4.56), (4.59) and (4.61) are satisfied with  $k$  given by (4.63), then this value of  $k$  is a valid estimated decay rate. If (4.56) and (4.61) are satisfied by this choice of  $k$  but (4.59) is not, then instead of (4.63), we choose

$$k^2 = \left(\frac{1}{\epsilon_1} - \frac{1}{\alpha|\epsilon_2|} - \frac{1}{\beta|\epsilon_3|}\right) \left(\frac{1}{\left(\frac{1}{\gamma|\epsilon_2|} + 1\right)}\right) \frac{\pi^2}{4h^2}, \quad (4.64)$$

and so equality holds in (4.59). It is easily verified that  $k$  given by (4.64) satisfies (4.62).

Equations (4.63) and (4.64) give two separate formulae for the estimated decay rate dependent on the choices of  $\alpha$ ,  $\beta$  and  $\gamma$  and valid under differing conditions. Furthermore, while there are many choices for  $\alpha$ ,  $\beta$  and  $\gamma$  which yield a valid estimated decay rate, we need a method to determine the proper choices of  $\alpha$ ,  $\beta$  and  $\gamma$  which yield the optimal decay rate. The two formulae (4.63) and (4.64) lead to two optimization formulations which will now be analyzed to determine the largest value for  $k$ .

### 4.3.1 Nonlinear Optimization Analysis

Of the three constraints (4.56), (4.59), and (4.61), that must be satisfied for the nonlinear optimization estimate, two of them, (4.56) and (4.61), may always be satisfied by proper choices of  $\alpha$  and  $\beta$ . The remaining constraint (4.59) may be equivalently expressed as the following two reduced conditions,

$$\left( \frac{1}{\epsilon_1} - \frac{1}{\alpha|\epsilon_2|} - \frac{1}{\beta|\epsilon_3|} \right) \geq 0, \quad (4.65)$$

$$k^2 \leq \frac{\pi^2}{4h^2} \left( \frac{1}{\epsilon_1} - \frac{1}{\alpha|\epsilon_2|} - \frac{1}{\beta|\epsilon_3|} \right) \frac{1}{\left( \frac{1}{\gamma|\epsilon_2|} + 1 \right)}, \quad (4.66)$$

where (4.65) is necessary in order for  $k^2$  to be nonnegative. From (4.56) and (4.61), we have

$$\alpha < |\epsilon_2| \quad \Rightarrow \quad \frac{1}{\alpha} > \frac{1}{|\epsilon_2|}, \quad (4.67)$$

$$\beta \leq |\epsilon_3| \quad \Rightarrow \quad \frac{1}{\beta} \geq \frac{1}{|\epsilon_3|}, \quad (4.68)$$

which in turn yield

$$\left( \frac{1}{\epsilon_1} - \frac{1}{\alpha|\epsilon_2|} - \frac{1}{\beta|\epsilon_3|} \right) < \left( \frac{1}{\epsilon_1} - \frac{1}{\epsilon_2^2} - \frac{1}{\epsilon_3^2} \right), \quad (4.69)$$

where we observe that right-hand side of (4.69) is positive due to the positive-definite assumption (4.9) on the the energy functional  $E_1(z)$ . As long as the right-hand side of (4.69) is strictly positive, we are guaranteed that there is *some* choice of  $\alpha$  and  $\beta$  for which (4.65) is satisfied. The remaining constraint (4.66) may or may not be satisfied by a proper choice of  $\gamma$ , and thus determines which of the two formulae (4.63) or (4.64) is valid. We then have the following two optimization formulations:

*Optimization Problem 1:*

$$\begin{aligned} \text{Maximize } F(\alpha, \beta, \gamma) = k^2 = & -\frac{\pi^2}{2h^2} \left( 1 - \frac{\alpha}{|\epsilon_2|} \right) \left( \frac{\gamma}{|\epsilon_2|} + \frac{1}{2\epsilon_1} \right) \\ & + \frac{\pi^2}{2h^2} \sqrt{\left( 1 - \frac{\alpha}{|\epsilon_2|} \right)^2 \left( \frac{\gamma}{|\epsilon_2|} + \frac{1}{2\epsilon_1} \right)^2 + 4 \left( 1 - \frac{\alpha}{|\epsilon_2|} \right) \left( 1 - \frac{\beta}{|\epsilon_3|} \right)} \end{aligned} \quad (4.70)$$

subject to

$$\left( 1 - \frac{\alpha}{|\epsilon_2|} \right) > 0 \quad (4.71)$$

$$\left( 1 - \frac{\beta}{|\epsilon_3|} \right) \geq 0 \quad (4.72)$$

$$\left( \frac{1}{\epsilon_1} - \frac{1}{\alpha|\epsilon_2|} - \frac{1}{\beta|\epsilon_3|} \right) \geq 0 \quad (4.73)$$

and

$$\begin{aligned} & \left( 1 - \frac{\alpha}{|\epsilon_2|} \right) \left( \frac{\gamma}{|\epsilon_2|} + \frac{1}{2\epsilon_1} \right) \left( \frac{1}{\epsilon_1} - \frac{1}{\alpha|\epsilon_2|} - \frac{1}{\beta|\epsilon_3|} \right) \left( \frac{\gamma|\epsilon_2|}{1 + \gamma|\epsilon_2|} \right) \\ & + \frac{1}{4} \left( \frac{1}{\epsilon_1} - \frac{1}{\alpha|\epsilon_2|} - \frac{1}{\beta|\epsilon_3|} \right)^2 \left( \frac{\gamma|\epsilon_2|}{1 + \gamma|\epsilon_2|} \right)^2 - 4 \left( 1 - \frac{\alpha}{|\epsilon_2|} \right) \left( 1 - \frac{\beta}{|\epsilon_3|} \right) \geq 0. \end{aligned} \quad (4.74)$$

*Optimization Problem 2:*

$$\text{Maximize } G(\alpha, \beta, \gamma) = k^2 = \frac{\pi^2}{4h^2} \left( \frac{1}{\epsilon_1} - \frac{1}{\alpha|\epsilon_2|} - \frac{1}{\beta|\epsilon_3|} \right) \left( \frac{\gamma|\epsilon_2|}{1 + \gamma|\epsilon_2|} \right) \quad (4.75)$$

*subject to*

$$\left( 1 - \frac{\alpha}{|\epsilon_2|} \right) > 0 \quad (4.76)$$

$$\left( 1 - \frac{\beta}{|\epsilon_3|} \right) \geq 0 \quad (4.77)$$

$$\left( \frac{1}{\epsilon_1} - \frac{1}{\alpha|\epsilon_2|} - \frac{1}{\beta|\epsilon_3|} \right) \geq 0 \quad (4.78)$$

*and*

$$\begin{aligned} & \left( 1 - \frac{\alpha}{|\epsilon_2|} \right) \left( \frac{\gamma}{|\epsilon_2|} + \frac{1}{2\epsilon_1} \right) \left( \frac{1}{\epsilon_1} - \frac{1}{\alpha|\epsilon_2|} - \frac{1}{\beta|\epsilon_3|} \right) \left( \frac{\gamma|\epsilon_2|}{1 + \gamma|\epsilon_2|} \right) \\ & + \frac{1}{4} \left( \frac{1}{\epsilon_1} - \frac{1}{\alpha|\epsilon_2|} - \frac{1}{\beta|\epsilon_3|} \right)^2 \left( \frac{\gamma|\epsilon_2|}{1 + \gamma|\epsilon_2|} \right)^2 - 4 \left( 1 - \frac{\alpha}{|\epsilon_2|} \right) \left( 1 - \frac{\beta}{|\epsilon_3|} \right) < 0. \end{aligned} \quad (4.79)$$

Condition (4.74) results from using (4.63) in (4.66) and condition (4.79) is the inequality that results when (4.74) is not satisfied.

To maximize the functions  $F(\alpha, \beta, \gamma)$  and  $G(\alpha, \beta, \gamma)$ , we now look at their partial derivatives with respect to the parameters  $\alpha, \beta$  and  $\gamma$ . From (4.70), it can be shown that

$$F_{,\alpha} < 0, \quad F_{,\beta} < 0, \quad F_{,\gamma} < 0. \quad (4.80)$$

Similarly from (4.75), it can be shown that

$$G_{,\alpha} > 0, \quad G_{,\beta} > 0, \quad G_{,\gamma} > 0. \quad (4.81)$$



Thus to maximize  $F(\alpha, \beta, \gamma)$  we seek the smallest possible values of  $\alpha, \beta$  and  $\gamma$  while to maximize  $G(\alpha, \beta, \gamma)$  we seek the largest possible values of  $\alpha, \beta$  and  $\gamma$ . It will now be shown that in fact the choices of  $\alpha, \beta, \gamma$ , call them  $\alpha^*, \beta^*$  and  $\gamma^*$ , which maximize  $F$  also maximize  $G$ .

For fixed values of  $\alpha$  and  $\beta$  such that (4.71) - (4.73) are satisfied,  $F$  is a *decreasing* function of  $\gamma$  and hence the choice  $\gamma_F^*$  which maximizes  $F$  is the *smallest* positive  $\gamma$  such that (4.74) is still satisfied. For fixed  $\alpha$  and  $\beta$ , the smallest positive  $\gamma$  for which (4.74) is satisfied occurs when equality is taken, yielding a cubic polynomial in  $\gamma$  with one positive root  $\gamma_F^*$ . At this value of  $\gamma = \gamma_F^*$ , the functions  $F(\alpha, \beta, \gamma)$  and  $G(\alpha, \beta, \gamma)$  are identical (recall that (4.74) results from (4.66)) and both are valid decay estimates. As  $\gamma$  decreases below  $\gamma_F^*$ , (4.79) is satisfied and  $G$  becomes the valid decay estimate. With  $\alpha$  and  $\beta$  still fixed such that (4.76) - (4.78) are satisfied,  $G$  is an *increasing* function of  $\gamma$  and the choice  $\gamma_G^*$  which maximizes  $G$  is the *largest* positive  $\gamma$  such that (4.79) is satisfied, i.e.

$$\gamma_G^* = \gamma_F^* \equiv \gamma^*. \quad (4.82)$$

Furthermore, we have

$$F(\alpha, \beta, \gamma^*) \equiv G(\alpha, \beta, \gamma^*). \quad (4.83)$$

So for *fixed values* of  $\alpha$  and  $\beta$ , the optimal choice  $\gamma^*$ , which maximizes both  $F$  and  $G$ , is found from computing the positive root of a cubic polynomial and, since  $F$  and  $G$  are identical at this choice of  $\gamma^*$ ,  $k$  is obtained from *either* (4.70) or (4.75), using  $h = 2$ . It then follows that over the *full range* of  $\alpha, \beta$  and  $\gamma$ , the choices  $\alpha^*, \beta^*$  and  $\gamma^*$  which maximize  $F$  also maximize  $G$  and that the two functions are identical at

these values.

While (4.70) and (4.75) yield two explicit formulae for a decay estimate, they are in terms of three parameters that must be optimally chosen and a numerical procedure was necessary to do this. A program was implemented to run through the possible ranges of the parameters  $\alpha$  and  $\beta$ , obtained from (4.71) - (4.73) or equivalently (4.76) - (4.78), and compute an optimal value  $k$  for each pair of  $\alpha$  and  $\beta$  (in the manner previously described), and thus an optimal  $k$  over the entire range of  $\alpha$ ,  $\beta$  and  $\gamma$ . The optimal decay estimate  $k$  in the nondimensional domain was then transformed back into the original domain so that

$$k^* = k \left( \frac{\beta_{11}}{\beta_{22}} \right)^{\frac{1}{4}} \quad (4.84)$$

and the stresses  $\tau$  have an exponential decay rate of  $\frac{2k^*}{2H}$ . These results are shown at the end of the chapter. It is observed that while this nonlinear optimization estimate produces explicit formulae for the estimated decay rate in terms of parameters which may be optimally chosen numerically, the formulae (4.70) and (4.75) will be different for each material since the parameters  $\alpha$ ,  $\beta$  and  $\gamma$  must be optimally chosen in each case. This is in contrast to the formulae (3.51), (3.55) and (3.102) obtained in Chapter 3 for orthotropic materials. These formulae did not change from one material to another. Ideally, we would like to determine the optimal choices of  $\alpha$ ,  $\beta$  and  $\gamma$  analytically in terms of the material parameters  $\epsilon_1$ ,  $\epsilon_2$  and  $\epsilon_3$ . Then the formulae (4.70) and (4.75) would be explicit in terms of  $\epsilon_1$ ,  $\epsilon_2$  and  $\epsilon_3$  and valid for all materials satisfying (4.9).

If we now consider the orthotropic limit for which  $\frac{1}{\epsilon_2}, \frac{1}{\epsilon_3} \rightarrow 0$ , this nonlinear optimization formulation reduces to the following:

*Problem 1*

$$k^2 = -\frac{\pi^2}{4h^2\epsilon_1} + \frac{\pi^2}{2h^2}\sqrt{\frac{1}{4\epsilon_1^2} + 4} \quad (4.85)$$

where

$$\frac{1}{\epsilon_1} \geq 0 \quad \text{and} \quad \frac{3}{4\epsilon_1^2} - 4 \geq 0. \quad (4.86)$$

$$\Rightarrow k = \frac{\pi}{2h\sqrt{\epsilon_1}} \left( \sqrt{1 + 16\epsilon_1^2} - 1 \right)^{\frac{1}{2}}, \quad \epsilon_1 \leq \frac{\sqrt{3}}{4}. \quad (4.87)$$

*Problem 2*

$$k^2 = \frac{\pi^2}{4h^2\epsilon_1} \quad (4.88)$$

where

$$\frac{1}{\epsilon_1} \geq 0 \quad \text{and} \quad \frac{3}{4\epsilon_1^2} - 4 < 0. \quad (4.89)$$

$$\Rightarrow k = \frac{\pi}{2h\sqrt{\epsilon_1}}, \quad \epsilon_1 > \frac{\sqrt{3}}{4}. \quad (4.90)$$

On comparing (4.87) and (4.90) with (3.49), we see that in the orthotropic limit the nonlinear optimization estimate reduces to the analytic estimate (3.49) developed in Chapter 3. This is not unexpected as the methods used to develop the two estimates are similar.

An alternative formulation for this nonlinear optimization method may be obtained using the physical energy  $E_p(z)$ , given by (4.4), instead of the energy functional  $E_1(z)$ . This leads to a nonlinear optimization estimate in *four* parameters  $\alpha$ ,  $\beta$ ,  $\gamma$  and  $\delta$  characterized by the following two problems:

*Optimization Problem 1:*

$$\begin{aligned} \text{Maximize } F(\alpha, \beta, \gamma, \delta) = k^2 = & -\frac{\pi^2}{2h^2} \left(1 - \frac{\alpha}{|\epsilon_2|} - \frac{|\beta_{12}|\delta}{\sqrt{\beta_{11}\beta_{22}}}\right) \left(\frac{\gamma}{|\epsilon_2|} + \frac{\beta_{66}}{2\sqrt{\beta_{11}\beta_{22}}}\right) \\ & + \frac{\pi^2}{2h^2} \left[ \left(1 - \frac{\alpha}{|\epsilon_2|} - \frac{|\beta_{12}|\delta}{\sqrt{\beta_{11}\beta_{22}}}\right)^2 \left(\frac{\gamma}{|\epsilon_2|} + \frac{\beta_{66}}{2\sqrt{\beta_{11}\beta_{22}}}\right)^2 \right. \\ & \left. + 4 \left(1 - \frac{\alpha}{|\epsilon_2|} - \frac{|\beta_{12}|\delta}{\sqrt{\beta_{11}\beta_{22}}}\right) \left(1 - \frac{\beta}{|\epsilon_3|} - \frac{|\beta_{12}|}{\delta\sqrt{\beta_{11}\beta_{22}}}\right) \right]^{\frac{1}{2}} \end{aligned} \quad (4.91)$$

subject to

$$\left(1 - \frac{\alpha}{|\epsilon_2|} - \frac{|\beta_{12}|\delta}{\sqrt{\beta_{11}\beta_{22}}}\right) > 0 \quad (4.92)$$

$$\left(1 - \frac{\beta}{|\epsilon_3|} - \frac{|\beta_{12}|}{\delta\sqrt{\beta_{11}\beta_{22}}}\right) \geq 0 \quad (4.93)$$

$$\left(\frac{\beta_{66}}{\sqrt{\beta_{11}\beta_{22}}} - \frac{1}{\alpha|\epsilon_2|} - \frac{1}{\beta|\epsilon_3|}\right) \geq 0 \quad (4.94)$$

and

$$\begin{aligned} & \left(1 - \frac{\alpha}{|\epsilon_2|} - \frac{|\beta_{12}|\delta}{\sqrt{\beta_{11}\beta_{22}}}\right) \left(\frac{\gamma}{|\epsilon_2|} + \frac{\beta_{66}}{2\sqrt{\beta_{11}\beta_{22}}}\right) \left(\frac{\beta_{66}}{\sqrt{\beta_{11}\beta_{22}}} - \frac{1}{\alpha|\epsilon_2|} - \frac{1}{\beta|\epsilon_3|}\right) \left(\frac{\gamma|\epsilon_2|}{1 + \gamma|\epsilon_2|}\right) \\ & + \frac{1}{4} \left(\frac{\beta_{66}}{\sqrt{\beta_{11}\beta_{22}}} - \frac{1}{\alpha|\epsilon_2|} - \frac{1}{\beta|\epsilon_3|}\right)^2 \left(\frac{\gamma|\epsilon_2|}{1 + \gamma|\epsilon_2|}\right)^2 \\ & - 4 \left(1 - \frac{\alpha}{|\epsilon_2|} - \frac{|\beta_{12}|\delta}{\sqrt{\beta_{11}\beta_{22}}}\right) \left(1 - \frac{\beta}{|\epsilon_3|} - \frac{|\beta_{12}|}{\delta\sqrt{\beta_{11}\beta_{22}}}\right) \geq 0. \end{aligned} \quad (4.95)$$

*Optimization Problem 2:*

$$\text{Maximize } G(\alpha, \beta, \gamma, \delta) = k^2 = \frac{\pi^2}{4h^2} \left( \frac{\beta_{66}}{\sqrt{\beta_{11}\beta_{22}}} - \frac{1}{\alpha|\epsilon_2|} - \frac{1}{\beta|\epsilon_3|} \right) \left( \frac{\gamma|\epsilon_2|}{1 + \gamma|\epsilon_2|} \right) \quad (4.96)$$

subject to

$$\left( 1 - \frac{\alpha}{|\epsilon_2|} - \frac{|\beta_{12}|\delta}{\sqrt{\beta_{11}\beta_{22}}} \right) > 0 \quad (4.97)$$

$$\left( 1 - \frac{\beta}{|\epsilon_3|} - \frac{|\beta_{12}|}{\delta\sqrt{\beta_{11}\beta_{22}}} \right) \geq 0 \quad (4.98)$$

$$\left( \frac{\beta_{66}}{\sqrt{\beta_{11}\beta_{22}}} - \frac{1}{\alpha|\epsilon_2|} - \frac{1}{\beta|\epsilon_3|} \right) \geq 0 \quad (4.99)$$

and

$$\begin{aligned} & \left( 1 - \frac{\alpha}{|\epsilon_2|} - \frac{|\beta_{12}|\delta}{\sqrt{\beta_{11}\beta_{22}}} \right) \left( \frac{\gamma}{|\epsilon_2|} + \frac{\beta_{66}}{2\sqrt{\beta_{11}\beta_{22}}} \right) \left( \frac{\beta_{66}}{\sqrt{\beta_{11}\beta_{22}}} - \frac{1}{\alpha|\epsilon_2|} - \frac{1}{\beta|\epsilon_3|} \right) \left( \frac{\gamma|\epsilon_2|}{1 + \gamma|\epsilon_2|} \right) \\ & + \frac{1}{4} \left( \frac{\beta_{66}}{\sqrt{\beta_{11}\beta_{22}}} - \frac{1}{\alpha|\epsilon_2|} - \frac{1}{\beta|\epsilon_3|} \right)^2 \left( \frac{\gamma|\epsilon_2|}{1 + \gamma|\epsilon_2|} \right)^2 \\ & - 4 \left( 1 - \frac{\alpha}{|\epsilon_2|} - \frac{|\beta_{12}|\delta}{\sqrt{\beta_{11}\beta_{22}}} \right) \left( 1 - \frac{\beta}{|\epsilon_3|} - \frac{|\beta_{12}|}{\delta\sqrt{\beta_{11}\beta_{22}}} \right) < 0. \end{aligned} \quad (4.100)$$

Numerical results were calculated for this  $E_p(z)$  formulation and compared with the  $E_1(z)$  formulation. As was the case previously for the basic energy estimate, the difference between the two energy formulations was insignificant and it is clear that the  $E_1(z)$  formulation is much simpler to work with, keeping in mind however that the physical energy formulation has a wider range of applicability.

## 4.4 Higher-Order Energy Estimates

In this section we adapt the conservation law approach, developed for orthotropic materials in Chapter 3, to anisotropic materials, making use of the higher-order energy functional  $E_2(z)$ . Thus for the estimates that follow, both of the anisotropic energies  $E_1(z)$  and  $E_2(z)$  given by (4.5) and (4.6) are used. Let the function  $F(z)$  be defined by

$$F(z) = [E_2(z) + mE_1(z)] + 2k \int_z^\infty [E_2(s) + mE_1(s)] ds, \quad (4.101)$$

where  $m$  and  $k$  are both positive constants to be determined. With  $F(z)$  defined in (4.101), we have

$$F'(z) + 2kF(z) = E_2'(z) + mE_1'(z) + 4k^2 \int_z^\infty [E_2(s) + mE_1(s)] ds. \quad (4.102)$$

We now wish to express the quantities  $E_2'(z)$  and  $\int_z^\infty E_2(s)ds$  as line integrals, as was done previously for  $E_1'(z)$  and  $\int_z^\infty E_1(s)ds$  in the basic energy estimate of section 4.2.

From its definition in (4.6), and using (3.20), we obtain a line integral representation for  $E_2'(z)$  as

$$E_2'(z) = - \int_{L_z} [\phi_{,\xi\xi\xi}^2 - \frac{2}{\epsilon_2} \phi_{,\xi\xi\xi} \phi_{,\xi\xi\eta} + \frac{1}{\epsilon_1} \phi_{,\xi\xi\eta}^2 - \frac{2}{\epsilon_3} \phi_{,\xi\eta\eta} \phi_{,\xi\xi\eta} + \phi_{,\xi\eta\eta}^2] d\eta. \quad (4.103)$$

Recalling (4.8), we obtain

$$E_2(z) = \frac{d}{dz} \int_{R_z} [\phi_{,\xi\xi} \phi_{,\xi\xi\xi} - \phi_{,\xi\eta} \phi_{,\eta\eta\eta}] dA, \quad (4.104)$$

which, when integrated and combined with the divergence theorem and boundary conditions, yields

$$\begin{aligned}\int_z^\infty E_2(s)ds &= -\int_{R_z} [\phi_{,\xi\xi}\phi_{,\xi\xi\xi} - \phi_{,\xi\eta}\phi_{,\eta\eta\eta}] dA \\ &= \int_{L_z} \left[ \frac{\phi_{,\xi\xi}^2}{2} + \frac{\phi_{,\eta\eta}^2}{2} \right] d\eta.\end{aligned}\quad (4.105)$$

We observe that (4.105) is identical to (3.60) obtained for the orthotropic case in section 3.4, i.e. the quantity  $\int_z^\infty E_2(s)ds$  has the same line integral representation regardless of whether  $E_2(s)$  is the *orthotropic* functional (3.8) or the *anisotropic* functional (4.6). This is because the line integral representation (4.8) for the anisotropic energy functional  $E_2(z)$  is independent of any material parameters. Substituting (4.12), (4.14), (4.103) and (4.105) into (4.102) results in

$$\begin{aligned}F'(z) + 2kF(z) &= -\int_{L_z} \left[ \phi_{,\xi\xi\xi}^2 + \phi_{,\xi\eta\eta}^2 - \frac{2}{\epsilon_2}\phi_{,\xi\xi\xi}\phi_{,\xi\xi\eta} - \frac{2}{\epsilon_3}\phi_{,\xi\eta\eta}\phi_{,\xi\xi\eta} \right. \\ &\quad + \frac{1}{\epsilon_1}\phi_{,\xi\xi\eta}^2 + (m - 2k^2)\phi_{,\xi\xi}^2 + (m - 2k^2)\phi_{,\eta\eta}^2 \\ &\quad - \frac{2m}{\epsilon_2}\phi_{,\xi\xi}\phi_{,\xi\eta} - \frac{2m}{\epsilon_3}\phi_{,\eta\eta}\phi_{,\xi\eta} + \frac{m}{\epsilon_1}\phi_{,\xi\eta}^2 - 4k^2m\phi_{,\xi}^2 \\ &\quad \left. + 4k^2m\phi\phi_{,\xi\xi} + \frac{8k^2m}{\epsilon_2}\phi_{,\xi}\phi_{,\eta} - \frac{2k^2m}{\epsilon_1}\phi_{,\eta}^2 \right] d\eta \\ &= -J(z).\end{aligned}\quad (4.106)$$

We will now investigate several methods to obtain positive values for  $m$  and  $k$  such that  $J(z)$  is nonnegative. This in turn yields the exponential decay estimate

$$F(z) \leq F(0)e^{-2kz}, \quad z \geq 0, \quad (4.107)$$

which, by following exactly the arguments outlined in (3.85) - (3.89), leads to bounds

on the energy functionals of the form

$$E_1(z) \leq 2 \left[ E_1(0) + \frac{1}{m} E_2(0) \right] e^{-2kz}, \quad z \geq 0, \quad (4.108)$$

$$E_2(z) \leq 2 [E_2(0) + m E_1(0)] e^{-2kz}, \quad z \geq 0, \quad (4.109)$$

where  $E_1(z)$  and  $E_2(z)$  now represent the anisotropic energy functionals. Again, the results (4.108) and (4.109) can be used to derive pointwise estimates for the stresses  $\tau$  such that

$$|\tau(\xi, \eta)| \leq K e^{-k\xi} \quad \text{for fixed } \eta. \quad (4.110)$$

#### 4.4.1 Quadratic Estimate

This estimate, while modelled after the conservation law approach of Chapter 3, does not actually involve either of the anisotropic conservation properties (4.2) or (4.3). It does however use the combination of energy functionals  $E_1(z)$  and  $E_2(z)$  that was used in Chapter 3 for the orthotropic conservation law estimate. The result is a somewhat simpler *quadratic* polynomial for  $m$  in contrast to the *sixth-order* polynomial developed in the orthotropic conservation law estimate.

Starting with (4.106) and completing squares, we obtain

$$\begin{aligned} J(z) = \int_{L_x} & \left[ \left( \phi_{,\xi\xi\xi} - \frac{1}{\epsilon_2} \phi_{,\xi\xi\eta} \right)^2 - \frac{1}{\epsilon_2^2} \phi_{,\xi\xi\eta}^2 + \left( \phi_{,\xi\eta\eta} - \frac{1}{\epsilon_3} \phi_{,\xi\xi\eta} \right)^2 - \frac{1}{\epsilon_3^2} \phi_{,\xi\xi\eta}^2 \right. \\ & + \frac{1}{\epsilon_1} \phi_{,\xi\xi\eta}^2 + (m - 2k^2) \phi_{,\xi\xi}^2 + (m - 2k^2) \phi_{,\eta\eta}^2 \\ & - \frac{2m}{\epsilon_2} \phi_{,\xi\xi} \phi_{,\xi\eta} - \frac{2m}{\epsilon_3} \phi_{,\eta\eta} \phi_{,\xi\eta} + \frac{m}{\epsilon_1} \phi_{,\xi\eta}^2 - 4k^2 m \phi_{,\xi}^2 \\ & \left. + 4k^2 m \phi \phi_{,\xi\xi} + \frac{8k^2 m}{\epsilon_2} \phi_{,\xi} \phi_{,\eta} - \frac{2k^2 m}{\epsilon_1} \phi_{,\eta}^2 \right] d\eta \end{aligned} \quad (4.111)$$



which, upon dropping the first and third terms, results in

$$\begin{aligned}
 J(z) \geq \int_{L_x} \left[ \left( \frac{1}{\epsilon_1} - \frac{1}{\epsilon_2^2} - \frac{1}{\epsilon_3^2} \right) \phi_{,\xi\xi\eta}^2 - 2k^2 \phi_{,\xi\xi}^2 - 2k^2 \phi_{,\eta\eta}^2 \right. \\
 + m(\phi_{,\xi\xi}^2 + \phi_{,\eta\eta}^2 - \frac{2}{\epsilon_2} \phi_{,\xi\xi} \phi_{,\xi\eta} - \frac{2}{\epsilon_3} \phi_{,\eta\eta} \phi_{,\xi\eta} + \frac{1}{\epsilon_1} \phi_{,\xi\eta}^2) \\
 \left. - 4k^2 m \phi_{,\xi}^2 + 4k^2 m \phi \phi_{,\xi\xi} + \frac{8k^2 m}{\epsilon_2} \phi_{,\xi} \phi_{,\eta} - \frac{2k^2 m}{\epsilon_1} \phi_{,\eta}^2 \right] d\eta. \quad (4.112)
 \end{aligned}$$

Completing squares again yields

$$\begin{aligned}
 J(z) \geq \int_{L_x} \left[ \left( \frac{1}{\epsilon_1} - \frac{1}{\epsilon_2^2} - \frac{1}{\epsilon_3^2} \right) \phi_{,\xi\xi\eta}^2 - 2k^2 \phi_{,\xi\xi}^2 - 2k^2 \phi_{,\eta\eta}^2 \right. \\
 + m \left\{ \left( \phi_{,\xi\xi} - \frac{1}{\epsilon_2} \phi_{,\xi\eta} \right)^2 - \frac{1}{\epsilon_2^2} \phi_{,\xi\eta}^2 + \phi_{,\eta\eta}^2 - \frac{2}{\epsilon_3} \phi_{,\eta\eta} \phi_{,\xi\eta} + \frac{1}{\epsilon_1} \phi_{,\xi\eta}^2 \right\} \\
 \left. - 4k^2 m \phi_{,\xi}^2 + 4k^2 m \phi \phi_{,\xi\xi} + \frac{8k^2 m}{\epsilon_2} \phi_{,\xi} \phi_{,\eta} - \frac{2k^2 m}{\epsilon_1} \phi_{,\eta}^2 \right] d\eta \quad (4.113)
 \end{aligned}$$

which upon dropping the completed square term gives

$$\begin{aligned}
 J(z) \geq \int_{L_x} \left[ \left( \frac{1}{\epsilon_1} - \frac{1}{\epsilon_2^2} - \frac{1}{\epsilon_3^2} \right) \phi_{,\xi\xi\eta}^2 - 2k^2 \phi_{,\xi\xi}^2 + (m - 2k^2) \phi_{,\eta\eta}^2 \right. \\
 + m \left( \frac{1}{\epsilon_1} - \frac{1}{\epsilon_2^2} \right) \phi_{,\xi\eta}^2 - \frac{2m}{\epsilon_3} \phi_{,\eta\eta} \phi_{,\xi\eta} - 4k^2 m \phi_{,\xi}^2 \\
 \left. + 4k^2 m \phi \phi_{,\xi\xi} + \frac{8k^2 m}{\epsilon_2} \phi_{,\xi} \phi_{,\eta} - \frac{2k^2 m}{\epsilon_1} \phi_{,\eta}^2 \right] d\eta. \quad (4.114)
 \end{aligned}$$

Next, we use several Wirtinger inequalities to simplify the expression for  $J(z)$ . Using

(4.23) and (4.24) in addition to (3.70) from Chapter 3, we obtain

$$\begin{aligned}
 J(z) \geq \int_{L_x} \left[ \left\{ \left( \frac{1}{\epsilon_1} - \frac{1}{\epsilon_2^2} - \frac{1}{\epsilon_3^2} \right) \frac{\pi^2}{h^2} - 2k^2 \right\} \phi_{,\xi\xi}^2 + \left\{ m - 2k^2 - \frac{2k^2 m h^2}{4\pi^2 \epsilon_1} \right\} \phi_{,\eta\eta}^2 \right. \\
 + \left\{ m \left( \frac{1}{\epsilon_1} - \frac{1}{\epsilon_2^2} \right) - \frac{4k^2 m h^2}{\pi^2} \right\} \phi_{,\xi\eta}^2 \\
 \left. + 4k^2 m \phi \phi_{,\xi\xi} + \frac{8k^2 m}{\epsilon_2} \phi_{,\xi} \phi_{,\eta} - \frac{2m}{\epsilon_3} \phi_{,\eta\eta} \phi_{,\xi\eta} \right] d\eta. \quad (4.115)
 \end{aligned}$$

Using the arithmetic-geometric mean inequalities (3.15) and (3.16), we have, for arbitrary constants  $\beta, \gamma, \alpha > 0$ ,

$$\int_{L_x} \frac{8k^2 m}{\epsilon_2} \phi_{,\xi} \phi_{,\eta} d\eta \geq - \int_{L_x} \frac{4k^2 m}{|\epsilon_2|} [\beta \phi_{,\xi}^2 + \frac{1}{\beta} \phi_{,\eta}^2] d\eta, \quad (4.116)$$

$$- \int_{L_x} \frac{2m}{\epsilon_3} \phi_{,\eta\eta} \phi_{,\xi\eta} d\eta \geq - \int_{L_x} \frac{m}{|\epsilon_3|} [\gamma \phi_{,\eta\eta}^2 + \frac{1}{\gamma} \phi_{,\xi\eta}^2] d\eta, \quad (4.117)$$

$$\begin{aligned} \int_{L_x} 4k^2 m \phi \phi_{,\xi\xi} d\eta &\geq - \int_{L_x} 2k^2 m [\alpha \phi^2 + \frac{1}{\alpha} \phi_{,\xi\xi}^2] d\eta \\ &> - \int_{L_x} 2k^2 m \left[ \frac{h^4}{\pi^4 (\frac{3}{2})^4} \alpha \phi_{,\eta\eta}^2 + \frac{1}{\alpha} \phi_{,\xi\xi}^2 \right] d\eta, \end{aligned} \quad (4.118)$$

where the last inequality follows on using (3.14), with  $w = \phi$ . Substituting these inequalities into (4.115) yields

$$\begin{aligned} J(z) &> \int_{L_x} \left[ \left\{ \left( \frac{1}{\epsilon_1} - \frac{1}{\epsilon_2^2} - \frac{1}{\epsilon_3^2} \right) \frac{\pi^2}{h^2} - 2k^2 - \frac{2k^2 m}{\alpha} \right\} \phi_{,\xi\xi}^2 \right. \\ &\quad + \left\{ m - 2k^2 - \frac{2k^2 m h^2}{4\pi^2 \epsilon_1} - \frac{2k^2 m h^4 \alpha}{\pi^4 (\frac{3}{2})^4} - \frac{m\gamma}{|\epsilon_3|} \right\} \phi_{,\eta\eta}^2 \\ &\quad + \left\{ m \left( \frac{1}{\epsilon_1} - \frac{1}{\epsilon_2^2} \right) - \frac{4k^2 m h^2}{\pi^2} - \frac{m}{|\epsilon_3| \gamma} \right\} \phi_{,\xi\eta}^2 \\ &\quad \left. - \frac{4k^2 m}{|\epsilon_2|} \left\{ \beta \phi_{,\xi}^2 + \frac{1}{\beta} \phi_{,\eta}^2 \right\} \right] d\eta. \end{aligned} \quad (4.119)$$

Again using (4.23) and (4.24) we obtain

$$\begin{aligned} J(z) &> \int_{L_x} \left[ \left\{ \left( \frac{1}{\epsilon_1} - \frac{1}{\epsilon_2^2} - \frac{1}{\epsilon_3^2} \right) \frac{\pi^2}{h^2} - 2k^2 - \frac{2k^2 m}{\alpha} \right\} \phi_{,\xi\xi}^2 \right. \\ &\quad + \left\{ m - 2k^2 - \frac{2k^2 m h^2}{4\pi^2 \epsilon_1} - \frac{2k^2 m h^4 \alpha}{\pi^4 (\frac{3}{2})^4} - \frac{m\gamma}{|\epsilon_3|} - \frac{4k^2 m h^2}{4\beta |\epsilon_2| \pi^2} \right\} \phi_{,\eta\eta}^2 \\ &\quad \left. + \left\{ m \left( \frac{1}{\epsilon_1} - \frac{1}{\epsilon_2^2} \right) - \frac{4k^2 m h^2}{\pi^2} - \frac{m}{|\epsilon_3| \gamma} - \frac{4k^2 m h^2 \beta}{|\epsilon_2| \pi^2} \right\} \phi_{,\xi\eta}^2 \right] d\eta. \end{aligned} \quad (4.120)$$

It now follows that  $J(z) \geq 0$  if the positive constants  $m$ ,  $k$ ,  $\alpha$ ,  $\beta$  and  $\gamma$  can be chosen so that the coefficients of  $\phi_{,\xi\xi}^2$ ,  $\phi_{,\eta\eta}^2$  and  $\phi_{,\xi\eta}^2$  in (4.120) are all nonnegative.

Thus we seek  $m$ ,  $k$ ,  $\alpha$ ,  $\beta$  and  $\gamma$  such that

$$k^2 \leq \frac{\left(\frac{1}{\epsilon_1} - \frac{1}{\epsilon_2^2} - \frac{1}{\epsilon_3^2}\right) \frac{\pi^2}{h^2}}{2 \left(1 + \frac{m}{\alpha}\right)} \quad (4.121)$$

$$k^2 \leq \frac{\left(\frac{1}{\epsilon_1} - \frac{1}{\epsilon_2^2} - \frac{1}{|\epsilon_3|\gamma}\right)}{\frac{4h^2}{\pi^2} \left(1 + \frac{\beta}{|\epsilon_2|}\right)} \quad (4.122)$$

$$k^2 \leq \frac{m \left(1 - \frac{\gamma}{|\epsilon_3|}\right)}{2 \left(1 + \frac{mh^2}{4\pi^2\epsilon_1} + \frac{\alpha mh^4}{\left(\frac{3}{2}\right)^4 \pi^4} + \frac{mh^2}{2\beta|\epsilon_2|\pi^2}\right)}. \quad (4.123)$$

In order for  $k^2$  to be positive, the right-hand sides of (4.121) - (4.123) must also be positive. Recalling our fundamental assumption (4.9) on the  $\epsilon_i$ , we see that the right-hand side of (4.121) is indeed positive. The remaining two conditions (4.122) and (4.123) imply the following bounds on  $\gamma$ ,

$$\frac{1}{|\epsilon_3|} \frac{1}{\left(\frac{1}{\epsilon_1} - \frac{1}{\epsilon_2^2}\right)} < \gamma < |\epsilon_3|. \quad (4.124)$$

It is readily verified that the right-hand sides of (4.121) - (4.123) are strictly monotone functions of the variables  $m$ ,  $\alpha$ ,  $\gamma$  and  $\beta$ . Thus the maximum choice for  $k$  satisfying (4.121) - (4.123) results from equating these three expressions. Equating (4.122) and (4.123) yields the following expression for  $m$ ,

$$m = - \frac{\frac{\pi^2}{h^2} \left(\frac{1}{\epsilon_1} - \frac{1}{\epsilon_2^2} - \frac{1}{|\epsilon_3|\gamma}\right)}{\left(\frac{1}{\epsilon_1} - \frac{1}{\epsilon_2^2} - \frac{1}{|\epsilon_3|\gamma}\right) \left(\frac{1}{4\epsilon_1} + \frac{\alpha h^2}{\left(\frac{3}{2}\right)^4 \pi^2} + \frac{1}{2\beta|\epsilon_2|}\right) - 2 \left(1 - \frac{\gamma}{|\epsilon_3|}\right) \left(1 + \frac{\beta}{|\epsilon_2|}\right)} \quad (4.125)$$

while equating (4.121) and (4.122) results in the following expression for  $\alpha$ ,

$$\alpha = \left[ \frac{\left( \frac{1}{\epsilon_1} - \frac{1}{\epsilon_2^2} - \frac{1}{|\epsilon_3|\gamma} \right)}{2 \left( 1 + \frac{\beta}{|\epsilon_2|} \right) \left( \frac{1}{\epsilon_1} - \frac{1}{\epsilon_2^2} - \frac{1}{\epsilon_3^2} \right) - \left( \frac{1}{\epsilon_1} - \frac{1}{\epsilon_2^2} - \frac{1}{|\epsilon_3|\gamma} \right)} \right] m \equiv F(\gamma, \beta)m. \quad (4.126)$$

It can be verified that

$$\beta > 0 \Rightarrow F(\gamma, \beta) > 0 \quad (4.127)$$

for  $\gamma$  in the range given by (4.124), so that positive values for  $\beta$  and  $m$  yield a positive value for  $\alpha$ . Substituting (4.126) into (4.125) gives the quadratic equation in  $m$

$$Am^2 + Bm + C = 0 \quad (4.128)$$

where

$$\begin{aligned} A &= \left[ \frac{\frac{h^2}{\pi^2(\frac{3}{2})^4} \left( \frac{1}{\epsilon_1} - \frac{1}{\epsilon_2^2} - \frac{1}{|\epsilon_3|\gamma} \right)^2}{2 \left( 1 + \frac{\beta}{|\epsilon_2|} \right) \left( \frac{1}{\epsilon_1} - \frac{1}{\epsilon_2^2} - \frac{1}{\epsilon_3^2} \right) - \left( \frac{1}{\epsilon_1} - \frac{1}{\epsilon_2^2} - \frac{1}{|\epsilon_3|\gamma} \right)} \right], \\ B &= \left[ \left( \frac{1}{\epsilon_1} - \frac{1}{\epsilon_2^2} - \frac{1}{|\epsilon_3|\gamma} \right) \left( \frac{1}{4\epsilon_1} + \frac{1}{2\beta|\epsilon_2|} \right) - 2 \left( 1 - \frac{\gamma}{|\epsilon_3|} \right) \left( 1 + \frac{\beta}{|\epsilon_2|} \right) \right], \\ C &= \frac{\pi^2}{h^2} \left( \frac{1}{\epsilon_1} - \frac{1}{\epsilon_2^2} - \frac{1}{|\epsilon_3|\gamma} \right). \end{aligned} \quad (4.129)$$

The roots of (4.128) may be found explicitly from the the quadratic formula as

$$m_{1,2} = \frac{-B \pm \sqrt{B^2 - 4AC}}{2A}. \quad (4.130)$$

It follows from (4.129) that  $A > 0$  and  $C > 0$  and hence for  $m$  given by (4.130) to be a *positive real root*, the following additional restrictions must hold,

$$B \leq 0 \quad (4.131)$$

$$B^2 - 4AC \geq 0. \quad (4.132)$$

Once  $m$ ,  $\alpha$ ,  $\beta$  and  $\gamma$  have been chosen to satisfy the necessary constraints,  $k$  can be determined from (4.122) with equality. This leads to the following formulation:

*Quadratic Estimate:*

$$\text{Maximize } H(\gamma, \beta) = k^2 = \frac{\pi^2}{4h^2} \frac{\left(\frac{1}{\epsilon_1} - \frac{1}{\epsilon_2^2} - \frac{1}{|\epsilon_3|\gamma}\right)}{\left(1 + \frac{\beta}{|\epsilon_2|}\right)} \quad (4.133)$$

*subject to*

$$\frac{1}{|\epsilon_3|} \frac{1}{\left(\frac{1}{\epsilon_1} - \frac{1}{\epsilon_2^2}\right)} < \gamma < |\epsilon_3|, \quad (4.134)$$

$$\begin{aligned} \beta \geq & \left[ \frac{4}{|\epsilon_2|} \left(1 - \frac{\gamma}{|\epsilon_3|}\right) \right]^{-1} \left[ - \left\{ 2 \left(1 - \frac{\gamma}{|\epsilon_3|}\right) - \frac{1}{4\epsilon_1} \left(\frac{1}{\epsilon_1} - \frac{1}{\epsilon_2^2} - \frac{1}{|\epsilon_3|\gamma}\right) \right\} \right. \\ & \left. + \sqrt{\left\{ 2 \left(1 - \frac{\gamma}{|\epsilon_3|}\right) - \frac{1}{4\epsilon_1} \left(\frac{1}{\epsilon_1} - \frac{1}{\epsilon_2^2} - \frac{1}{|\epsilon_3|\gamma}\right) \right\}^2 + \frac{4}{\epsilon_2^2} \left(\frac{1}{\epsilon_1} - \frac{1}{\epsilon_2^2} - \frac{1}{|\epsilon_3|\gamma}\right) \left(1 - \frac{\gamma}{|\epsilon_3|}\right)} \right] \end{aligned} \quad (4.135)$$

*and*

$$\begin{aligned} & \left[ 2 \left(1 - \frac{\gamma}{|\epsilon_3|}\right) \left(1 + \frac{\beta}{|\epsilon_2|}\right) - \left(\frac{1}{\epsilon_1} - \frac{1}{\epsilon_2^2} - \frac{1}{|\epsilon_3|\gamma}\right) \left(\frac{1}{4\epsilon_1} + \frac{1}{2\beta|\epsilon_2|}\right) \right]^2 \geq \\ & 4 \left(\frac{1}{\epsilon_1} - \frac{1}{\epsilon_2^2} - \frac{1}{|\epsilon_3|\gamma}\right)^2 \left(\frac{2}{3}\right)^4 \left[ \frac{\left(\frac{1}{\epsilon_1} - \frac{1}{\epsilon_2^2} - \frac{1}{|\epsilon_3|\gamma}\right)}{2 \left(1 + \frac{\beta}{|\epsilon_2|}\right) \left(\frac{1}{\epsilon_1} - \frac{1}{\epsilon_2^2} - \frac{1}{\epsilon_3^2}\right) - \left(\frac{1}{\epsilon_1} - \frac{1}{\epsilon_2^2} - \frac{1}{|\epsilon_3|\gamma}\right)} \right]. \end{aligned} \quad (4.136)$$

The inequality (4.135) results from (4.131) which gives a quadratic inequality for  $\beta$  while the inequality (4.136) results from (4.132). Of the three constraints (4.134) - (4.136) that must hold for this quadratic estimate, (4.134) can always be satisfied by a proper choice of  $\gamma$  while (4.135) then gives a *lower bound* on the choice of  $\beta$  in terms of  $\gamma$ . Furthermore, it can be observed that the left-hand side of (4.136) grows without bound for  $\beta$  large and increasing, while the right-hand side decreases with respect to  $\beta$ , so that (4.136) is always satisfied for  $\beta$  sufficiently large. Thus, we are guaranteed *some* choice for  $\gamma$  and  $\beta$  that yields a valid estimated decay rate  $k$ . While (4.133) gives an explicit formula for  $k$ , numerical procedures are necessary to determine the parameters  $\beta$  and  $\gamma$  that maximize  $k$ .

Without implementing any numerical techniques to maximize  $k$ , we observe from (4.122) and (4.124) that

$$k^2 \leq \frac{\pi^2}{4h^2} \left( \frac{1}{\epsilon_1} - \frac{1}{\epsilon_2^2} - \frac{1}{\epsilon_3^2} \right), \quad (4.137)$$

where the right-hand side of (4.137) is positive by virtue of (4.9). Transforming this result back to the original domain and setting  $h = 2$  yields the following bound on the *estimated decay rate*  $k^*$

$$k^* < \frac{\pi}{4} \sqrt{\frac{1}{\epsilon_1} - \frac{1}{\epsilon_2^2} - \frac{1}{\epsilon_3^2}} \left( \frac{\beta_{11}}{\beta_{22}} \right)^{\frac{1}{4}}. \quad (4.138)$$

We recall that the stresses  $\tau$  have a decay factor of  $\frac{2k^*}{2H}$ . The inequality (4.138) yields an *upper bound* for the estimated decay rate solely in terms of the elastic parameters of the material, i.e. independent of  $\gamma$  and  $\beta$ , and will be used later to assess the range of validity of the method given here. It will be shown that the quadratic estimate

is limited in certain ranges of the material parameters. For this reason, numerical optimization techniques were not pursued.

We now return to (4.121) - (4.123) and consider the orthotropic limit as  $\frac{1}{\epsilon_2}, \frac{1}{\epsilon_3} \rightarrow 0$ . Equating the three orthotropic versions of (4.121) - (4.123) leads to a quadratic equation in  $m$  that is simpler than in the anisotropic case and leads to the following *orthotropic quadratic estimate*:

$$k^2 = \frac{\pi^2}{4h^2\epsilon_1} \quad (4.139)$$

provided

$$\frac{1}{4\epsilon_1} - 2\epsilon_1 \leq -2\left(\frac{3}{2}\right)^{-2} \quad (4.140)$$

which implies

$$\epsilon_1 \geq N \approx 0.639. \quad (4.141)$$

The inequality (4.140) is a condition that is necessary for  $m$  to be a positive real quantity. Equation (4.139) is identical to the analytic estimate (3.49)<sub>2</sub>, however the range of  $\epsilon_1$  given by (4.141) is more restrictive than the range  $\epsilon_1 > 0.433$  required for validity of the analytic estimate.

#### 4.4.2 Quartic Estimate

This estimate starts with  $J(z)$  given by (4.106) and makes use of the anisotropic conservation property (4.2) to simplify terms. This leads to a *quartic* equation for the undetermined constant  $m$ , in contrast to the *quadratic* equation for  $m$  which resulted in the the previous section.

The conservation property (4.2) may be rewritten using the arithmetic-geometric

mean inequality (3.15) as

$$\begin{aligned} \int_{L_x} \left[ \frac{4}{\epsilon_2} \phi_{,\xi\xi} \phi_{,\xi\eta} - \phi_{,\xi\xi}^2 + \phi_{,\eta\eta}^2 - \frac{1}{\epsilon_1} \phi_{,\xi\eta}^2 \right] d\eta &= - \int_{L_x} 2\phi_{,\xi} \phi_{,\xi\xi\xi} d\eta \\ &\leq \int_{L_x} \left[ \omega \phi_{,\xi}^2 + \frac{1}{\omega} \phi_{,\xi\xi\xi}^2 \right] d\eta \quad (4.142) \end{aligned}$$

for  $\omega > 0$ . Thus we have from (4.142) that

$$-\frac{4}{\epsilon_2} \int_{L_x} \phi_{,\xi\xi} \phi_{,\xi\eta} d\eta \geq - \int_{L_x} \left[ \omega \phi_{,\xi}^2 + \frac{1}{\omega} \phi_{,\xi\xi\xi}^2 + \phi_{,\xi\xi}^2 - \phi_{,\eta\eta}^2 + \frac{1}{\epsilon_1} \phi_{,\xi\eta}^2 \right] d\eta. \quad (4.143)$$

Returning to (4.106) and using (4.143) leads to the inequality

$$\begin{aligned} J(z) \geq \int_{L_x} \left[ \left(1 - \frac{m}{2\omega}\right) \phi_{,\xi\xi\xi}^2 + \phi_{,\xi\eta\eta}^2 - \frac{2}{\epsilon_2} \phi_{,\xi\xi\xi} \phi_{,\xi\xi\eta} - \frac{2}{\epsilon_3} \phi_{,\xi\eta\eta} \phi_{,\xi\xi\eta} \right. \\ \left. + \frac{1}{\epsilon_1} \phi_{,\xi\xi\eta}^2 + \left(m - 2k^2 - \frac{m}{2}\right) \phi_{,\xi\xi}^2 + \left(m - 2k^2 + \frac{m}{2}\right) \phi_{,\eta\eta}^2 \right. \\ \left. - \frac{2m}{\epsilon_3} \phi_{,\eta\eta} \phi_{,\xi\eta} + \left(\frac{m}{\epsilon_1} - \frac{m}{2\epsilon_1}\right) \phi_{,\xi\eta}^2 - \left(4k^2m + \frac{\omega m}{2}\right) \phi_{,\xi}^2 \right. \\ \left. + 4k^2m \phi \phi_{,\xi\xi} + \frac{8k^2m}{\epsilon_2} \phi_{,\xi} \phi_{,\eta} - \frac{2k^2m}{\epsilon_1} \phi_{,\eta}^2 \right] d\eta. \quad (4.144) \end{aligned}$$

Completing squares in the higher-order cross terms results in

$$\begin{aligned} J(z) \geq \int_{L_x} \left[ \left(1 - \frac{m}{2\omega}\right) \left\{ \phi_{,\xi\xi\xi} - \frac{1}{\epsilon_2(1 - \frac{m}{2\omega})} \phi_{,\xi\xi\eta} \right\}^2 - \frac{1}{(1 - \frac{m}{2\omega})\epsilon_2^2} \phi_{,\xi\xi\eta}^2 \right. \\ \left. + \left\{ \phi_{,\xi\eta\eta} - \frac{1}{\epsilon_3} \phi_{,\xi\xi\eta} \right\}^2 - \frac{1}{\epsilon_3^2} \phi_{,\xi\xi\eta}^2 \right. \\ \left. + \frac{1}{\epsilon_1} \phi_{,\xi\xi\eta}^2 + \left(m - 2k^2 - \frac{m}{2}\right) \phi_{,\xi\xi}^2 + \left(m - 2k^2 + \frac{m}{2}\right) \phi_{,\eta\eta}^2 \right. \\ \left. - \frac{2m}{\epsilon_3} \phi_{,\eta\eta} \phi_{,\xi\eta} + \frac{m}{2\epsilon_1} \phi_{,\xi\eta}^2 - \left(4k^2m + \frac{\omega m}{2}\right) \phi_{,\xi}^2 \right. \\ \left. + 4k^2m \phi \phi_{,\xi\xi} + \frac{8k^2m}{\epsilon_2} \phi_{,\xi} \phi_{,\eta} - \frac{2k^2m}{\epsilon_1} \phi_{,\eta}^2 \right] d\eta \quad (4.145) \end{aligned}$$

from which, upon dropping positive terms, we get



$$\begin{aligned}
J(z) \geq \int_{L_z} & \left[ \left( \frac{1}{\epsilon_1} - \frac{1}{(1 - \frac{m}{2\omega})\epsilon_2^2} - \frac{1}{\epsilon_3^2} \right) \phi_{,\xi\xi\eta}^2 \right. \\
& + \left( m - 2k^2 - \frac{m}{2} \right) \phi_{,\xi\xi}^2 + \left( m - 2k^2 + \frac{m}{2} \right) \phi_{,\eta\eta}^2 \\
& - \frac{2m}{\epsilon_3} \phi_{,\eta\eta} \phi_{,\xi\eta} + \frac{m}{2\epsilon_1} \phi_{,\xi\eta}^2 - \left( 4k^2 m + \frac{\omega m}{2} \right) \phi_{,\xi}^2 \\
& \left. + 4k^2 m \phi \phi_{,\xi\xi} + \frac{8k^2 m}{\epsilon_2} \phi_{,\xi} \phi_{,\eta} - \frac{2k^2 m}{\epsilon_1} \phi_{,\eta}^2 \right] d\eta, \quad (4.146)
\end{aligned}$$

provided

$$\left( 1 - \frac{m}{2\omega} \right) > 0. \quad (4.147)$$

On using (3.66) from Chapter 3, we have

$$\begin{aligned}
J(z) > \int_{L_z} & \left[ \left\{ \frac{1}{\epsilon_1} - \frac{1}{(1 - \frac{m}{2\omega})\epsilon_2^2} - \frac{1}{\epsilon_3^2} \right\} \phi_{,\xi\xi\eta}^2 + \left\{ m - 2k^2 - \frac{m}{2} - \frac{2k^2 m}{\nu} \right\} \phi_{,\xi\xi}^2 \right. \\
& + \left\{ m - 2k^2 + \frac{m}{2} - \frac{2k^2 m \nu h^4}{(\frac{3\pi}{2})^4} \right\} \phi_{,\eta\eta}^2 - \frac{2m}{\epsilon_3} \phi_{,\eta\eta} \phi_{,\xi\eta} + \frac{m}{2\epsilon_1} \phi_{,\xi\eta}^2 \\
& \left. - \left( 4k^2 m + \frac{\omega m}{2} \right) \phi_{,\xi}^2 + \frac{8k^2 m}{\epsilon_2} \phi_{,\xi} \phi_{,\eta} - \frac{2k^2 m}{\epsilon_1} \phi_{,\eta}^2 \right] d\eta, \quad (4.148)
\end{aligned}$$

where  $\nu > 0$  is an arbitrary parameter. Now, using the arithmetic-geometric mean inequalities (3.15) and (3.16), we obtain

$$\int_{L_z} \frac{2}{\epsilon_2} \phi_{,\xi} \phi_{,\eta} d\eta \geq - \int_{L_z} \frac{1}{|\epsilon_2|} [\delta \phi_{,\xi}^2 + \frac{1}{\delta} \phi_{,\eta}^2] d\eta, \quad (4.149)$$

$$- \int_{L_z} \frac{2}{\epsilon_3} \phi_{,\eta\eta} \phi_{,\xi\eta} d\eta \geq - \int_{L_z} \frac{1}{|\epsilon_3|} [\mu \phi_{,\eta\eta}^2 + \frac{1}{\mu} \phi_{,\xi\eta}^2] d\eta, \quad (4.150)$$

for arbitrary  $\delta, \mu > 0$ . Using these inequalities in (4.148) yields

$$\begin{aligned}
J(z) > \int_{L_z} & \left[ \left\{ \frac{1}{\epsilon_1} - \frac{1}{(1 - \frac{m}{2\omega})\epsilon_2^2} - \frac{1}{\epsilon_3^2} \right\} \phi_{,\xi\xi\eta}^2 + \left\{ \frac{m}{2} - 2k^2 - \frac{2k^2 m}{\nu} \right\} \phi_{,\xi\xi}^2 \right. \\
& + \left\{ \frac{3m}{2} - 2k^2 - \frac{2k^2 m \nu h^4}{(\frac{3\pi}{2})^4} - \frac{\mu m}{|\epsilon_3|} \right\} \phi_{,\eta\eta}^2 + \left\{ \frac{m}{2\epsilon_1} - \frac{m}{\mu |\epsilon_3|} \right\} \phi_{,\xi\eta}^2 \\
& \left. - \left( 4k^2 m + \frac{\omega m}{2} + \frac{4k^2 m \delta}{|\epsilon_2|} \right) \phi_{,\xi}^2 - \left( \frac{2k^2 m}{\epsilon_1} + \frac{4k^2 m}{\delta |\epsilon_2|} \right) \phi_{,\eta}^2 \right] d\eta. \quad (4.151)
\end{aligned}$$

Upon using (4.23) and (4.24) in the last two terms of (4.151), we obtain

$$\begin{aligned}
 J(z) > \int_{L_z} \left[ \left\{ \frac{1}{\epsilon_1} - \frac{1}{(1 - \frac{m}{2\omega})\epsilon_2^2} - \frac{1}{\epsilon_3^2} \right\} \phi_{,\xi\xi\eta}^2 + \left\{ \frac{m}{2} - 2k^2 - \frac{2k^2m}{\nu} \right\} \phi_{,\xi\xi}^2 \right. \\
 &\quad + \left\{ \frac{3m}{2} - 2k^2 - \frac{2k^2m\nu h^4}{(\frac{3\pi}{2})^4} - \frac{\mu m}{|\epsilon_3|} - \frac{k^2mh^2}{2\epsilon_1\pi^2} - \frac{k^2mh^2}{\delta|\epsilon_2|\pi^2} \right\} \phi_{,\eta\eta}^2 \\
 &\quad \left. + \left\{ \frac{m}{2\epsilon_1} - \frac{m}{\mu|\epsilon_3|} - \frac{4k^2mh^2}{\pi^2} - \frac{m\omega h^2}{2\pi^2} - \frac{4k^2mh^2\delta}{\pi^2|\epsilon_2|} \right\} \phi_{,\xi\eta}^2 \right] d\eta. \quad (4.152)
 \end{aligned}$$

On using (3.70) we obtain

$$\begin{aligned}
 J(z) > \int_{L_z} \left[ \left\{ \frac{\pi^2}{h^2} \left( \frac{1}{\epsilon_1} - \frac{1}{(1 - \frac{m}{2\omega})\epsilon_2^2} - \frac{1}{\epsilon_3^2} \right) + \frac{m}{2} - 2k^2 - \frac{2k^2m}{\nu} \right\} \phi_{,\xi\xi}^2 \right. \\
 &\quad + \left\{ m \left( \frac{3}{2} - \frac{\mu}{|\epsilon_3|} \right) - 2k^2 \left( 1 + \frac{m\nu h^4}{(\frac{3\pi}{2})^4} + \frac{mh^2}{4\epsilon_1\pi^2} + \frac{mh^2}{2\delta|\epsilon_2|\pi^2} \right) \right\} \phi_{,\eta\eta}^2 \\
 &\quad \left. + \left\{ m \left( \frac{1}{2\epsilon_1} - \frac{1}{\mu|\epsilon_3|} - \frac{\omega h^2}{2\pi^2} \right) - 4k^2mh^2 \left( \frac{1}{\pi^2} + \frac{\delta}{\pi^2|\epsilon_2|} \right) \right\} \phi_{,\xi\eta}^2 \right] d\eta, \quad (4.153)
 \end{aligned}$$

provided

$$\left( \frac{1}{\epsilon_1} - \frac{1}{(1 - \frac{m}{2\omega})\epsilon_2^2} - \frac{1}{\epsilon_3^2} \right) \geq 0. \quad (4.154)$$

It then follows that the integral  $J(z)$  given by (4.153) will be positive if we can choose positive constants  $\omega$ ,  $\nu$ ,  $\delta$ ,  $\mu$ ,  $m$  and  $k$  such that the coefficients of  $\phi_{,\xi\xi}^2$ ,  $\phi_{,\xi\eta}^2$  and  $\phi_{,\eta\eta}^2$  are nonnegative and such that the conditions (4.147) and (4.154) are both satisfied. Since (4.9) implies that  $\epsilon_3^2 > \epsilon_1$ , these last two conditions may be combined together to yield the single constraint

$$\left( 1 - \frac{m}{2\omega} \right) \geq \frac{\epsilon_1\epsilon_3^2}{\epsilon_2^2(\epsilon_3^2 - \epsilon_1)}, \quad (4.155)$$

which shall be used henceforth.

Thus the problem is to find positive constants  $\omega$ ,  $\nu$ ,  $\delta$ ,  $\mu$ ,  $m$  and  $k$  such that

$$k^2 \leq \frac{\left( \frac{1}{2\epsilon_1} - \frac{1}{\mu|\epsilon_3|} - \frac{\omega h^2}{2\pi^2} \right)}{4h^2 \left( \frac{1}{\pi^2} + \frac{\delta}{\pi^2|\epsilon_2|} \right)}, \quad (4.156)$$

$$k^2 \leq \frac{\frac{m}{2} \left( \frac{3}{2} - \frac{\mu}{|\epsilon_3|} \right)}{1 + \frac{m\nu h^4}{\left(\frac{3\pi}{2}\right)^4} + \frac{mh^2}{4\epsilon_1\pi^2} + \frac{mh^2}{2\delta|\epsilon_2|\pi^2}}, \quad (4.157)$$

$$k^2 \leq \frac{\frac{4\pi^2}{h^2} \left\{ \frac{1}{\epsilon_1} - \frac{1}{\epsilon_2^2(1 - \frac{m}{2\omega})} - \frac{1}{\epsilon_3^2} \right\} + 2m}{8 \left( 1 + \frac{m}{\nu} \right)}, \quad (4.158)$$

and

$$\frac{m}{2\omega} \leq 1 - \frac{\epsilon_1\epsilon_3^2}{\epsilon_2^2(\epsilon_3^2 - \epsilon_1)} \equiv f(\epsilon_1, \epsilon_2, \epsilon_3). \quad (4.159)$$

For convenience, we now choose equality in (4.159) to obtain a valid decay estimate although this may or may not yield the *optimal* decay estimate. Upon choosing equality in (4.159) and introducing the notation

$$m = \frac{\pi^2}{h^2}M, \quad \nu = \frac{\pi^2}{h^2}\Delta, \quad k^2 = \frac{\pi^2}{h^2}K^2, \quad (4.160)$$

where  $h = 2$ , the inequalities (4.156) - (4.158) then read

$$K^2 \leq \frac{\left( \frac{1}{2\epsilon_1} - \frac{1}{\mu|\epsilon_3|} - \frac{M}{4f} \right)}{4 \left( 1 + \frac{\delta}{|\epsilon_2|} \right)}, \quad (4.161)$$

$$K^2 \leq \frac{\frac{M}{2} \left( \frac{3}{2} - \frac{\mu}{|\epsilon_3|} \right)}{1 + M\Delta \left( \frac{3\pi}{2} \right)^{-4} + \frac{M}{4\epsilon_1} + \frac{M}{2\delta|\epsilon_2|}}, \quad (4.162)$$

$$K^2 \leq \frac{M}{4 \left( 1 + \frac{M}{\Delta} \right)}. \quad (4.163)$$

The problem is now to find positive  $M$ ,  $\Delta$ , and  $K$  such that (4.161) - (4.163) hold, where  $\delta$  and  $\mu$  are arbitrary positive parameters yet to be determined.

First, we observe that in order for  $K^2$  to be positive, the right-hand sides of (4.161) and (4.162) imply the following restrictions,

$$\frac{1}{2\epsilon_1} - \frac{1}{\mu|\epsilon_3|} - \frac{M}{4f} > 0, \quad (4.164)$$

$$\mu < \frac{3}{2}|\epsilon_3|. \quad (4.165)$$

Since the right-hand sides of (4.161) - (4.163) are monotone functions of their arguments, the optimal value for  $K$  will be obtained by equating these three expressions.

This leads to a *fourth-order* equation for  $M$  as

$$\begin{aligned} & \left(\frac{3}{2}\right)^4 \left\{ M \left(1 + \frac{\delta}{|\epsilon_2|}\right) - \left(\frac{1}{2\epsilon_1} - \frac{1}{\mu|\epsilon_3|} - \frac{M}{4f}\right) \right\} \times \\ & \left\{ 2M \left(\frac{3}{2} - \frac{\mu}{|\epsilon_3|}\right) \left(1 + \frac{\delta}{|\epsilon_2|}\right) - \left(1 + \frac{M}{4\epsilon_1} + \frac{M}{2\delta|\epsilon_2|}\right) \left(\frac{1}{2\epsilon_1} - \frac{1}{\mu|\epsilon_3|} - \frac{M}{4f}\right) \right\} \\ & - M^2 \left(\frac{1}{2\epsilon_1} - \frac{1}{\mu|\epsilon_3|} - \frac{M}{4f}\right)^2 = 0. \end{aligned} \quad (4.166)$$

Once  $\mu$ , subject to (4.165), and  $\delta$  have been chosen, equation (4.166) may then be solved numerically for  $M$ . Of the four possible roots,  $M$  must be chosen such that the constraint (4.164) is satisfied.  $K$  may then be found on equality in (4.161) and  $\Delta$  in turn may be found from (4.163) with equality. Due to the complexity of this formulation and the number of parameters involved, numerical calculations were not pursued.

One can, however, obtain a bound on this quartic estimate as was done for the previous quadratic estimate. Returning to (4.161), we observe that

$$K^2 \leq \frac{\frac{1}{2\epsilon_1} - \frac{1}{\mu|\epsilon_3|}}{4} < \frac{1}{8\epsilon_1} - \frac{1}{6\epsilon_3^2} \quad (4.167)$$

where the condition (4.165) has been used in the last step. Referring back to the notation in (4.160) and transforming (4.167) back into the original  $x_1 - x_2$  domain yields the following *upper bound* on the estimated decay rate  $k^*$ ,

$$k^* < \frac{\pi}{2} \sqrt{\frac{1}{8\epsilon_1} - \frac{1}{6\epsilon_3^2}} \left( \frac{\beta_{11}}{\beta_{22}} \right)^{\frac{1}{4}}, \quad (4.168)$$

where the stresses  $\tau$  have a decay factor of  $\frac{2k^*}{2H}$ . This bound, solely in terms of the elastic parameters of the material, will be used later to assess the range of validity of the present analysis. It will be shown that the quartic estimate, like the quadratic estimate, is limited in certain ranges of the material parameters.

Again, it is easier to obtain results from this method in the orthotropic limit, i.e. as  $\frac{1}{\epsilon_2}, \frac{1}{\epsilon_3} \rightarrow 0$ . The inequalities (4.156) - (4.158) then reduce to

$$k^2 \leq \frac{\pi^2}{8h^2\epsilon_1} - \frac{\omega}{8}, \quad (4.169)$$

$$k^2 \leq \frac{3m}{4 \left( 1 + \frac{m\nu h^4}{(\frac{3\pi}{2})^4} + \frac{mh^2}{4\epsilon_1\pi^2} \right)}, \quad (4.170)$$

$$k^2 \leq \frac{\frac{4\pi^2}{h^2\epsilon_1} + 2m}{8 \left( 1 + \frac{m}{\nu} \right)}. \quad (4.171)$$

Taking the limit in (4.159) also gives

$$\omega \geq \frac{m}{2}. \quad (4.172)$$

From (4.169) we see that  $k$  is a decreasing function of  $\omega$  and therefore choosing equality in (4.172) will yield the optimal decay estimate. Upon using the notation in (4.160), the remaining conditions (4.169) - (4.171) become

$$K^2 \leq \frac{\frac{2}{\epsilon_1} - M}{16}, \quad (4.173)$$

$$K^2 \leq \frac{3M}{4 \left[ 1 + \frac{M}{4\epsilon_1} + M\Delta \left( \frac{2}{3} \right)^4 \right]}, \quad (4.174)$$

$$K^2 \leq \frac{\frac{4}{\epsilon_1} + 2M}{8 \left( 1 + \frac{M}{\Delta} \right)}. \quad (4.175)$$

In order for  $K^2$  to be positive, (4.173) implies that

$$M < \frac{2}{\epsilon_1}. \quad (4.176)$$

Due to the monotone nature of the right-hand sides of (4.173) - (4.175), the maximum value for  $K$  will be achieved by equating these three expressions. This leads to the following fourth-order equation for  $M$ ,

$$\left( \frac{3}{2} \right)^4 \left\{ \frac{6}{\epsilon_1} + 5M \right\} \left\{ 12M - \left( 1 + \frac{M}{4\epsilon_1} \right) \left( \frac{2}{\epsilon_1} - M \right) \right\} - M^2 \left( \frac{2}{\epsilon_1} - M \right)^2 = 0. \quad (4.177)$$

The roots of (4.177) may then be used to obtain  $K$  by taking equality in (4.173), where it is observed that the smallest value for  $M$  yields the largest value for  $K$ . The fourth-order equation (4.177) was solved numerically using MACSYMA for the set of materials shown in Table 3.1 from Chapter 3. For each of the materials, the smallest positive root  $M$  gave positive values for  $\Delta$  and  $K^2$  and hence gave the desired

maximum  $K$  satisfying (4.173) - (4.175). Using (4.160) and transforming this result back to the original domain yields

$$k^* = \frac{\pi}{h} K \left( \frac{\beta_{11}}{\beta_{22}} \right)^{\frac{1}{4}}, \quad (4.178)$$

where the stresses  $\tau$  have a decay factor of  $\frac{2k^*}{2H}$ . Although this estimate does not yield an explicit formula for the decay rate in terms of the elastic constants, it does yield a numerical estimate. These results are shown in Table 4.1 together with the conservation law estimate of section 3.4. It is seen that the latter method yields a better estimate.

## 4.5 Exact Decay Rates

Exact solutions of the anisotropic equation (4.1) subject to the boundary conditions (2.23) - (2.25) are much more complicated and difficult to obtain than the solutions of the orthotropic equation (3.3) subject to the same boundary conditions. As in section 3.5, we seek solutions of the form

$$\phi = e^{-\gamma\zeta} F(\eta), \quad \gamma = \text{constant}, \quad (4.179)$$

which leads to the following eigenvalue problem

$$\begin{aligned} F'''' + \frac{2}{\epsilon_2} \gamma F''' + \frac{1}{\epsilon_1} \gamma^2 F'' + \frac{2}{\epsilon_3} \gamma^3 F' + \gamma^4 F &= 0, \quad \text{on } (-1, 1) \\ F(-1) &= F(1) = 0, \\ F'(-1) &= F'(1) = 0, \end{aligned} \quad (4.180)$$

which is the anisotropic generalization of (3.104). Seeking solutions to (4.180) of the form

$$F = Ae^{\mu\eta}, \quad \mu \text{ constant}, \quad (4.181)$$

leads to the characteristic polynomial

$$P(\mu) = \mu^4 + \frac{2}{\epsilon_2}\mu^3 + \frac{1}{\epsilon_1}\mu^2 + \frac{2}{\epsilon_3}\mu + 1 = 0 \quad (4.182)$$

whose roots  $\mu$  are complex and occur in conjugate pairs (Equation (4.182) is actually the nondimensional version of (2.47)). Let the roots  $\mu$  of (4.182) be denoted by

$$\mu_{1,2} = p_1 \pm iq_1, \quad \mu_{3,4} = p_2 \pm iq_2, \quad (4.183)$$

where  $p_\alpha, q_\alpha$  depend on  $\epsilon_i$  ( $i = 1, 2, 3$ ). Substituting the general form for  $F$  given in (4.181) into the boundary conditions given in (4.180) results in the following eigencondition for  $\gamma$  (see Choi and Horgan [6]),

$$\begin{aligned} & [(p_1 - p_2)^2 + (q_1 + q_2)^2] \cos 2(q_1 - q_2)\gamma - \\ & [(p_1 - p_2)^2 + (q_1 - q_2)^2] \cos 2(q_1 + q_2)\gamma = 4q_1q_2 \cosh 2(p_1 - p_2)\gamma. \end{aligned} \quad (4.184)$$

The roots of (4.184) are complex in general and depend on the three elastic parameters  $\epsilon_1, \epsilon_2$  and  $\epsilon_3$ . Recently, in [19], this eigencondition has been simplified using a spherical representation to yield a *reduced eigencondition* for a *modified eigenvalue*  $\zeta$  in terms of *two* parameters  $\psi$  and  $\omega$  which may be determined from the elastic constants of the material (in [19], the quantity  $\omega$  is denoted by  $\theta$ ). The actual eigenvalue  $\gamma$  is related to the modified eigenvalue  $\zeta$  by the scaling

$$\zeta = \rho\gamma, \quad (4.185)$$

where  $\rho$  is a third material parameter which may be determined from the elastic constants of the material. The reduced eigencondition can be solved for various values



of  $\psi$  and  $\omega$ , see [19]. By interpolating from tables in [19] and scaling by the factor  $\rho$ , one obtains the real and imaginary parts of the eigenvalue  $\gamma$  of smallest real part, which must then be transformed back into the original domain. The procedure from [19] was automated for this dissertation to produce exact decay rates with which to compare the estimates. While the procedure just outlined has already been developed in [19], the numerical results for specific materials are new and show some interesting trends. We note that an alternative analysis of exact decay rates has also been given recently in [28].

Exact decay rates were computed for each of the materials listed in Table 3.1 of Chapter 3. The materials were initially oriented with their fibers parallel to the axial direction, making a fiber angle of  $0^\circ$  with the  $x_1$ -axis. For this situation, the strip is specially orthotropic. See Figure 4.1 for an illustration of the fiber angle  $\theta$ , for general  $\theta$ .

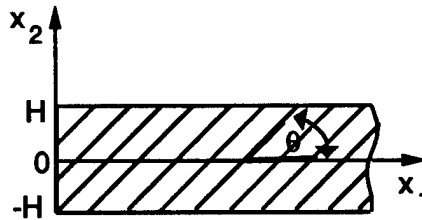


Figure 4.1: Fiber angle  $\theta$

The principle axes of the materials were then rotated through a fiber angle range of  $0^\circ - 90^\circ$ . For values of  $0^\circ < \theta < 90^\circ$ , the principal axes of the material and the axes shown in Figure 4.1 do not coincide. For this situation the strip exhibits

anisotropy in the form of coupling between stretching and shearing in the  $x_1 - x_2$  plane. For  $\theta = 90^\circ$ , the materials are specially orthotropic, but with their fibers parallel to the transverse direction. At each of the intermediate fiber angles, for which the strip is *anisotropic*, the techniques of [19] were used to calculate the exact decay rate. A plot of actual decay rates is shown below in Figure 4.2. For convenience we have chosen the three materials HS1, HS2 and UM for which to plot results. Decay rate curves for the other materials listed in Table 3.1 are similar in shape.

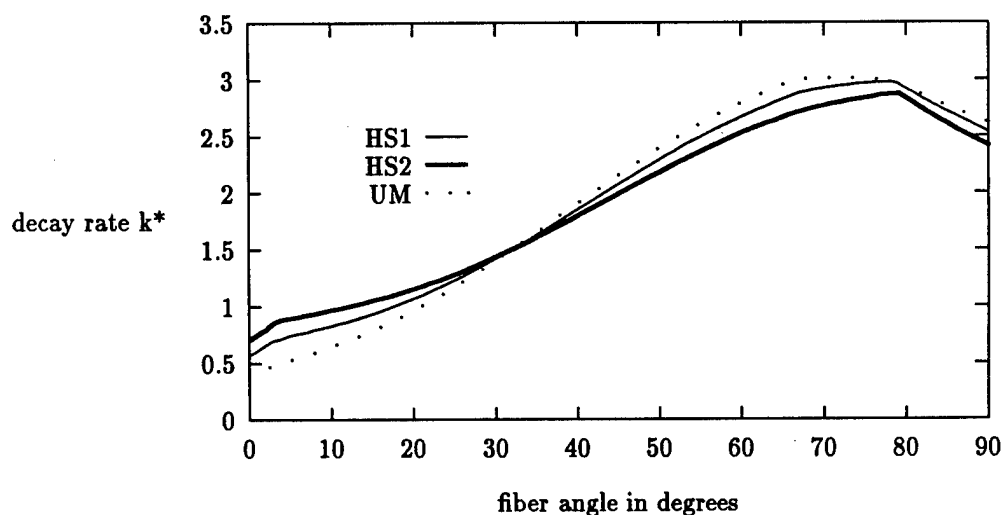


Figure 4.2: Exact decay rates vs. fiber angle

It is of interest to note that for each of these materials while  $\theta = 0$  produces the smallest decay rate (as expected), there is a fiber orientation angle in the range  $60^\circ - 80^\circ$  at which the decay rate is largest. This initially unexpected result has also been observed in other structural mechanics problems for laminates [20]. A similar non-monotonic behavior of decay rate with material properties has also been observed by Choi and Horgan [29] for a sandwich strip. Mathematically, this peak in the decay

rate can be traced back to the existence of a multiple eigenvalue which was found in [19]. There, the real and imaginary parts of the modified eigenvalue  $\zeta$  were plotted as functions of  $\psi$  and  $\omega$ , forming surfaces in three-dimensional coordinate space, and a cusp was found to exist in the *real* surface, corresponding to a multiple eigenvalue at that point. This cusp is responsible for the two "kinks" in the decay rate curves of Figure 4.2. For each material, as the fiber angle is rotated, the real part of the modified eigenvalue  $\zeta$  traverses a path along the three-dimensional surface mentioned above, crossing over the cusp region twice. Due to the scaling factor  $\rho$  which yields the actual eigenvalue  $\gamma$ , the effects of the cusp are small the first time the cusp is crossed and exaggerated the second time. Thus we observe in each of the curves of Figure 4.2 a small "kink" when the fiber angle is near  $0^\circ$  and a large "kink", or peak, as the fiber angle approaches  $90^\circ$ .

Physically, this peak behavior in the decay rate curves may be related to the severe non-monotone behavior of the elastic parameters  $\epsilon_2$  and  $\epsilon_3$  with  $\theta$  in the particular fiber angle range (see e.g. Figure 4.17 below for HS1). This peak behavior may also occur because as the fiber angle increases, the effects of the matrix on deformation become increasingly more important. Thus for fiber angles near  $90^\circ$  the material behavior is dominated by the matrix in contrast to angles near  $0^\circ$  where the fibers have the dominant effect on the decay rate.

We also observe from Figure 4.2 that for each of the materials there is a fiber orientation angle (roughly in the range  $30^\circ - 50^\circ$ ) at which the decay rate coincides with that for an *isotropic* material ( $k^* = 2.106$ ).

## 4.6 Discussion of Results

In this section, we refer to Figures 4.3 - 4.16 as well as Table 4.1 to discuss the basic energy estimate, nonlinear optimization estimate and higher-order energy estimates developed in this chapter. In contrast to the estimates of the previous chapter, the estimates of the present chapter do not produce explicit formulae for the decay rate, but rather require numerical methods of evaluation. For convenience we choose the three materials HS1, HS2 and UM as representative materials for which to show results. We also wish to thank Dr. M.P. Nemeth of NASA Langley Research Center for providing some of the numerical codes that were used in producing many of the figures.

Figures 4.3 - 4.5 show the exact decay rate together with the basic energy estimate and the nonlinear optimization estimate, for each of the three materials HS1, HS2 and UM respectively. Recall that these two estimates were the only estimates in the anisotropic case that yielded a numerical result (the higher-order energy estimates were not implemented numerically for the anisotropic case). It is observed for each of the materials that both the basic energy estimate and the nonlinear optimization estimate (lower bounds for the exact decay rate) greatly underestimate the exact decay rate, particularly in the middle fiber angle range of  $20^\circ - 70^\circ$ . For the fiber angles near  $0^\circ$  and  $90^\circ$ , i.e. where the material is closer to being orthotropic, the estimates are better, though there is still room for improvement. The nonlinear optimization estimate is seen to be slightly better than the basic energy estimate as the fiber angle increases.

It is noted that in these preceding figures the estimates correspond to mathematical energy formulations using the energy functional  $E_1(z)$ . As mentioned previously, these estimates did not change significantly when the real physical strain-energy  $E_p(z)$  was used. This is now seen in Figures 4.6 - 4.8, where the basic energy estimate is shown using the two different energy formulations, again for the materials HS1, HS2 and UM, respectively. The exact decay rate is reproduced for convenience. While the  $E_1(z)$  formulation is slightly better in the outer ranges of the fiber angle and the  $E_p(z)$  formulation is slightly better in the middle range of the fiber angle, these differences are very small. Similar results are seen in Figures 4.9 - 4.11 where comparisons of the nonlinear optimization estimate with the two different energy formulations are shown for HS1, HS2 and UM.

As mentioned earlier in this chapter, the estimates using  $E_p(z)$  have the advantage that they apply to all physical materials, while the estimates using  $E_1(z)$  require a stricter positive-definite condition that may fail to hold for some materials. This can be seen from Figure 4.12 and Figure 4.13. Figure 4.12 shows the materials from Table 3.1 for which the energy functional  $E_1(z)$  is a positive definite quadratic form, i.e. materials for which  $\frac{1}{\epsilon_1} - \frac{1}{\epsilon_2} - \frac{1}{\epsilon_3} > 0$  (see equation (4.9)). This includes five of the seven materials listed in Table 3.1. Figure 4.13 shows the remaining two materials for which the positive definite condition (4.9) fails to hold at certain fiber angles. Thus, we observe that the  $E_1(z)$  formulations of this chapter cannot be applied to KE or BE in the middle fiber angle region.

Figure 4.12 also indicates why the basic energy estimate and nonlinear optimization estimate shown in Figures 4.3 - 4.5 yield poor results in the middle fiber angle

range. For most of the materials shown in Figure 4.12, the positive-definite condition on  $E_1(z)$  is barely satisfied in the middle fiber angle range. This weakness of the energy norm  $E_1(z)$  in this range limits the accuracy of the estimates of this chapter. For the basic energy estimate given by (4.40) and (4.45), we see that  $k^*$  is proportional to  $\sqrt{\lambda}$  where  $\lambda$  is the smallest eigenvalue of the positive-definite matrix (4.18) arising in the quadratic form  $W_1$  in  $E_1(z)$ . It then follows that the weaker the positive-definiteness of  $E_1(z)$ , the smaller the value for  $\lambda$  and hence the poorer the estimated decay rate  $k^*$ . Similarly, in the nonlinear optimization estimate given by (4.70) - (4.74), we obtained a result that was dependent on the positive-definiteness of  $E_1(z)$ . Specifically, we found that in order for the conditions (4.71) - (4.73) to be satisfied for *some* choice of the parameters  $\alpha$  and  $\beta$ , the positive-definite condition on  $E_1(z)$  must hold (see (4.67) - (4.69)). It can further be observed that the weaker the positive-definiteness of the energy norm  $E_1(z)$ , the less freedom there is in choosing the parameters  $\alpha$  and  $\beta$  to maximize the decay estimate and hence the poorer the results expected. Thus the accuracy of both the basic energy estimate and the nonlinear optimization estimate is very closely linked to the degree of positive-definiteness of the energy norm involved.

In Figures 4.14 - 4.16, we show some results for the higher-order energy estimates of this chapter, i.e. the quadratic and quartic estimates. For the anisotropic case, neither the quadratic estimate nor the quartic estimate yielded results that were very tractable numerically. However, *explicit upper bounds were obtained for both of these estimated decay rates* and are plotted in Figures 4.14 - 4.16 for HS1, HS2 and UM respectively. The quadratic estimate upper bound comes from (4.138) while the

quartic estimate upper bound is given in (4.168). For each of the materials shown, we observe that both the quadratic estimate upper bound and the quartic estimate upper bound are well below the exact decay rate in the middle fiber angle range. In the outer fiber angle ranges, these two bounds are much higher and in some cases exceed the actual decay rate. Since these are *upper bounds* for the estimated decay rates (which are, in turn, *lower bounds* on the exact decay rate), Figures 4.14 - 4.16 show that these techniques will yield very poor results in the middle fiber angle ranges. In the outer fiber angle ranges there is the potential for accurate results as the upper bounds on the estimates exceed the exact decay rates, however the estimates themselves could lie well below the bounding curves. In fact, for the HS1 and HS2 materials at  $15^\circ$  fiber orientation angle, attempts were made through trial and error to determine a numerical result from the quadratic estimate. The decay rate estimates so obtained were inadequate, however. For these reasons, numerical techniques were not further pursued. We also note from Figures 4.14 and 4.16 that for HS1 and UM there are certain fiber angle ranges for which the quartic estimate upper bound becomes negative. This implies that for these ranges the quartic estimate is invalid and cannot be applied.

Results in the orthotropic limits for both the quadratic and quartic estimates were obtained earlier in this chapter. The orthotropic quadratic estimate required that  $\epsilon_1 > .63$  and hence this estimate does not apply to any of the materials in Table 3.1. The orthotropic quartic estimate, however, does apply to these materials and numerical results are shown in Table 4.1. Here, the exact decay rates and the conservation law estimate of Chapter 3 are included for comparison. It can be seen

that for orthotropic materials the quartic estimate is not quite as good as the conservation law estimate, particularly for materials with larger values of  $\epsilon_1$ . It is, however, better than the analytic estimate (3.51), excepting the BA and isotropic materials, and better than (3.55) for small  $\epsilon_1$ .

Finally, in Figures 4.17 and 4.18 we show typical curves for the elastic parameters of the material as functions of the fiber orientation angle. Figure 4.17 provides plots for  $\epsilon_1$ ,  $\epsilon_2$  and  $\epsilon_3$  for the HS1 material, and is representative of most of the other materials used in this dissertation. As the fiber angle increases, the elastic parameters all vary smoothly. We observe that  $\epsilon_1$  is symmetric about  $45^\circ$  where it reaches its maximum value while  $\epsilon_2$  and  $\epsilon_3$  are symmetric with respect to each other, and suffer a rapid variation near  $\theta = 90^\circ$  and  $\theta = 0^\circ$  respectively. In Figure 4.18 these elastic parameters are plotted for the KE material and we observe some atypical properties. Here,  $\epsilon_1$  still varies smoothly and is symmetric about  $45^\circ$ , however  $\epsilon_2$  and  $\epsilon_3$  show sharp jumps in sign. Such extreme behavior helps to explain the difficulty involved with obtaining accurate decay rate estimates for such materials.



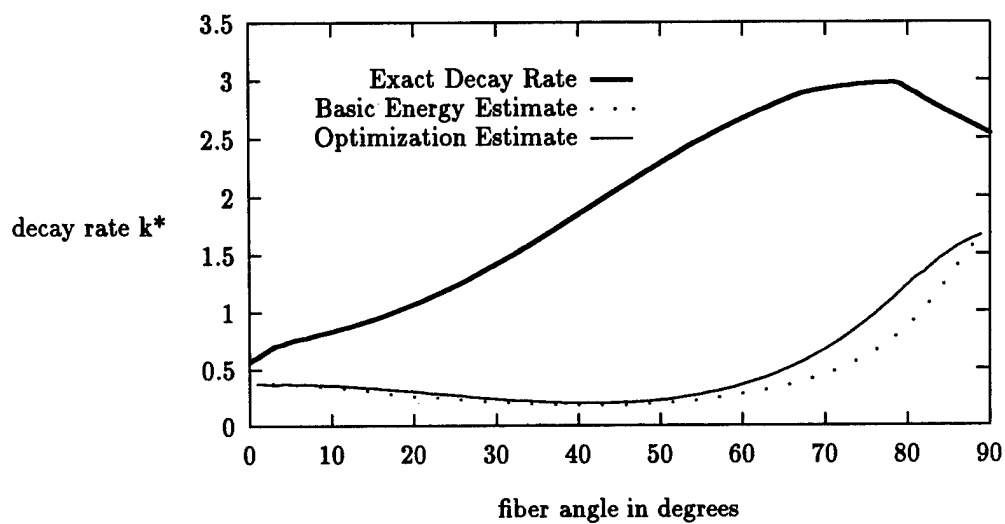


Figure 4.3: Exact decay rate and estimates for HS1

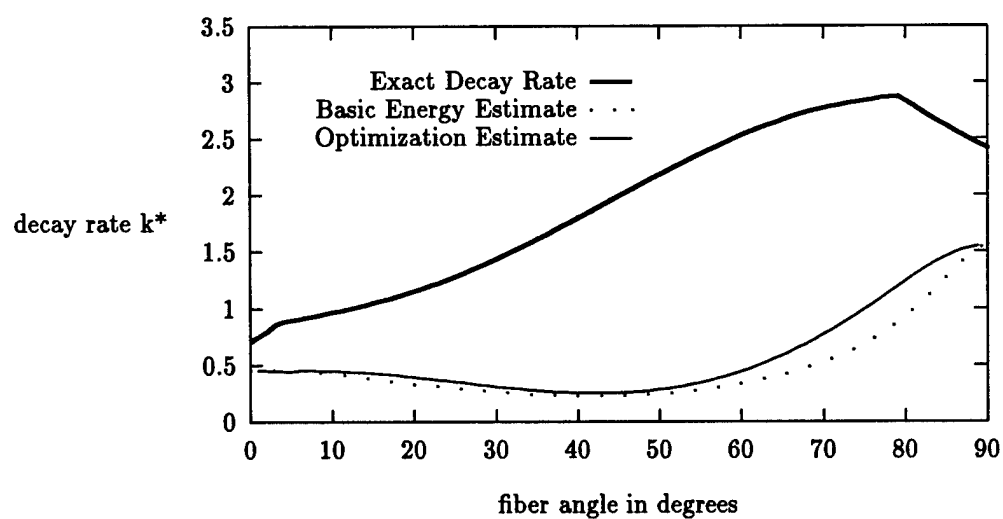


Figure 4.4: Exact decay rate and estimates for HS2

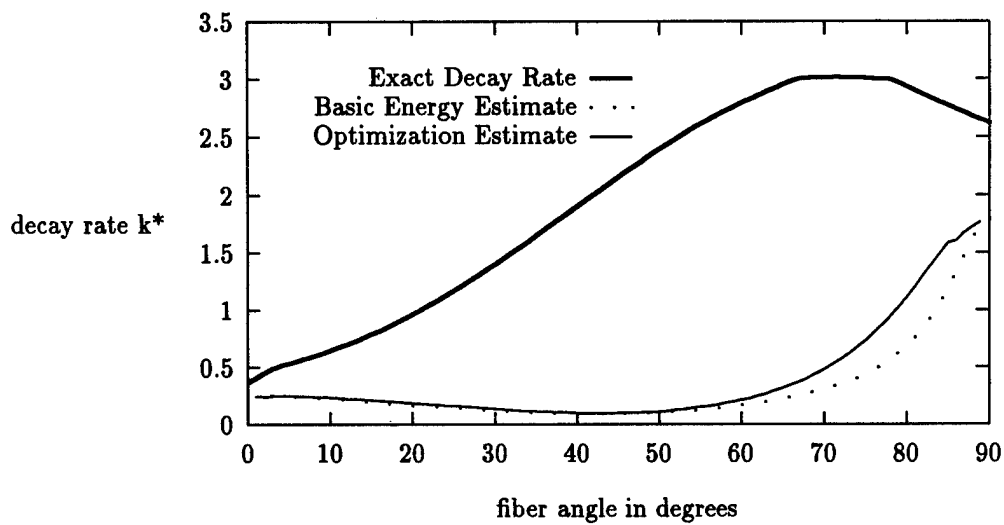


Figure 4.5: Exact decay rate and estimates for UM

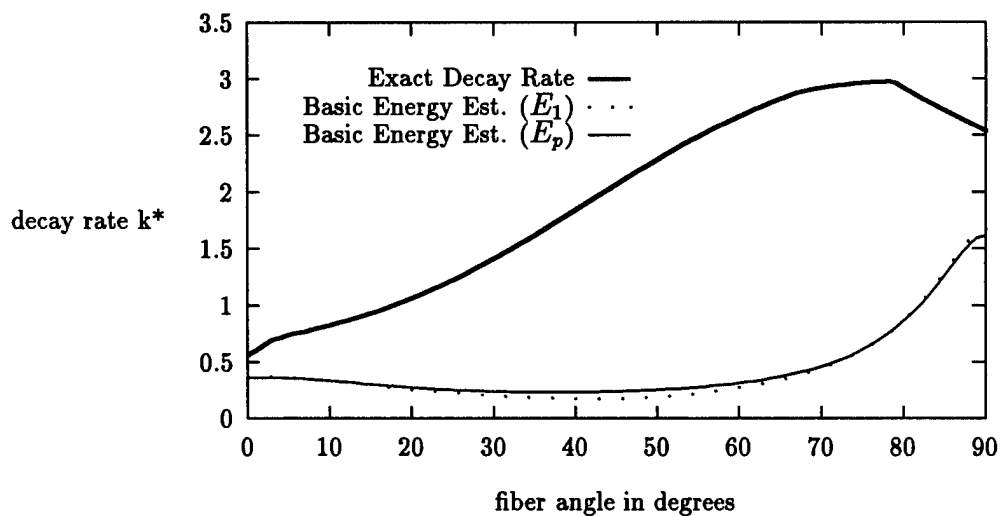


Figure 4.6: Basic energy estimate for HS1 with different energy functionals

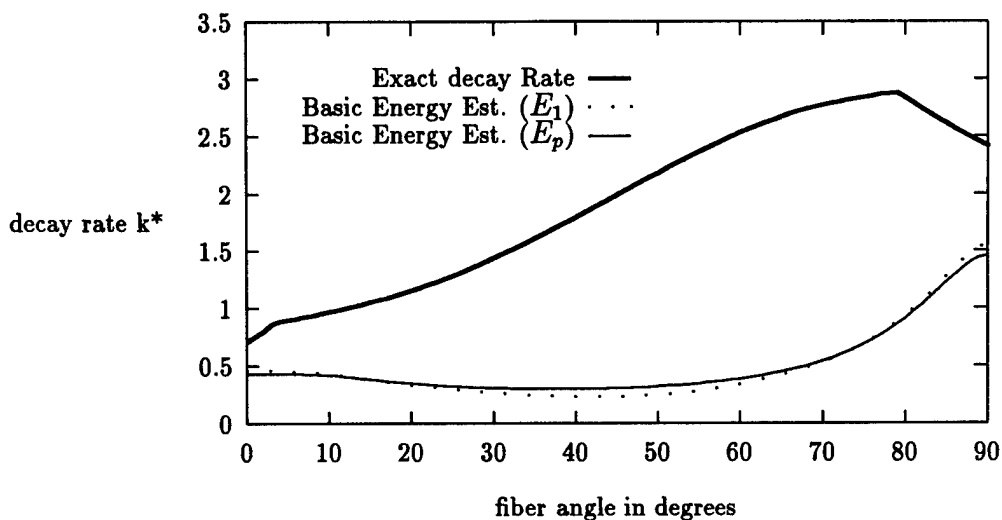


Figure 4.7: Basic energy estimate for HS2 with different energy functionals

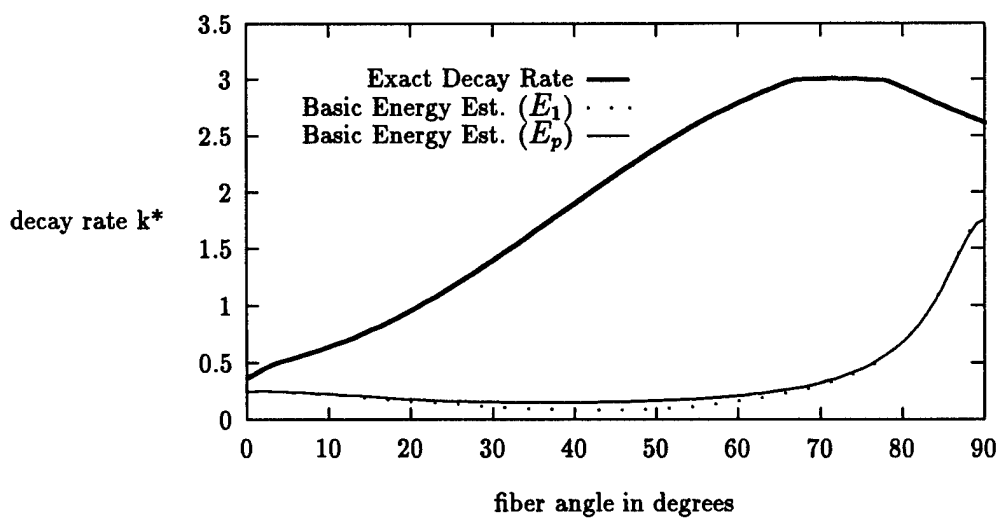


Figure 4.8: Basic energy estimate for UM with different energy functionals

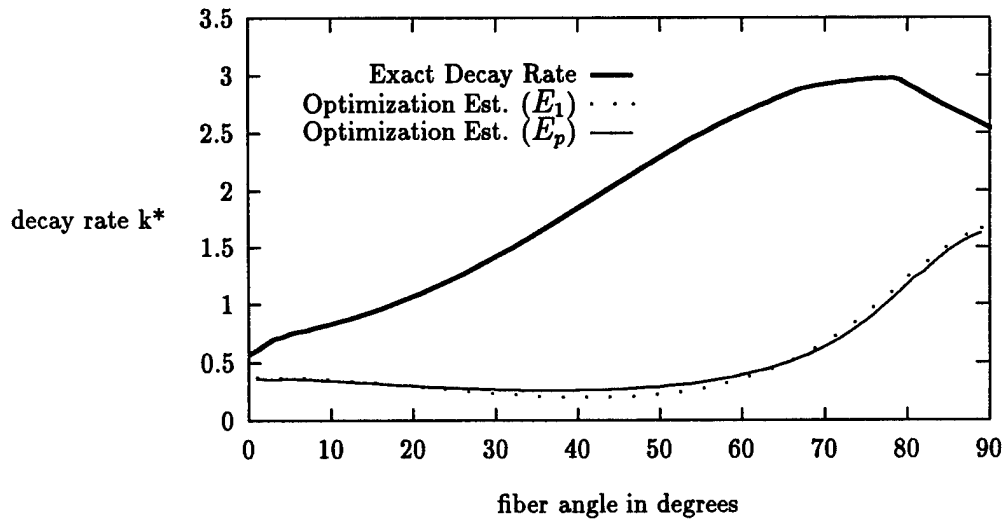


Figure 4.9: Nonlinear optimization estimate for HS1 with different energy functionals

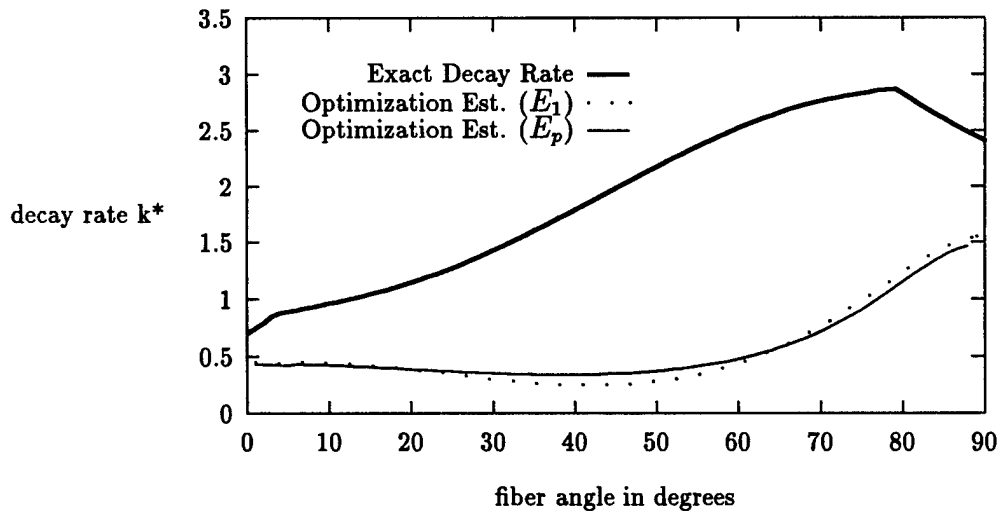


Figure 4.10: Nonlinear optimization estimate for HS2 with different energy functionals

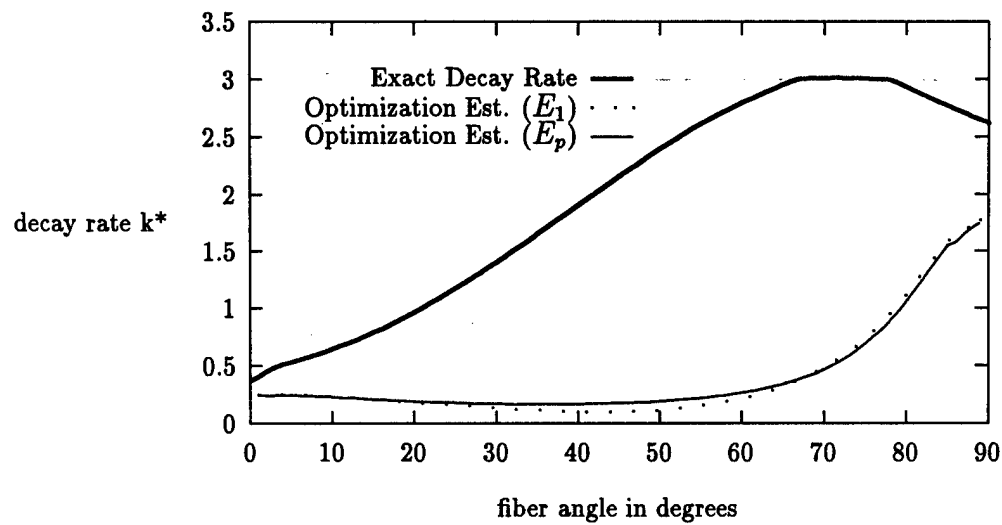


Figure 4.11: Nonlinear optimization estimate for UM with different energy functionals

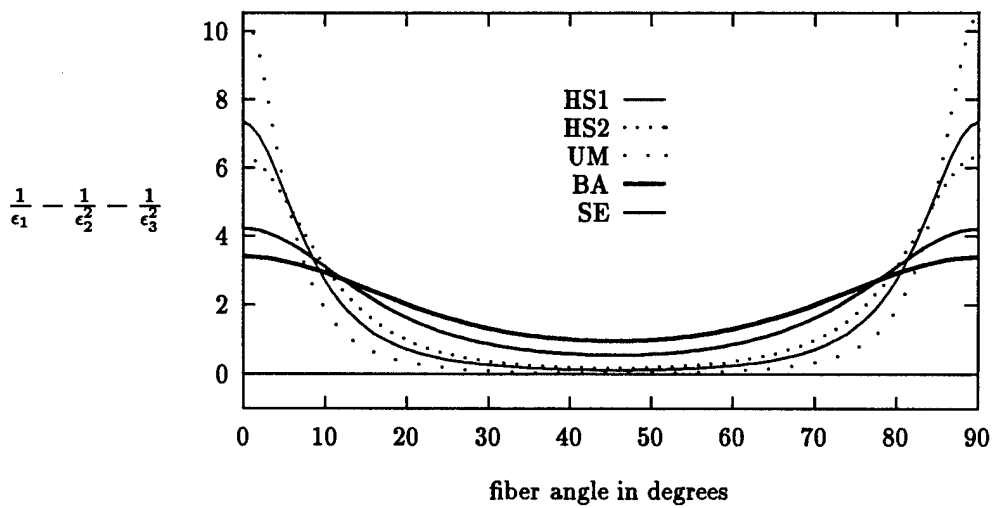


Figure 4.12: Materials for which the positive-definite condition (4.9) is satisfied

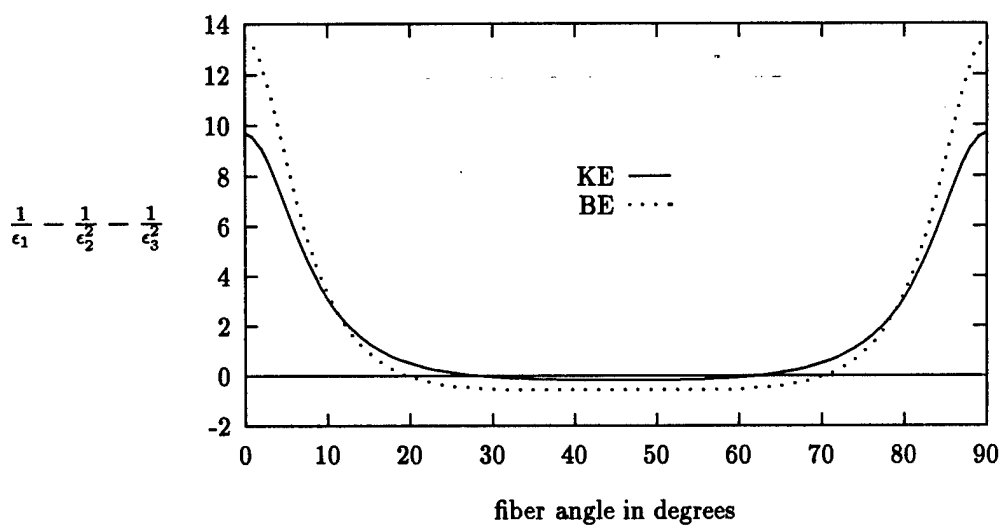


Figure 4.13: Materials for which the positive-definite condition (4.9) fails

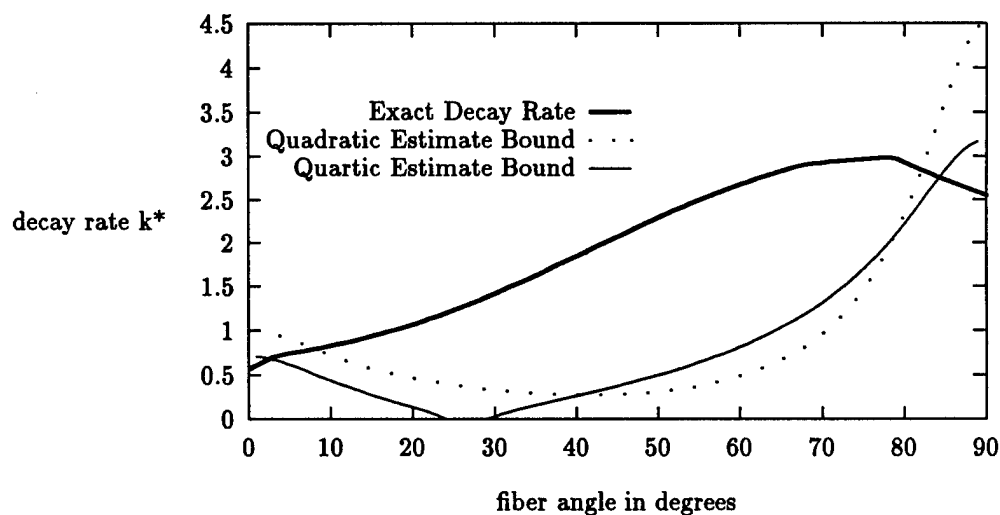


Figure 4.14: Upper bounds (4.138), (4.168) on estimated decay rate for HS1

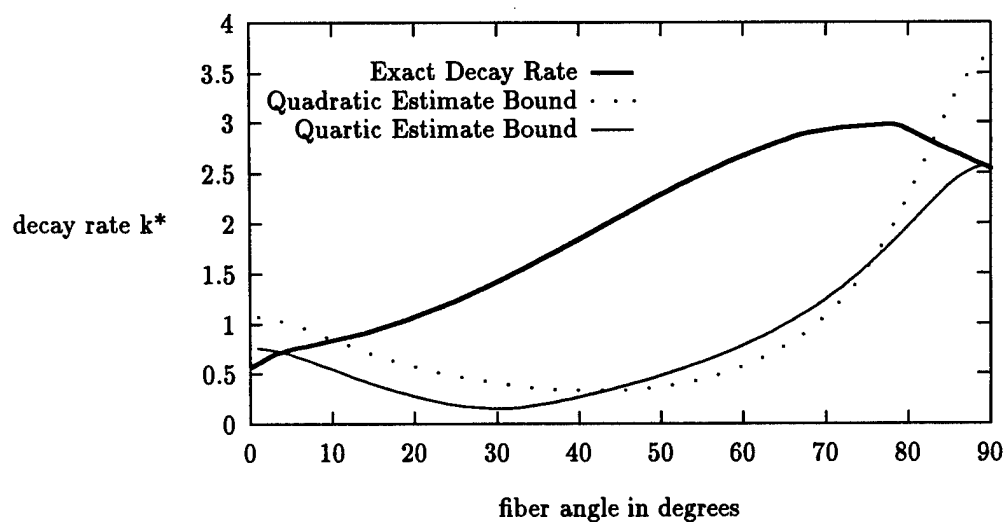


Figure 4.15: Upper bounds (4.138), (4.168) on estimated decay rate for HS2

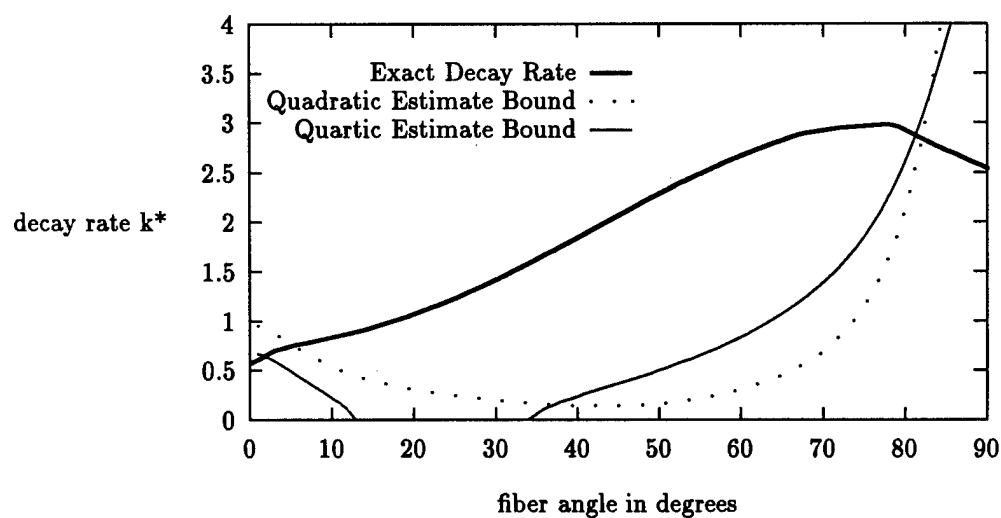


Figure 4.16: Upper bounds (4.138), (4.168) on estimated decay rate for UM

Material ( $\epsilon_1$ )	Quartic Estimate	Cons. Law Estimate	Exact Decay Rate $k^*$
<b>BE</b> (0.0745)	0.409	0.445	0.487
<b>UM</b> (0.0949)	0.306	0.328	0.369
<b>KE</b> (0.1030)	0.438	0.467	0.534
<b>HS1</b> (0.1362)	0.447	0.468	0.567
<b>HS2</b> (0.1578)	0.522	0.564	0.708
<b>SE</b> (0.2366)	0.709	0.794	1.195
<b>BA</b> (0.2946)	0.853	1.069	1.942
<b>Isotropic</b> (0.500)	0.749	1.220	2.106

Table 4.1: Quartic estimate for orthotropic materials :  $\tau \sim e^{-\frac{k^* x_1}{H}}$  as  $x_1 \rightarrow \infty$ .



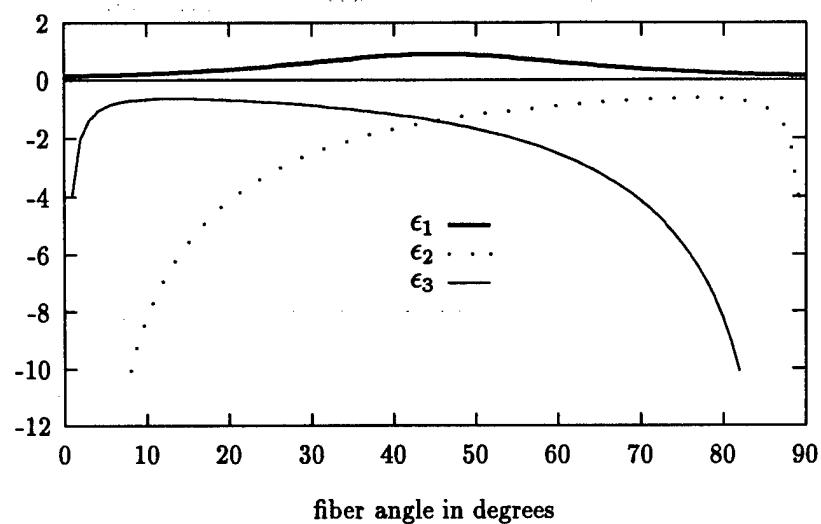


Figure 4.17: Nondimensional parameters for HS1

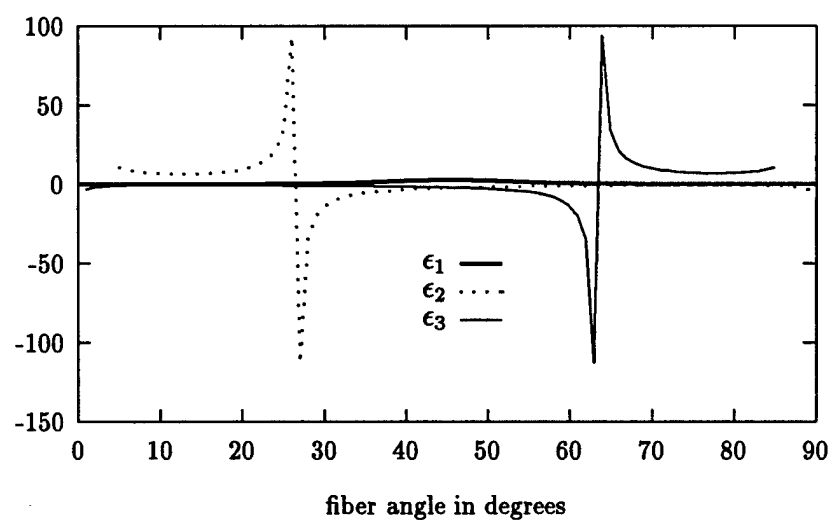


Figure 4.18: Nondimensional parameters for KE

## Chapter 5

# SUMMARY AND CONCLUSIONS

Several methods have been developed in this dissertation for deriving decay rate estimates for stresses in an anisotropic linearly elastic semi-infinite strip subject to a plane stress/strain deformation. The goal of the present study has been to examine the effects of material orthotropy and anisotropy on the decay rate of local stresses generated by self-equilibrated edge loadings.

The problem was analyzed first for the important subclass of *specially orthotropic materials*, where two estimates (the analytic estimate and the conservation law estimate) were obtained that provide lower bounds on the decay rate for stresses in the material. The analytic estimate gave an *explicit* formula in terms of nondimensional material parameters and thus directly revealed the effects of material orthotropy on the stress decay rate. Two essential parameters required for determining the stress decay rates have been identified as the dimensionless parameter  $\epsilon_1$  and the beta ratio

$(\frac{\beta_{11}}{\beta_{22}})^{\frac{1}{4}}$ . Upon expressing these parameters in terms of the usual engineering material constants, the stress decay behavior can be found and trends can be identified for a wide class of materials. It has been shown that, in general, materials with the smallest values of  $\epsilon_1$  have the smallest decay rates and hence the largest decay lengths. When compared with the corresponding exact stress decay rates, the analytic estimate has been shown to preserve relative ordering of the decay rates among the various materials from Table 3.1 and, although an *underestimate* for the exact decay rate (and a *overestimate* for the exact decay length), the analytic estimate yields a conservative and useful result that captures the overall behavioral trends of specially orthotropic materials. While the conservation law estimate *did not* produce an explicit formula, numerical results were obtained that are significantly better than the corresponding results obtained using the analytic estimate, and for some materials were in good agreement with the exact stress decay rates. The improved accuracy of the conservation law approach, particularly for the strongly orthotropic materials considered, suggests the usefulness of such a method for estimating solutions to similar problems. For both the analytic and conservation law estimates, an asymptotic analysis resulted in asymptotic formulae for the estimated decay rates for materials with small values of  $\epsilon_1$ . For strongly orthotropic materials these asymptotic formulae resulted in stress decay rate estimates that are proportional to  $(\frac{G_{LT}}{E_L})^{\frac{1}{2}}$ , a result that has already been applied to many practical problems involving composite materials. It has been further shown that for all of the analyses presented here for the orthotropic strip, the most accurate decay rate estimates are obtained for materials with small values of the orthotropic parameter  $\epsilon_1$ .

The strip problem has also been examined for *anisotropic materials*, where the difficulty encountered in obtaining results greatly increases. For this problem, four decay rate estimates have been derived; i.e., a basic energy estimate, a nonlinear optimization estimate and two higher-order energy estimates. Unlike the analyses for the orthotropic strip, explicit decay rate formulae for the anisotropic strip in terms of the elastic material constants were not obtained due to the increased analytical complexity caused by the presence of anisotropy. Both the basic energy estimate and the nonlinear optimization estimate yield *numerical* results that depend implicitly on the elastic parameters of the material,  $\epsilon_1$ ,  $\epsilon_2$ ,  $\epsilon_3$  in addition to the beta ratio. These estimates have been compared with corresponding exact decay rates computed numerically for a set of specially orthotropic materials in which the principal material axes were rotated through a fiber angle varying from  $0^\circ$  to  $90^\circ$ . Both the basic energy estimate and the nonlinear optimization estimate exhibited similar characteristics; they gave more accurate estimates for the fiber angles near  $0^\circ$  and  $90^\circ$ , where the material is close to being orthotropic, while giving less accurate results in the middle fiber angle region where more general anisotropy is observed. The limitations of both of these approximate methods for anisotropic strips has been found to be directly related to the positive-definiteness conditions on the energy norms. The higher-order energy estimates were modelled after the conservation law approach of Chapter 3 and resulted in optimization problems which, due to the number of undetermined parameters involved, did not result in tractable numerical results. These higher-order estimates were found to simplify considerably in the orthotropic limit. However the numerical results obtained were not better than the orthotropic estimates of Chapter

3. Asymptotic analyses were not pursued for the anisotropic strip since small values of the parameters  $\epsilon_2$  and  $\epsilon_3$  do not have the physical significance that small values of  $\epsilon_1$  do for the orthotropic strip, i.e. corresponding to strong orthotropy. In particular, small values of  $\epsilon_2$  and  $\epsilon_3$  are not exhibited by common materials of technological interest. In general, the methods of this dissertation when extended to the anisotropic strip were found to be difficult to implement and were not able to provide as accurate results as desired. Nevertheless, the results indicate some of the difficulties involved in modelling the anisotropic strip and give insight into what may be done to improve the estimates. Furthermore, since the results yield *lower bounds* for the decay rates and thus *upper bounds* for the decay lengths, the results are conservative and thus immediately useful from an engineering design perspective.

We conclude with an outline of some areas of future research. Ideally, an explicit decay rate formula in terms of  $\epsilon_1$ ,  $\epsilon_2$  and  $\epsilon_3$  is desirable for the anisotropic strip. This would clearly reveal the importance of anisotropy on the decay rate of edge effects and would be applicable to a broad range of materials. This insight could stimulate the investigations of many other problems using a classical approach with anisotropic elasticity. Such insight could greatly assist in tailoring composite structures and provide guidance for modelling complex structures with powerful computational tools such as the finite element method. One promising approach to solving the anisotropic strip problem is the conservation law method. While one of the two conservation laws developed in this research was shown to yield highly accurate results for orthotropic materials, it remains to be seen whether the remaining conservation law can be used in a similar fashion or if additional conservation laws can be developed to improve the

results. Finally, as the anisotropic analysis revealed, the decay rate estimates obtained here are not accurate whenever the positive-definiteness of the energy norm is weakly satisfied. This suggests that alternate energy norms might be more appropriate for the analysis of the anisotropic strip.

# Bibliography

- [1] C. O. Horgan and J. K. Knowles. Recent developments concerning Saint-Venant's principle. In T. Y. Wu and J. W. Hutchinson, editors, *Advances in Applied Mechanics*, volume 23, pages 179–269. Academic Press, 1983.
- [2] C. O. Horgan. Recent developments concerning Saint-Venant's principle: an update. *Applied Mechanics Reviews*, 42:295–303, 1989.
- [3] C. O. Horgan. Decay estimates for the biharmonic equation with applications to Saint-Venant principles in plane elasticity and Stokes flows. *Quarterly of Applied Mathematics*, 47:147–157, 1989.
- [4] C. O. Horgan. On Saint-Venant's principle in plane anisotropic elasticity. *Journal of Elasticity*, 2:169–180, 1972.
- [5] C. O. Horgan. Some remarks on Saint-Venant's principle for transversely isotropic composites. *Journal of Elasticity*, 2:335–339, 1972.
- [6] I. Choi and C. O. Horgan. Saint-Venant's principle and end effects in anisotropic elasticity. *Journal of Applied Mechanics*, 44:424–430, 1977.
- [7] C. O. Horgan. Saint-Venant end effects in composites. *Journal of Composite Materials*, 16:411–422, 1982.
- [8] C. O. Horgan and J. G. Simmonds. Asymptotic analysis of an end-loaded, transversely isotropic, elastic, semi-infinite strip weak in shear. *Int. J. Solids and Structures*, 27:1895–1914, 1991.
- [9] C. O. Horgan and J. G. Simmonds. Saint-Venant end effects in composite structures. *Composites Engineering*, 3:279–286, 1994.
- [10] L. A. Carlsson and R. B. Pipes. *Experimental Characterization of Advanced Composite Materials*. Prentice-Hall, 1987.
- [11] J. K. Knowles. On Saint-Venant's principle in the two-dimensional linear theory of elasticity. *Archive for Rational Mechanics and Analysis*, 21:1–22, 1966.
- [12] J. N. Flavin. On Knowles' version of Saint-Venant's principle in two-dimensional elastostatics. *Arch. Rat. Mech. Anal.*, 53:366–375, 1974.

- [13] O. A. Oleinik and G. A. Yosifian. On Saint-Venant's principle in plane elasticity theory. *Dokl. Akad. Nauk. SSSR*, **239**:530-533, 1978. (translated in *Soviet Math. Dokl.* **19**, 364-368 (1978)).
- [14] O. A. Oleinik and G. A. Yosifian. The Saint-Venant principle in the two-dimensional theory of elasticity and boundary problems for a biharmonic equation in unbounded domains. *Sibirsk. Mat. Zh.*, **19**:1154-1165, 1978. (translated in *Siberian Math. J.* **19**, 813-822 (1978)).
- [15] J. K. Knowles. An energy estimate for the biharmonic equation and its application to Saint-Venant's principle in plane elastostatics. *Indian Journal of Pure and Applied Mathematics*, **14**:791-805, 1983.
- [16] S. G. Lekhnitskii. *Theory of Elasticity of an Anisotropic Elastic Body*. Mir Publishers, 1981.
- [17] M. P. Nemeth. Buckling behavior of long symmetrically laminated plates subjected to combined loadings. Technical Report 3195, NASA, 1992.
- [18] K. L. Miller and C. O. Horgan. Conservation properties for plane deformations of isotropic and anisotropic linearly elastic strips. *Journal of Elasticity*, **33**:311-318, 1993.
- [19] E. C. Crafter, R. M. Heise, C. O. Horgan and J. G. Simmonds. The eigenvalues for a self-equilibrated, semi-infinite, anisotropic elastic strip. *Journal of Applied Mechanics*, **60**:276-281, 1993.
- [20] M. P. Nemeth. NASA Langley Research Center, Hampton, VA (private communication).
- [21] S. G. Mikhlin. *Variational Methods in Mathematical Physics*. Macmillan, 1964.
- [22] J. E. Littlewood G. H. Hardy and G. Polya. *Inequalities*, 2<sup>nd</sup> edition. Cambridge University Press, 1967.
- [23] C. O. Horgan. A note on a class of integral inequalities. *Proc. Cambridge Phil. Soc.*, **74**:127-131, 1973.
- [24] P. Vafeades and C. O. Horgan. Exponential decay estimates for solutions of the von Karman equations on a semi-infinite strip. *Arch. Rat. Mech. Anal.*, **104**:1-25, 1988.
- [25] J. G. Simmonds and J. E. Mann, Jr. *A First Look at Perturbation Theory*. Robert E. Krieger Publishing Company, 1986.
- [26] S. P. Timoshenko and J. N. Goodier. *Theory of Elasticity*, third ed. McGraw-Hill, 1970.
- [27] J. M. Ortega. *Matrix Theory*. Plenum Press, 1987.



- [28] M. Z. Wang, T. C. T. Ting and G. Yan. The anisotropic elastic semi-infinite strip. *Quart. Appl. Math.*, **51**:283-297, 1993.
- [29] I. Choi and C. O. Horgan. Saint-Venant end effects for plane deformation of sandwich strips. *Int. J. Solids and Structures*, **14**:187-195, 1978.